Scientific Research and Essays

Volume 9 Number 17 15 September 2014
ISSN 1992-2248

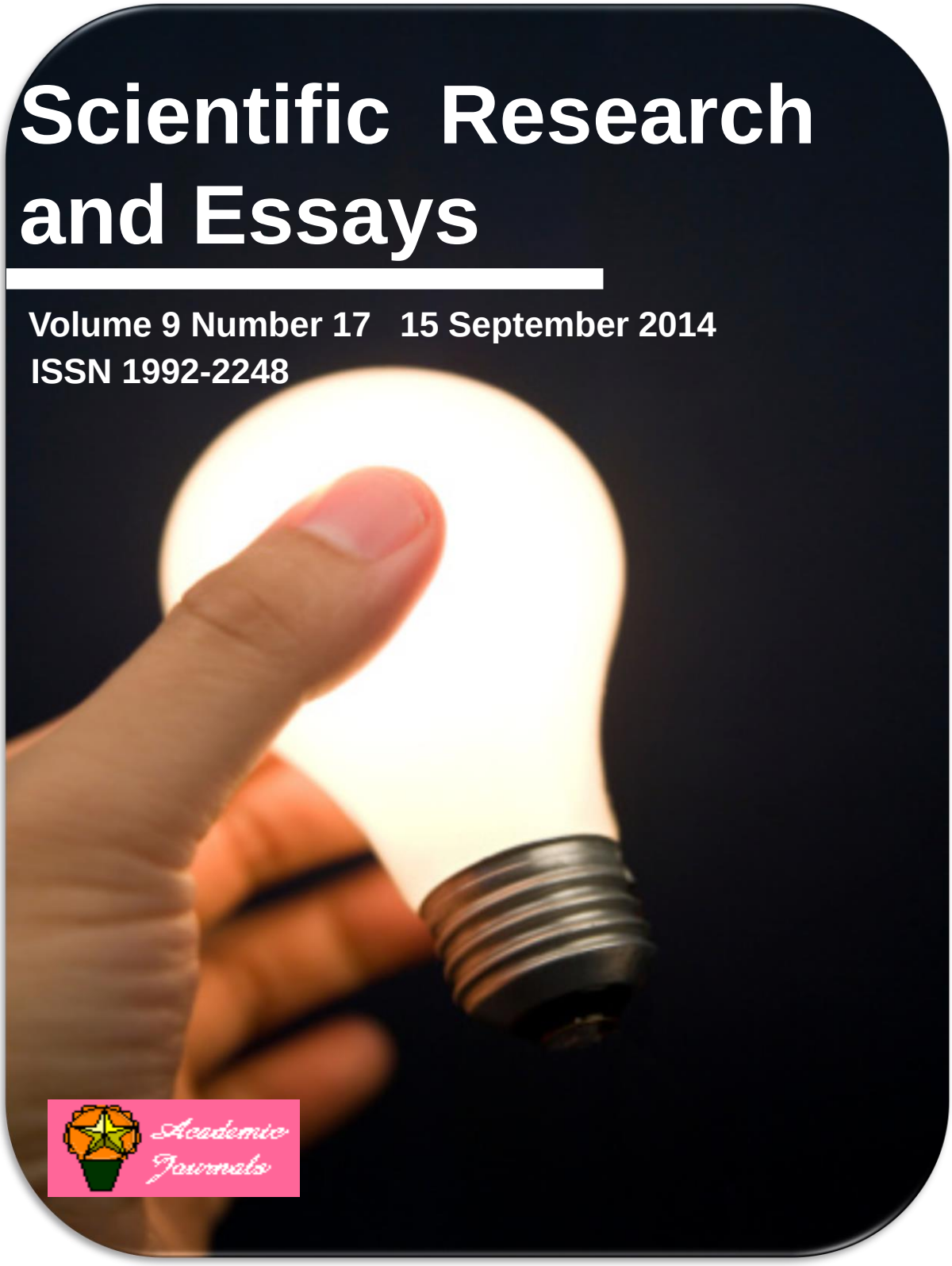

Academic Journals

ABOUT SRE

The **Scientific Research and Essays (SRE)** is published twice monthly (one volume per year) by Academic Journals.

Scientific Research and Essays (SRE) is an open access journal with the objective of publishing quality research articles in science, medicine, agriculture and engineering such as Nanotechnology, Climate Change and Global Warming, Air Pollution Management and Electronics etc. All papers published by SRE are blind peer reviewed.

Submission of Manuscript

Submit manuscripts as e-mail attachment to the Editorial Office at: sre@academicjournals.org. A manuscript number will be mailed to the corresponding author shortly after submission.

The Scientific Research and Essays will only accept manuscripts submitted as e-mail attachments.

Please read the **Instructions for Authors** before submitting your manuscript. The manuscript files should be given the last name of the first author.

Editors

Editorial Board

n detail.

Fees and Charges: Authors are required to pay a $550 handling fee. Publication of an article in the Scientific Research and Essays is not contingent upon the author's ability to pay the charges. Neither is acceptance to pay the handling fee a guarantee that the paper will be accepted for publication. Authors may still request (in advance) that the editorial office waive some of the handling fee under special circumstances.

Submission of a manuscript implies: that the work described has not been published before (except in the form of an abstract or as part of a published lecture, or thesis) that it is not under consideration for publication elsewhere; that if and when the manuscript is accepted for publication, the authors agree to automatic transfer of the copyright to the publisher.

Scientific Research and Essays

Table of Contents: Volume 9 Number 17 15 September, 2014

ARTICLES

Research Articles

academicJournals

Vol. 9(17), pp. 744-751, 15 September, 2014
DOI: 10.5897/SRE2014.6108
Article Number: 00B16DA47283
ISSN 1992-2248 © 2014

http://www.academicjournals.org/SRE

Scientific Research and Essays

Full Length Research Paper

Results of treatment of tibial plafond fractures with articulated external fixation

Reşit SEVİMLİ[1*], M. Fatih KORKMAZ[1] and MD Ökkeş BİLAL[2]

[1]Department of Orthopedic and Traumatology, Medical Faculty, İnönü University, 4400 Malatya/Turkey.
[2]Department of Orthopedic and Traumatology, Medical Faculty, Sütçü imam University, 4600 Kahramanmaraş/Turkey.

Received 16 November, 2013; Accepted 16 June, 2014

The aim of this study is to assessor the tibial pilon fractures treated primarily with results of the articulated external fixation. The study included 24 patients (18 male, 6 female) with mean age of 26 ± 4.2 (range 18-51). According to the classification of AO/OTA, 6 cases were diagnosed as Type A, 4 cases as Type B and 14 cases as type C. Also, according to the Gustilo and Anderson method four of the cases were classified as grade I, two grade II and six grade III open fracture. For eight cases only the articulated external fixation was used, and for sixteen of the cases who have fibula injury at the syndesmosis level both articulated external fixation and plate-screw osteosynthesis for the restoration of the fibula was performed. While the articulated external fixation duration ranged from 8 to 14 weeks (10 ± 3.2 SD); follow up period was between 7 and 32 months (25 ± 4.6 SD). The results were evaluated according to the Teeny and Wiss criteria. The operation results of the patients were as follow: excellent for three, good for four, moderate for three, and poor for two of them. The complications encountered were bulla skin lesion for two of the cases at post-operative third day and non-union for one of the patients. There was no bone or soft tissue infection. The open tibial pilon fractures result from high-energy trauma; carry risk of serious injuries, loss of the range of the motion and infection can be safely treated with external fixation technique.

Key words: External fixators, tibial fractures, intra-articular fractures.

INTRODUCTION

Fractures of the tibial pilon fractures, representing 1% of the lower extremity distal to the articular surface of the tibia metaphyseal extension and internal fixation techniques indicate and commonly used in the treatment of a fracture of the classic traditional type (Taylor, 1992). These fractures, low energy and they occur, not cause injury to surrounding soft tissue sheath is an important, high-energy injuries, associated soft tissue problems and intra-articular fractures are prone to trouble because it is a multi-part fracture. Pilon fractures of the metaphyseal fragments with high energy trauma are multiple, it is associated with the articular surface of the displaced fragments often. As a result of severe compression of the joint surface, oppression and violent fragmentation of the articular surface causes. Not created at the time of the trauma due to the anatomical joint surface cartilage and early osteoarthritis is an inevitable occurrence.

Pilon fractures with severe soft tissue damage can be seen. The amount of soft tissue injury associated with significant complications. Excessive edema is caused by

*Corresponding author. E-mail: resitsevimli@mynet.com, Tel: +90 5345738724.

the formation of bulla on the skin. Appropriate radiological evaluation is very important in determining the properties of the fracture. Anterior-posterior and lateral radiograph of the ankle mortis must also be drawn in addition to X-rays. The main purpose of treatment, open reduction and re-creation of the joint surface, good to a solid early action to detect and identify the sound to start (Bottlang et al., 1999). High-energy pylon fractures with soft-tissue loss and with fracture split is attempted to be treated the same way, a serious infection, wound problems and complications such as nonunion becomes inevitable to encounter(Dichristina et al., 1996). Recent studies noting the importance of treatment of tibial pilon fractures, external fixation techniques, study platform tibial pilon fractures were treated with external fixation evaluated the results of early motion. So the aim of this study is to assess the results of the primarily treated tibial pilon fractures with articulated external fixation.

MATERIALS AND METHODS

Working with sufficient follow-up and platform ankle fixator was performed on 24 patients treated with tibial pilon fractures. Included in the study 24 patients (18 males, 6 females) average age of 26 ± 4.2 (min: 18, max: 51), respectively. Broken cause a traffic accident in 16 cases, 4 cases of gunshot wounds and 4 had a fall from height. Fractures, 16 right leg, and 8 left leg respectively. According to the classification of AO/OTA, 6 cases were diagnosed as Type A, 4 cases as Type B and 14 cases as Type C. Also, according to the Gustilo and Anderson method four of the cases were classified as grade I, two grade II and six grade III open fracture. Fractures with the first day of the period between the 9th day of surgery (3.5 ± 3SS) and, 12 patients with open fractures were the first responders in the emergency department, patients with grade III open fracture wounds were washed with saline solution for at least 10 L. Cut-off bone chips removed cleaned of soft tissue foreign bodies. Open fractures brought closer to becoming partially closed with interrupted sutures, fixation during the implementation of the second debridement was performed. A single dose of tetanus immunoglobulin for prophylaxis and for the prophylaxis of infection 1 week cefazolin sodium 3 g/day and 5 days 200 to 400 mg/day was used netilmicin. Temporary limb with skeletal traction splint or calcaneus were passed. Before the procedure, all patients with informed consent forms after obtaining permission from the nine patients with spinal anesthesia, general anesthesia applied to three patients were operated on with the supine position, and fluoroscopy. In all cases, C-arm monolateral articulated external fixator bridging the ankle (Biomet) was used. One of the distal fixation screws schanz to kalkaneus, placing one of the talus, the fracture surface of the proximal anteromedial tibial screw placed at the transmigrate articulated external fixator placed together in all cases sufficient enough distraction and reduction of Type III patients is also confirmed under fluoroscopy after fixation in neutral ankle was stabilized.

A 38-year-old man had a traffic accident cases, preoperative tibial pilon fractures, tibial joint on the crash and the displacement is evident on radiographs AO/OTA classified as Type C fractures according to the classification (Figure 1a and b). With articulated external fixator with distraction and reduction of post-operative articular surface of the tibia and fibula restored and made repairs syndesmosis AP-Lateral radiograph of the same patient (Figure 1c).

Only four of the cases articulated external fixation, fibula injury at the level of the eight patients syndesmos articulated external fixator with the plate-screw osteosynthesis of fibula made for the restoration of the ankle joint in neutral while the screw syndesmoz applied parallel to the face. If syndesmosis leave the tibia we must restoration this area. For restoration of syndesmosis we use only plate and screw. Outside of three cases we do not use multiple incision. AO/OTA two cases of Type C according to the classification of Type III open fractures closed reduction was performed in all patients except one case.

Cases of compartment syndrome in the early postoperative period and were closely monitored for infection. Radiographic checks every two weeks, transmission case was dressing daily. In all cases, passive ankle range of motion was started after the third week after surgery, radiographic union fixators were removed after being identified. X-ray anatomic alignment check first month of the same phenomenon seen enough and started fracture union (Figure 2a and b). The mean duration of external fixation platform for ten weeks (8 to 14 weeks), mean follow-up period was twenty-five months (7 to 32 months).

Evidences

All patients with grade I or II according to the criteria of Paley pin tract problems, but it was enough to remove the screw schanz grade III infection was observed. Schanz three pin tract infections nail care and resolved with oral antibiotics. Teeny results were evaluated according to the criteria (Table 1). In 6 cases excellent, good in 8 cases, 6 cases moderate, poor results were obtained in 4 cases. In all cases, the ankle range of motion was measured immediately after removal of the fixation. Close to normal in all patients except 4 cases ROM's angle values were obtained. Complications in the early postoperative period in two of the cases were blisters on the skin. Nonunion was seen in one patient.

A 42-year-old male patient traffic accidents in the first week of postoperative partial necrosis of the skin and skin integrity is seen from the front and sides appears to be a complete and good circulation (Figure 3a to c). There was no bone or soft tissue infection. Complaints resolved with oral anti-inflammatory treatment in patients with pain, while a single case was ankle arthrodesis. After releasing the first month after the operation the patient started articulated external fixation apparatus passive ankle range of motion exercises and be seen (Figure 4a and b).

RESULTS

Tibial pilon fractures with metaphyseal defects before applying the external fixation, to facilitate reduction of the articular surface of the distal tibia, fibula and the tibia, fibula osteosynthesis may be necessary to ensure that the actual length (Bourne, 1989). Reduction of capsular not connected to the intra-articular fractures need to be applied to a limited open reduction and minimal osteosynthesis. Also, the joint surface and resulting arthro diastazis ligamentotaxis ensure full tilt and should be identified to avoid the talus do (Fitzpatrick et al., 1995; Russell et al., 1991). This type of joint fractures as early as possible to start the movement of used articulated fixation. Except for those two cases, we do not have any osteoarthritis. In the treatment of tibial pilon fractures, infection and wound problems, are important factors affecting the result. By we if caused by high energy and high rate when treated with conventional methods tibial pilon fractures are at risk of wound problems and secure

Figure 1. A 38-year-old man car traffic accident the patient's preoperative and postoperative radiographs of tibial pilon fractures.

Figure 2. X-ray control the same hospital as the first month.

Table 1. According to Wiss and Teeny clinical evaluation.

Very good	No pain, normal gait, normal ROM, no swelling.
Good	Minimal pain, normal walking, ¾ normal ROM, mild swelling.
Medium	By using the pain, normal walking, ½ the normal ROM, moderate swelling of using NSAID's.
Bad	Walking and rest pain, claudication, ½ the normal ROM, swelling.

with hinged external fixator technique can be successfully treated. A longer follow-up studies with larger patient series should be considered.

DISCUSSION

Pilon fractures of the distal articular surface of the tibia into the joint surface with varying degrees of extension fractures with articular disruption. 7% of all fractures of the tibia and comprises 1% of all lower extremity fractures. Pilon fractures of causes in motor vehicle accidents, falls and injuries include gunshot. For the first time since 1979 when the surgical principles were described by Ruedi and Allgower (1979), despite the use of the same techniques different results have been used to explain this phenomenon (Bottlang et al., 1999; Dichristina et al., 1996). Therefore AO/OTA groups, exploration and use of space to find new treatment methods have been mentioned. The principles used in the treatment of tibial fractures:

(1) Conservative treatment: The unallocated to allow for surgical treatment of fractures, or can be applied in the presence of local or systemic problems (Michelson et al., 2004).
(2) Surgical treatment: (i) Classic open reduction and internal fixation, (ii) Hybrid external fixation, (iii) Percutaneous plating, external fixation, (iv) External fixation and limited internal fixation, (v) Temporary external fixation and open reduction and internal fixation followed by known methods (Borrelli and Ellis 2002; Ebraheim et al., 2000; Fracture and Dislocation Compendium, 1996).

Be successful in the treatment of pilon fractures and

Figure 3. A 42-year-old male patient vehicle traffic accident in the first postoperative week, the front and side view of a partial skin necrosis.

Figure 4. After the operation the patient was started in the first month after the passive ankle range of motion exercises.

sufficient for the acquisition of the ankle joint surface anatomy of the function to be restored and the injured soft tissues should heal without complications (Sirkin and Sanders, 2001; Sirkin et al., 1999; Dickson et al., 2001) treatment planning pilon fractures sometimes dramatic situations can not occur below knee amputations, orthopedic surgeons have turned to the search for new solutions to protect the soft tissue (Scheck, 1965; Paley, 1990).

Though the classification presented by Ruedi and Allgower (1979) is still being used, we generally use AO/OTA classification today (Paley, 1990; Ruedi and Allgower, 1979). The AO long bone group universal classification of fractures groups distal tibia fractures as 43. The first sub-grouping is on the degree of continuity between diaphysis and metaphysis (Figure 5).

43A: Extra-articular – most would not recognise these as pilon fractures, although in some series non-articular fractures are included and it can be difficult to tell how many were articular.

43B: Partial articular fractures with some connection between part of the joint surface and the diaphysis - again, some series appear to include these but most do not clearly differentiate between them and those with complete separation between diaphysis and metaphysis. Posterior partial fracture overlap with malleolar fractures with posterior malleolar components (Klammer, 2013), and anterior partial fractures were included by Lauge-Hansen (1950) in his classification of malleolar fractures.

43C: Complete articular fractures with no connection between the joint surface and diaphysis – most pilon fractures fall into this group

Tibial pilon fractures treated by conventional methods in the literature complication rate of 0 to 36% have been reported by Akkaya and Okcu (2007). Described by AO/OTA conventional treatment, open reduction fibula, distal tibial articular surface reconstruction, bone grafting of the metaphyseal defect, and with the support plate includes support for the medial tibia (Bayraktar and Yücesir (2010). On the tibial metaphyseal region reductions need to occur when more soft tissue dissection and removal of the external fixation for stabilization of tibial diaphyseal widespread use, this situation, soft tissue tension and displacement of the soft tissue around the ankle and preventing deterioration of nutrition, infection and wound problems, such as severe reduced complications (Atesalp et al., 1999; Kim et al., 1997).

Pilon fractures, fracture stabilization with external fixation of the fracture addition, the metaphyseal region, especially broken fragments, with the reduction of the effect of soft tissue provides ligamentotaxis without stripping (Barbieri et al., 1996; Bourne, 1989). Ligamentotaxis is the period used to emphasize that, for traction to be effective it must be stable by counter traction provided by ligaments and soft tissue surrounding the main bone. The pull and the counter pull restore the length and fracture fragments, which are otherwise difficult to excellent control. This tissue tension can be maintained by external fixator or by a some distractor (Fitzpatrick et al., 1995; Treadwell and Fallat, 1994). Teeny

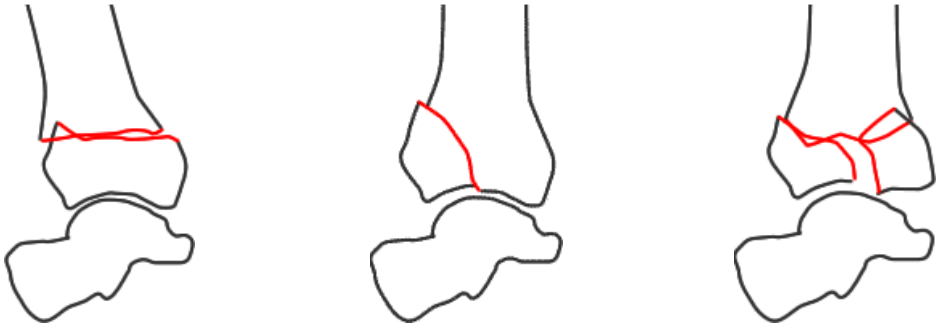

Figure 5. AO/OTA classification.

and Wiss (1993) AO/OTA come into contact with Type A and B fractures, but deep infection developed in 37% of Type C fractures reported (Watson et al., 2000). Depending on the type of soft tissue injury, the severity of fractures and fracture fixation, open reduction and limited open reduction with minimal-just treated with external fixation methods (Saleh et al., 1993; Blauthet al., 2001).

According to AO classification, complete-articular (Type C) fractures are treated with open reduction-minimal osteosynthesis nonunion, malunion, and wound complications than patients treated with external fixation method is much higher than reported (Kapukaya et al., 2005; Oh et al., 2003). Based on this information, the tibial pilon fractures in the region, especially the high-energy trauma, minimal soft tissue dissection and minimal use of material should be obvious (Helfet et al., 1997; Watson et al., 2000). 60% of cases (AO/OTA Type C) with the mechanism of high-energy trauma fractures have occurred, although infection, wound problems, post-surgical edema development of long-term complications, such as the amount of soft tissue is lower than the rate in the literature. This is just a series which this is due to the formation of the patients treated with articulated external fixation. Bonar and Marsh (1994) as well as to ensure ligamentotaxis unilateral external fixation in our application platform talus and calcaneus detected with separate schanz nails (Watson et al., 2000; Bonar and Marsh, 1994).

In our study of high-energy pilon fractures as a result of trauma patients, wound problems, reduce early range of motion, ensuring early return home and bed occupation in order to reduce their daily activities outside the three cases instead of open reduction and fixation with closed reduction and platform ankle and clinically applied method 72% of the cases' part of the results were good (Russell et al., 1991; Aktuğlu et al., 1998).

Conflict of Interests

The authors have not declared any conflict of interests.

REFERENCES

Akkaya MG, Okcu G (2007). Managmet of tibial pylon fractures. Turkiye Klinikleri J. Surg. Med. Sci. 3(39):76-90.

Aktuğlu K, Özsoy MH, Yensel U (1998). Treatment of displaced pylon fractures with circular external fixators of Ilizarov. Foot Ankle Int.19(4):208-216. http://dx.doi.org/10.1177/107110079801900404

Atesalp S, Koseoglu E, Demiralp PA (1999). [Tibial plafond fractures treated with the Ilizarov method.] In: Ege R, Antalya, Turkey, 3-7 (11):344-346.

Barbieri R, Schenk R, Koval K, Aurori K, Aurori B (1996). Hybrid external fixation in the treatment of tibial plafond fractures. Clin. Orthop. 332(11):16-22. http://dx.doi.org/10.1097/00003086-199611000-00004

Bayraktar B, Yücesir İ (2010). Athletic Injuries of Foot and Ankle and Their Treatment. Turkiye Klinikleri J PM & R-Special Topics. 3(2):69-77.

Blauth M, Bastian L, Krettek C, Knop C, Evans S (2001). Surgical options for the treatment of severe tibial pilon fractures: A study of three techniques. J. Orthop. Trauma. 15(3):153-160. http://dx.doi.org/10.1097/00005131-200103000-00002

Bonar SK, Marsh JL (1994). Tibial plafond fractures: Changing principles of treatment. J. Am. Acad. Orthop. Surg. 2(6):297-305.

Borrelli J Jr, Ellis E (2002). Pilon fractures: assessment and treatment. Orthop. Clin. North Am. 33(1):231-245. http://dx.doi.org/10.1016/S0030-5898(03)00082-8

Bottlang M, Marsh JL, Brown TD (1999). Articulated external fixation of the ankle: Minimizing motion resistance by accurate axis alignment. J. Biomech. 32(1):63-70. http://dx.doi.org/10.1016/S0021-9290(98)00143-2

Bourne RB (1989). Pilon fractures of the distal tibia. Clin. Orthop. 240(9):42-46.

Dichristina D, Riemer BL, Butterfield SL, Burke CJ (1996). 3rd. Pilon fractures treated with an articulated external fixator: A preliminary report. Orthopedics 19(12):1019-1024.

Dickson KF, Montgomery S, Field J (2001). High energy plafond fractures treated by a spanning external fixator initially and followed by a second stage open reduction internal fixation of the articular surface--preliminary report. Injury 32(Suppl 4):S92-S98. http://dx.doi.org/10.1016/S0020-1383(01)00163-2

Ebraheim N, Sabry FF, Mehalik JN (2000). Intraoperative imaging of the tibial plafond fracture: A potential pitfall. Foot Ankle Int. 21(1):67-72.

Fitzpatrick DC, Marsh JL, Brown TD (1995). Articulated external fixation of pilon fractures: The effects on ankle joint kinematics. J. Orthop. Trauma. 9(1):76-82. http://dx.doi.org/10.1097/00005131-199502000-00012

Helfet DL, Shonnard PY, Levine D, Borrelli J Jr (1997). Minimally invasive plate osteosynthesis of distal fractures of the tibia. Injury. 28(Suppl 1):S42-S47. http://dx.doi.org/10.1016/S0020-1383(97)90114-5

Kapukaya A, Subasi M, Arslan H (2005). Management of comminuted

closed tibial plafond fractures using circular external fixators. Acta Orthop. Belg. 71(5):582-589.
Kim HS, Jahng JS, Kim SS, Chun CH, Han HJ (1997). Treatment of tibial pilon fractures using ring fixators and arthroscopy. Clin. Orthop. 334(12):244-250.
Michelson J, Moskovitz P, Labropoulos P (2004). The nomenclature for intra-articular vertical impact fractures of the tibial plafond: Pilon versus pylon. Foot Ankle Int. 25(3):149-50.
Oh CW, Kyung HS, Park IH, Kim PT, Ihn JC (2003). Distal tibia metaphyseal fractures treated by percutaneous plate osteosynthesis. Clin. Orthop. Relat. Res. 408:286-91. http://dx.doi.org/10.1097/00003086-200303000-00038
Paley D (1990). Problems, obstacles, and complications of limb lengthening by the Ilizarov technique. Clin. Orthop. 250(12):81-104.
Ruedi TP, Allgower M (1979). The operative treatment of intraarticular fractures of the lower end of the tibia. Clin. Orthop. 138(5):105-110.
Russell TA, Taylor JC, Lavelle DG (1991). Fractures of the tibial plafond. In: Rockwood CA, Wilkins KE, King RE, editors. Fractures in adults. 3rd ed. New York: Lippincott. p. 1968-1972.
Saleh M, Shanahan MD, Fern ED (1993). Intra-articular fractures of the distal tibia: Surgical management by limited internal fixation and articulated distraction. Injury 24(1):37-40. http://dx.doi.org/10.1016/0020-1383(93)90081-G
Scheck M (1965). Treatment of comminuted distal tibial fractures by combined dual-pin fixation and limited open reduction. J. Bone Joint Surg. Am. 47(8):1537-1553.
Sirkin M, Sanders R (2001). The treatment of pilon fractures. Orthop. Clin. North Am. 32(1):91-102. http://dx.doi.org/10.1016/S0030-5898(05)70196-6
Sirkin M, Sanders R, DiPasquale T, Herscovici D Jr (1999). A staged protocol for soft tissue management in the treatment of complex pilon fractures. J. Orthop. Trauma. 13(2):78-84. http://dx.doi.org/10.1097/00005131-199902000-00002

academicJournals

Vol. 9(17), pp. 752-757, 15 September, 2014
DOI: 10.5897/SRE2014.5997
Article Number: 352632D47287
ISSN 1992-2248 © 2014

http://www.academicjournals.org/SRE

Scientific Research and Essays

Full Length Research Paper

Some multistep higher order iterative methods for non-linear equations

Nazir Ahmad Mir[1*] and Naila Rafiq[2]

[1]Department of Basic Sciences, Riphah International University, I-14 Islamabad, Pakistan.
[2]Centre for Advanced Studies in Pure and Applied Mathematics, Bahauddin Zakariya University, Multan, Pakistan.

Received 6 June, 2014; Accepted 20 August, 2014

We establish here new three and four-step iterative methods of convergence order seven and fourteen to find roots of non-linear equations. The new developed iterative methods are variants of Newton's method that use different approximations of first derivatives in terms of previously known function values, thus improving efficiency indices of the methods. The seventh and fourteenth order iterative methods use four and five function values including one derivative of a function. So, the efficiency indices of these methods are $\sqrt[4]{7} = 1.6265$ and $\sqrt[5]{14} = 1.6952$, respectively. Numerical examples are given to show the performance of described methods.

Key words: Non-linear equation, Iterative methods, convergence order, efficiency index.

INTRODUCTION

Newton's method is a well known and commonly used quadratically convergent iterative method for finding roots of non-linear equation:

$$f(x) = 0, \tag{1}$$

which is given by

$$x_{n+1} = x_n + \frac{f(x_n)}{f'(x_n)} \tag{2}$$

In recent years, researchers have made many modifications in this method to get higher order iterative methods. These methods are developed using various techniques by introducing some more steps to Newton's method. In this way, not only the convergence order but efficiency index of the method may also be increased (Chun, 2007; Mir and Rafiq, 2013; Osada, 1998; Potra and Ptak, 1984; Sharma, 2005).

Recently, the researchers introduced three-step iterative methods of convergence order seven to eight (Kou and Wang, 2007; Mir and Rafiq, 2014; Bi et al., 2009). Most recently, Neta and Petkovic (2010) introduced four-step iterative method of optimal convergence order sixteen for solving non-linear equations. In 2011, Sargolzaei and Soleymani (2011) introduced 4-step method of convergence order fourteen with five function evaluation and thus have efficiency index $\sqrt[5]{14} = 1.6952$. In 1981, Neta introduced 4-step method but did not prove its convergence order. In 2010

*Corresponding author. E-mail: nazirahmad.mir@gmail.com

Mathematics Subject Classification (2010): 65H05, 65B99.

(Geum and Kim, 2010) prove that the order of convergence of Neta's method is fourteen. To see more in this direction, we refer to Neta (1981), Sargolzaei and Soleymani (2011), Soleymani and Sharifi (2011).

Motivated in this direction, we also introduce here three-step and four-step iterative methods of convergence order seven and fourteen with efficiency indices, namely $\sqrt[4]{7} = 1.6265$ and $\sqrt[5]{14} = 1.6952$ respectively.

THE ITERATIVE METHODS

Consider two-step optimal convergent order four methods for solution of non-linear equation by Mir et al. (2013):

$$x_{n+1} = x_n - \{\alpha\boldsymbol{\mu}(x_n) + \beta\boldsymbol{v}(x_n)\}; for\ \alpha = -1, \beta = 2$$
$$x_{n+1} = x_n - \{\alpha\boldsymbol{\mu}(x_n) + \beta\boldsymbol{\psi}(x_n) + \gamma\boldsymbol{v}(x_n)\};$$
$$for\ \alpha = 1, \beta = 1, \gamma = -1$$

Where

$$\boldsymbol{\mu}(x_n) = \frac{f(x_n) + f(y_n)}{f'(x_n)},$$
$$\boldsymbol{v}(x_n) = \frac{f^2(x_n)}{f'(x_n)[f(x_n) - f(y_n)]},$$
$$\boldsymbol{\psi}(x_n) = \frac{f(x_n) + 2f(y_n)}{f(x_n) + f(y_n)}\frac{f(x_n)}{f'(x_n)}$$

and

$$y_n = x_n - \frac{f(x_n)}{f'(x_n)}.$$

At third step, we add Newton's method with an approximation of derivative $f'(z_n)$ from Mir et al. (2014) which is given by:

$$f'(z_n) = f[x_n, z_n] - f[x_n, y_n, z_n](x_n - z_n) \quad (3)$$

where $f[x_n, z_n]$ and $f[x_n, y_n, z_n]$ are the divided differences which are defined by:

$$f[x_n, z_n] = \frac{f(x_n) - f(z_n)}{x_n - z_n}$$

and

$$f[x_n, y_n, z_n] = \frac{f[x_n, y_n] - f[y_n, z_n]}{x_n - z_n}$$

We therefore propose the following three-step algorithms:

$$\begin{cases} y_n = x_n - \dfrac{f(x_n)}{f'(x_n)} \\ z_n = x_n - \dfrac{f(x_n)}{f'(x_n)}\left(\dfrac{2f(x_n)}{f(x_n) - f(y_n)} - \dfrac{f(x_n) + f(y_n)}{f'(x_n)}\right) \\ x_{n+1} = z_n - \dfrac{f(z_n)}{f[x_n, z_n] - f[x_n, y_n, z_n](x_n - z_n)} \end{cases} \quad (4)$$

and

$$\begin{cases} y_n = x_n - \dfrac{f(x_n)}{f'(x_n)} \\ y_n = x_n - \dfrac{f(x_n)}{f'(x_n)} * q \\ where\ q = \left(\dfrac{f(x_n) + f(y_n)}{f'(x_n)} + \dfrac{f(x_n) + 2f(y_n)}{f(x_n) + f(y_n)} - \dfrac{f(x_n)}{f(x_n) - f(y_n)}\right) \\ x_{n+1} = z_n - \dfrac{f(z_n)}{f[x_n, z_n] - f[x_n, y_n, z_n](x_n - z_n)} \end{cases} \quad (5)$$

We can further improve the efficiency indices of Methods (4) and (5) by adding Newton's method as one more step with the approximation of derivative $f'(w_n)$ which is given by

$$f'(w_n) = f[x_n, w_n] + (f[y_n, x_n, z_n] - f[y_n, x_n, w_n] - f[z_n, x_n, w_n])(x_n - w_n) \quad (6)$$

from Sargolzaei and Soleymani (2011) and Soleymani and Sharifi (2011) which increase just one function value. Thus, we propose the following four-step algorithms:

$$\begin{cases} y_n = x_n - \dfrac{f(x_n)}{f'(x_n)} \\ y_n = x_n - \dfrac{f(x_n)}{f'(x_n)}\left(\dfrac{2f(x_n)}{f(x_n) - f(y_n)} - \dfrac{f(x_n) + f(y_n)}{f'(x_n)}\right) \\ w_n = z_n - \dfrac{f(z_n)}{f[x_n, z_n] - f[x_n, y_n, z_n](x_n - z_n)} \\ x_{n+1} = w_n - \dfrac{f(w_n)}{f'(w_n)},\ where\ f'(w_n)\ is\ given\ by\ (6) \end{cases} \quad (7)$$

and

$$\begin{cases} y_n = x_n - \dfrac{f(x_n)}{f'(x_n)} \\ y_n = x_n - \dfrac{f(x_n)}{f'(x_n)} * q \\ where\ q = \left(\dfrac{f(x_n) + f(y_n)}{f'(x_n)} + \dfrac{f(x_n) + 2f(y_n)}{f(x_n) + f(y_n)} - \dfrac{f(x_n)}{f(x_n) - f(y_n)}\right) \\ w_n = z_n - \dfrac{f(z_n)}{f[x_n, z_n] - f[x_n, y_n, z_n](x_n - z_n)} \\ x_{n+1} = w_n - \dfrac{f(w_n)}{f'(w_n)},\ where\ f'(w_n)\ is\ given\ by\ (6) \end{cases} \quad (8)$$

Convergence analysis

We now use Maple 10.0 to derive error equations of the iterative methods described by Equations (4), (5), (7) and (8). We prove that the iterative Methods (4) and (5) are of convergence order seven and Methods (7) and (8) are of convergence order fourteen.

Theorem 1: Let $\omega \in I$ be a simple root of a sufficiently differentiable function $f: I \subseteq \mathbb{R} \to \mathbb{R}$ in an open interval I. If x_0 is sufficiently close to ω then the convergence order of three-step method described by (4) is seven and the error equation is given by:

$$e_{n+1} = c_3c_2(c_3c_2 - 3c_2^3)e_n^7 + O(e_n^8).$$

Proof: Let ω be a simple root of f and $x_n = \omega + e_n$. By Taylor's expansion, we have:

$$f(x_n) = f'(\omega)\left(e_n + c_2e_n^2 + c_3e_n^3 + c_4e_n^4 + c_5e_n^5 + c_6e_n^6\right) + O\left(e_n^7\right), \quad (9)$$

$$f'(x_n) = f'(\omega)\left(1 + 2c_2e_n + 3c_3e_n^2 + 4c_4e_n^3 + 5c_5e_n^4 + 6c_6e_n^5\right) + O(e_n^6), \quad (10)$$

where $c_k = \left(\frac{1}{k!}\right)\frac{f^{(k)}(\omega)}{f'(\omega)}$, $k = 2,3,\ldots$.

Substituting Equations (9) and (10) in Equation (4), we obtain:

$$y_n = \omega + c_2e_n^2 + \left(-2c_2^2 + 2c_3\right)e_n^3 - \left(7c_2c_3 - 4c_2^3 - 3c_4\right)e_n^4 + O\left(e_n^5\right). \quad (11)$$

Thus, using Taylor's series, we have:

$$f(y_n) = f'(\omega)\left(c_2e_n^2 + 2\left(c_3 - c_2^2\right)e_n^3 + \left(-7c_2c_3 + 3c_4 + 5c_2^3\right)e_n^4 + O(e_n^5)\right). \quad (12)$$

Substituting Equations (9), (10), (11) and (12) in Equation (4), we have:

$$z_n = \omega + (-c_2c_3 + 3c_2^3)e_n^4 + (-2c_3^2 - 18c_2^4 - 2c_2c_4 + 20c_3c_2^2)e_n^5 + (70c_2^5 - 130c_3c_2^3 - 7c_4c_3 - 3c_2c_5 + 42c_2c_3^2 + 30c_4c_2^2)e_n^6 + O\left(e_n^7\right). \quad (13)$$

Now, we expand $f(z_n)$ at ω using Taylor expansion:

$$f(z_n) = f'(\omega)((-c_2c_3 + 3c_2^3)e_n^4 + (-18c_2^4 + 20c_3c_2^2 - 2c_2c_4 - 2c_3^2)e_n^5 + (30c_4c_2^2 - 7c_4c_3 + 70c_2^5 - 3c_2c_5 + 42c_2c_3^2 - 130c_3c_2^3)e_n^6 + (18c_3c_5 - 16c_2^3c_4 - 16c_2^2c_5 + 12c_2c_6 - 2c_2^2c_3^2 + 152c_2^4c_3 + 10c_4^2 - 4c_7 - 52c_2c_4c_3 - 12c_3^3 - 92c_2^6)e_n^7) + O\left(e_n^8\right). \quad (14)$$

Using Taylor series, we have from Equation (4)

$$f'(z_n) = f'(\omega)(1 + c_2c_3e_n^3 - (6c_2^4 - c_2c_4 - 2c_3^2)e_n^4 + O\left(e_n^5\right)). \quad (15)$$

Further substituting (13), (14) and (15) in three-step method (4), we have:

$$x_{n+1} = \omega + c_3c_2(c_3c_2 - 3c_2^3)e_n^7 + O(e_n^8).$$

This implies,

$$e_{n+1} = c_3c_2(c_3c_2 - 3c_2^3)e_n^7 + O(e_n^8).$$

Hence, the theorem is proved.

Theorem 2: Let $\omega \in I$ be a simple root of a sufficiently differentiable function $f: I \subseteq \mathbb{R} \to \mathbb{R}$ in an open interval I. If x_0 is sufficiently close to ω then the convergence order of three-step method described by algorithm (5) is seven and the error equation is given by:

$$e_{n+1} = c_3c_2(c_3c_2 - 5c_2^3)e_n^7 + O(e_n^8).$$

Proof: Similar to Theorem 1.

Theorem 3: Let $\omega \in I$ be a simple root of a sufficiently differentiable function $f: I \subseteq \mathbb{R} \to \mathbb{R}$ in an open interval I. If x_0 is sufficiently close to ω then the convergence order of three-step method described by algorithm (7) has order of convergence fourteen and satisfy the error equation:

$$e_{n+1} = (b_7c_2a_4c_4)e_n^{14} + O(e_n^{15}),$$

where $a_4 = -c_2c_3 + 3c_2^3$ *and* $b_7 = -a_4c_2c_3$.

Proof: Let us consider the error Equation (13) as follows:

$$z_n = \omega + a_4e_n^4 + a_5e_n^5 + a_6e_n^6 + + a_7e_n^7 + O\left(e_n^8\right), \quad (16)$$

Where

$$a_4 = -c_2c_3 + 3c_2^3,$$
$$a_5 = 20c_3c_2^2 - 18c_2^4 - 2c_2c_4 - 2c_3^2,$$
$$a_6 = -130c_3c_2^3 - 3c_2c_5 + 30c_4c_2^2 + 42c_2c_3^2 - 7c_4c_3 + 70c_2^5,$$
$$a_7 = 18c_3c_5 - 16c_2^3c_4 - 16c_2^2c_5 + 12c_2c_6 - 2c_2^2c_3^2 + 152c_2^4c_3 + 10c_4^2 - 4c_7 - 52c_2c_4c_3 - 12c_3^3 - 92c_2^6$$

and $c_k = \left(\frac{1}{k!}\right)\frac{f^{(k)}(\omega)}{f'(\omega)}$, for $k = 2,3,\ldots$.

Now,

$$f(z_n) = f'(\omega)[a_4e_n^4 + a_5e_n^5 + a_6e_n^6 + + a_7e_n^7 + (a_8 + c_2a_4^2)e_n^8 + O\left(e_n^9\right)]. \quad (17)$$

From Equation (3):

$$f'(z_n) = f'(\omega)(1 - c_2c_3e_n^3 + (2c_3c_2^2 - c_2c_4 - 2c_3^2 + 2c_2a_4)e_n^4 + + O\left(e_n^5\right)).$$

Thus,

$$\frac{f(z_n)}{f'(z_n)} = a_4e_n^4 + a_5e_n^5 + a_6e_n^6 + (a_7 + c_2c_3a_4)e_n^7 + O\left(e_n^8\right) \quad (18)$$

Now, substituting Equations (16) and (18) in Equation (7), we get:

$$w_n = \omega - a_4c_2c_3e_n^7 + (-a_4c_2c_4 + 2a_4c_3c_2^2 - a_5c_2c_3 - 2a_4c_3^2 + c_2a_4^2)e_n^8 + (2c_2^2c_3a_5 - 2c_3^2a_5 - c_2c_3a_6 - c_2c_4a_5)e_n^9 + \ldots + O\left(e_n^{15}\right). \quad (19)$$

We rewrite the error Equation (19) as follows:

$$w_n = \omega + b_7e_n^7 + b_8e_n^8 + b_9e_n^9 + \ldots + O\left(e_n^{15}\right). \quad (20)$$

where $b_7 = -a_4c_2c_3$,
$b_8 = -2a_4c_3^2 + 2a_4c_3c_2^2 - a_5c_2c_3 - a_4c_2c_4 + c_2a_4^2$ and
$b_9 = -2c_3^2a_5 - c_2c_3a_6 + 2c_2^2c_3a_5 - c_2c_4a_5$

Now, by Taylor expansion,

$$f(w_n) = f'(\omega)[b_7e_n^7 + b_8e_n^8 + b_9e_n^9 + \ldots + O\left(e_n^{14}\right)]. \quad (21)$$

Substituting Equations (9-12), (16), (17), (20) and (21) in Equation (6), we have

$$f'(w_n) = f'(\omega)(1+(c_2a_4c_4+c_2b_7)e_n^7+O(e_n^8)). \quad (22)$$

Substituting Equations (20), (21) and (22) we have the following error equation for the four-step method (7):

$$x_{n+1} = \omega+(b_7c_2a_4c_4)e_n^{14}+O(e_n^{15}).$$

This implies $e_{n+1} = (b_7c_2a_4c_4)e_n^{14}+O(e_n^{15})$.

Theorem 4: Let $\omega \in I$ be a simple root of a sufficiently differentiable function $f:I \subseteq \mathbb{R} \to \mathbb{R}$ in an open interval I. If x_0 is sufficiently close to ω then the convergence order of three-step method described by algorithm (8) has order of convergence fourteen:

$$e_{n+1} = (b_7c_2a_4c_4)e_n^{14}+O(e_n^{15}),$$

$$where\ b_7 = c_3c_2(c_3c_2-5c_2^3)\ and\ a_4 = -c_2c_3+5c_2^3.$$

Proof: Similar to Theorem 3.

NUMERICAL EXAMPLES

Comparison of 7th order convergent methods

Now, we compare our seventh order convergent methods, namely MN_7-1 and MN_7-2 described by (4) and (5) respectively, with second order convergent Newton's method NW (11) sixth order convergent method (G6) Grau and Diaz-Barrero (2006) and seventh order convergent method (G7) Kou et al. (2007). The result of the numerical comparison of various methods is shown in Table 3 on the same number of function evaluations (TNFE=12), that is, on the third iteration with 350 significant digits and convergence criterion as follows:

$$|f(x_n)| < 10^{-300}.$$

Examples are taken from (Bi et al., 2009) which are used for comparison as follows (Table 1):

Comparison of 14th order methods

We compare our methods namely $MN_{14}-1$ and $MN_{14}-2$ described by (7) and (8) with Neta's fourteenth order method (N14) (1981) at the same number of function evaluations TNFE=12. The absolute values of the given test functions at first three iterations are given in Table 4. The computation is carried out with 2500 significant digits and with the following stopping criteria:

$$|f(x_n)| < \epsilon, \quad \text{where } \epsilon = 10^{-2450}$$

Table 1. Examples for 7th order methods.

Example	Roots
$f_1(x) = x^5+x^4+4x^2-15$	1.347428098968305
$f_2(x) = \sin x - x/3$	2.278862660075828
$f_3(x) = 10xe^{-x^2}-1$	1.679630610428450
$f_4(x) = \cos x - x$	0.7390851332151606
$f_5(x) = e^{-x^2+x+2}-1$	1.000000000000000
$f_6(x) = e^{-x}+\cos x$	1.746139530408012
$f_7(x) = ln(x^2+x+2)-x+1$	4.152590736757158
$f_8(x) = \sin^{-1}(x^2-1)-\frac{1}{2}x+1$	0.5948109683983692

Table 2. Examples for 14th order methods.

Example	Roots
$f_1(x) = e^x+x-20,$	$\omega \approx 2.8424389537844470...,$
$f_2(x) = \sqrt{x^2+2x+5}-2\sin x-x^2+3$	$\omega \approx 2.3319676558839640...,$
$f_3(x) = 2x\cos x+x-3,$	$\omega \approx -3.0346643069740450...,$
$f_4(x) = (x-1)^6-1$	$\omega = 2$

Here, we use the following test functions (Parviz and Soleymani, 2011) for comparison (Table 2). We observe that the numerical results are comparable or better in some cases.

Conclusion

In this article, we modified the existing methods of Mir et al. (2014) with the introduction of one and two steps more in such a way that the modified methods have improved convergence order that is, from fourth order to seventh order and then to fourteenth order as well as with their efficiencies improved. Modified methods are comparable and have better results as compared to the existing methods shown in Tables 3 and 4. The three-step methods are of seventh order convergent with four function evaluations per iteration and thus having computational efficiency $\sqrt[4]{7} = 1.6265$. The four-step methods are of fourteenth order convergent methods with five function evaluations per iteration and thus having computational efficiency $\sqrt[5]{14} = 1.6952$.

Conflict of Interest

The authors have not declared any conflict of interest.

Table 3. TNFE=Total number of function evaluation.

Comparison of 7th order methods on the same TNFE=12					
Example	**Methods**				
	NW	**G6**	**G7**	**MN_7-1**	**MN_7-2**
$f_1, x_0 = 1.6$	3.6e-39	8.2e-140	1.62e-216	1.3e-233	4.7e-321
$f_2, x_0 = 2.0$	4.20e-57	5.3e-166	1.14e-244	2.3e-315	2.3e-251
$f_3, x_0 = 1.8$	1.22e-57	9.3e-187	1.34e-281	4.7e-297	9.0e-264
$f_4, x_0 = 1.0$	3.00e-83	4.1e-237	0.0e+00	0.0e+00	0.0e+00
$f_5, x_0 = -0.5$	1.04e-26	3.28e-79	8.94e-118	1.9e-145	8.7e-135
$f_6, x_0 = 2.0$	9.24e-85	1.5e-233	1.29e-338	3.0e-350	3.0e-350
$f_7, x_0 = 3.2$	2.81e-74	1.0e-207	2.88e-312	1.0e-349	3.8e-343
$f_8, x_0 = 1.0$	1.78e-54	1.0e-165	1.30e-215	3.2e-269	1.6e-241

Table 4. TNFE=Total number of function evaluation.

Comparison of 14th order methods on the same TNFE=12				
Example	$\lvert f(x_n)\rvert$	**Methods**		
		N_{14}	$MN_{14}-1$	$MN_{14}-2$
$f_1, x_0 = 3.5$	$\lvert f_1(x_1)\rvert$	0.2e-6	1.0e-7	1.8e-7
	$\lvert f_1(x_2)\rvert$	0.4e-113	9.3e-119	4.4e-115
	$\lvert f_1(x_3)\rvert$	0.1e-1608	1.1e-1673	1.2e-1621
$f_2, x_0 = 0.5$	$\lvert f_2(x_1)\rvert$	0.1e-7	1.2e-8	2.5e-8
	$\lvert f_2(x_2)\rvert$	0.6e-124	1.5e-125	1.6e-121
	$\lvert f_2(x_3)\rvert$	0.3e-1751	2.8e-1762	4.9e-1760
$f_3, x_0 = -3.2$	$\lvert f_3(x_1)\rvert$	0.5e-3	4.6e-3	2.2e-1
	$\lvert f_3(x_2)\rvert$	0.3e-44	1.7e-33	8.0e-11
	$\lvert f_3(x_3)\rvert$	0.7e-621	1.5e-459	4.2e-142
$f_4, x_0 = 2.6$	$\lvert f_4(x_1)\rvert$	0.1	2.7e-2	5.0e-2
	$\lvert f_4(x_2)\rvert$	0.3e-16	1.6e-27	1.2e-23
	$\lvert f_4(x_3)\rvert$	0.3e-235	1.5e-380	5.9e-326

REFERENCES

Bi W, Ren H, Wu Q (2009). Three-step iterative methods with eighth order convergence for solving non-linear equations. J. Comput. Appl. Math. 225:105-112. http://dx.doi.org/10.1016/j.cam.2008.07.004

Chun C (2007). Some third-order families of iterative methods, methods for solving nonlinear equation, Appl. Math. Comput. 188:924-933. http://dx.doi.org/10.1016/j.amc.2006.10.043

Grau M, Diaz-Barrero JL (2006). An improvement to Ostrowski root-finding method. Appl. Math. Comput. 173: 450-456. http://dx.doi.org/10.1016/j.amc.2005.04.043

Kou J, Li Y, Wang X (2007).Some variants of Ostrowski's method with seventh-order convergence, J. Comput. Appl. Math. 209:153-159. http://dx.doi.org/10.1016/j.cam.2006.10.073

Mir NA, Rafiq N (2013). Some new efficient Iterative method for solving non-linear equations. WASJ 27(12):1664-1668.

Mir NA, Rafiq N (2014). Some families of three-step optimal convergent order iterative methods for solving non-linear equations. Accepted, Abstr. Anal. Appl.

Neta B (1981). On a family of multi-points methods for non-linear equations. Int. J. Comput. Math. 9:353-361. http://dx.doi.org/10.1080/00207168108803257

Neta B, Petkovic MS (2010). Construction of optimal order nonlinear solvers using inverse interpolation. Appl. Math. Comput. 217(6):2448–2455. http://dx.doi.org/10.1016/j.amc.2010.07.045

Osada N (1998). Improving the order of convergence of iterative functions. J. Comput. Appl. Math. 98:311-315. http://dx.doi.org/10.1016/S0377-0427(98)00131-9

Potra FA, Pták V (1984). Non discrete Induction and Iterative Processes, Research Notes in Mathematics, 103:, Pitman, Boston,

Sargolzaei P, Soleymani F (2011). Accuarte fourteenth-order method for solving non-linear equations. Numer. Algor. 58:513-527. http://dx.doi.org/10.1007/s11075-011-9467-4

Sharma JR (2005). A Composite third order Newton-Steffensen method for solving nonlinear equations. Appl. Math. Comput.169:242-246. http://dx.doi.org/10.1016/j.amc.2004.10.040

Soleymani F, Sharifi M (2011). On a class of fifteenth-order iterative formulas for simple roots. Int. Elect. J. Pure Appl. Math. 3(3):245-252.

academicJournals

Vol. 9(17), pp. 758-767, 15 September, 2014
DOI: 10.5897/SRE07.099
Article Number: F0B3C9047290
ISSN 1992-2248 © 2014

http://www.academicjournals.org/SRE

Scientific Research and Essays

Full Length Research Paper

Applying robust variance components models in the analyses of major gene effects within fragile X families

Latunji Charles A.

Cell Biology and Molecular Genetics Unit, Zoology Department, University of Ibadan, Ibadan, Nigeria.

Received 13 June, 2007; Accepted 11 February, 2011

The effect of the fragile X allele on ridge breadth, height and testicular volume was examined using robust statistical techniques for the data collected from 8 families from Ibadan, south west Nigeria, afflicted with this disorder. There is the presence of outliers, an estimated 6.5% for testicular volume and 1.3% for ridge breadth and height data respectively. It is shown that fragile X affects ridge breadth, height and testicular volume in a different manner. Fragile X women had a greater mean ridge breadth than normal women; a pattern similar to normal and fragile X men but the differences were not significant. Fragile X men were shorter than normal men, but no significant difference between the mean height of normal and fragile X women was observed. Whereas fragile X girls were shown to grow more quickly and to stop growth earlier than normal girls, normal women were taller than fragile X women. Testicular volume in fragile X boys continue in development long after normal boys have stopped; an observation that could explain the significant difference in means of adult males. An examination of the covariance between relatives classified according to fragile X status showed that for the three traits the influence of fragile X alleles was to reduce the covariance between parents and offspring, the effect of which produces a departure from an additive polygenic model of inheritance.

Key words: Fragile X allele, ridge breadth, testicular volume, single-gene disorder.

INTRODUCTION

Of one of the most frequent single-gene disorders recognised in humans, the fragile X is of particular interest and concern because it is one of the most frequent and it represents a wide spectrum of clinical manifestations including intellectual capability and physical defects (Garber et al., 2008; Kabakus et al., 2006). The molecular basis of fragile X has the form of an unstable CGG repeat within the “fragile X mental retardation” (FMR1) gene (Glover-Lopez and Guillen-Navarro, 2006; Verkerk et al., 1991). The expansion of this repeat beyond a particular threshold causes transcriptional suppression. The instability of the CGG repeat combined with other features of the fragile X genotype (Terracciano et al., 2005; Heitz, et al., 1992; Warren and Nelson, 1994) complicates the genotype-phenotype relationship in this condition. Extensive variability of clinical expressions between different families and particularly between different generations within a family could be observed because of the phenomenon of anticipation, that gradual deterioration of clinical status (Korneluk and Narang, 1997; Van Esch et al., 2005). If the effect of the unstable fragile X mutation on a quantitative trait is considered, simple descriptive procedures such as scatter plots, typically reveal a

E-mail: ca.latunji@ui.edu.ng. Tel: 234-8055200995.

number of outliers. The analysis of such data requires a methodology which is specifically tailored to handle data where data exist with extensively varying observations are the rule rather than the exception (Huggins and Loesch, 1995).

Concerning genetic and non-genetic effects on quantitative traits, there had been various hypotheses concerning testing a trait using maximum likelihood techniques under the assumption of multivariate normality. However, despite the fact that (Lange, 1978) has given theoretical justification of the assumption of multivariate normality for polygenic traits, it is relatively common that this assumption is violated (Huggins, 1993).

Huggins (1993) has developed a robustified likelihood procedure which supposes that the bulk of the data is multivariate normal with a proportion of contamination due to outliers, and that the analysis is only interested in modelling the central multivariate portion of the data. This differs from the procedures employed by other authors such as (White, 1982; Beaty, 1985; Royall, 1986) and those who obtained estimates which are robust against model misspecification, of the variance of the maximum likelihood estimates computed under the assumption of multivariate normality.

In the past, standard maximum likelihood methods were largely used to analyse data on some physical and intellectual measures in human pedigrees affected with fragile X (Loesch et al., 1992; Loesch et al., 1993).

Robust statistical methodology have previously been used by Huggins (1993) to derive a test for the detection of major gene effects in the presence of the fragile X mutation in the highly heritable polygenic trait, ridge count. A similar application on ridge breadth and height was also reported in Huggins and Loesch (1995). Here the use of pedigree data and the highly sophisticated statistical analysis was employed to eliminate the effect of the fragile X mutation on the means and variance components of height, ridge breadth and testicular volume in which averages of the ridge breadth and the testicular volumes were taken on the left and the right hands for ridge breadth, and bilaterally for testicular volume respectively. This approach fits models to the central multivariate central portion of the data and precludes the use of subjective screening procedures to determine if there is an atypical observation to be removed from the data sets.

These traits were chosen for the following reasons. Firstly, they were found to be affected in adult fragile X individuals by simple group comparisons (Loesch 1986; Loesch et al., 1988). Therefore, they can conveniently be used in the application of robustified likelihood procedures for the analysis of quantitative traits which are normally determined by a larger number of additive genes but which in abnormal conditions are modified by the effect of a gene mutation. Moreover the result of the analysis are of interest to biologists and clinicians as they contribute to a better understanding of the extent and of the pathomechanisms of growth abnormalities in fragile X.

MATERIALS AND METHODS

The data

Data was collated from a previous study on 8 African Negroid families living in south western Nigeria (Latunji, 2008). Data on two antropometric and one dermatoglyphic phenotypic traits for fragile X individuals and their participating relatives. Ridge breadth was estimated between two palmer interdigital triradii, a and b, by dividing the distance between these triradii by the number of ridges between them plus 1, as described in Huggins and Loesch' (1995)

Length (l) and width (w) of the testis was measured with a caliper and the volume (V) was calculated according to the formular $V= w^2l\pi/6$ (Mingroni-Netto et al., 1990). The average volume of the two testis per individual was taken.

A total of 78 individuals (31 males and 47 females) aged 8 to 78 years, participated in the study (Table 1). Measurements on ridge breadth and height were available from all while the males supplied the data on testicular volume. The composition of the data set by sex and fragile X status is given in Table 2. The number of individuals per pedigree upon which observations on height and ridge breadth is available ranged from 7 to 13 with an average of 9.75. The number per pedigree upon which observations on testicular volume is available ranged from 2 to 8 with an average of 3.88. The average number of generations per pedigree upon which observations on the three traits are available was 2.5.

Scatter plots of the values of ridge breadth in relation to palm width, height to age and testicular volume to age are given in Figures 1, 2 and 3 respectively.

Statistical methods

Robust estimates were computed according to (Huggins, 1993) who gave a similar modification of a log-likelihood which down weights outliers. Residuals were computed according to the methods of (Hopper and Mathews, 1982) but using robust rather than maximum likelihood estimates. If residuals larger than 2.3 are regarded as extreme outliers (that is, observations which are more than 2.3 standard deviations from their expected values) it is was then estimated that there were 1.3% extreme outliers in the ridge breadth data, 1.3% for height and 6.5% extreme outliers for testicular volume. The choice of 2.3 as the threshold for screening extreme outliers is somewhat arbitrary and perhaps conservative. However, it is pertinent for descriptive purposes, as under the multivariate normal model there is a probability of only 0.006 that any particular residual exceeds this amount. In particular under the multivariate normal model, the probability that 1.6% of the residuals in the height and ridge breadth data exceed 2.3 in absolute value is extremely small (0.003), and testicular volume data where 6.5% of these extreme outliers were observed respectively, the probability is far smaller.

Modelling the means

Means were modelled according to Loesch and Huggins (1995). This was based on the clear evidence that ridge breadth is linearly related to palm width in boys and girls but not in adults as observed from scatter plots. Motivated by these plots the model for mean ridge breadth (ridge breadth) was in the form of a regression on palm width for individuals less than 19 years old, and a mean for individuals aged greater than 19 years.

Table 1. Anthropocentric and dermatoglyphic data from the 8 pedigrees.

Pedigrees	Individuals	Palm width	Ridge	Age	Height volume	Testicular breadth
	I – I	7.7	525	38	1590.8	
	I – I*	9.6	580	61	1601.1	27.7
	II - I	7.4	473.1	37	1720	
	II – II*	7.3	495.1	35	1566.1	
	II – III*	8	540.1	48	1690	32.5
A	II – IV	7.2	490	42	1750.8	
	II – V*	9	505.1	40	1791.2	19.4
	II – VI*	5.8	473	13	1355	
	III – I**	7.8	550	17	1670	24.5
	III – II	5.9	518.1	15	1535	
	III – III*	5.5	531.3	12	1355.9	
	I – I*	8	530	61	1520	
	II – I*	9.4	550	39	1840	24.6
	II – II	7.4	475.5	30	1611	
	II – III	7.3	465	28	1551	
	II – IV	7.5	460.5	26	1423	
B	II – V	7.2	550.6	41	1453.7	
	II – VI*	6.2	500.4	51	1710.6	23.8
	III – I*	6.6	490.3	10	1290	15.9
	III – II**	5.6	520.9	13	1390.8	
	III – III	7	490.1	15	1500.9	26.3
	III – IV	6.9	510	18	1580	25
	I – I	7.6	528	46	1550	
	I – II	8.9	682.9	53	1610	25.9
	II – I	7.7	620.2	13	1416.1	
C	II – II**	7.4	513	15	1410.5	26.3
	II – III*	7.1	640.1	16	1485.2	
	II – IV*	7.7	594	16	1510.1	
	II – V	8.5	601.7	22	1473	
	I – I	7.7	498	58	1553.2	
	I – II	7.7	650.1	57	1600	25.4
	I – III	7.3	620.1	41	1580.1	
	I – IV*	6.8	560.6	51	1694	
D	II – I	5.6	420	24	1583	
	II – II*	7.6	575	20	1690.6	20.6
	II – III**	7.9	520	17	1650	28.1
	II – IV	8.2	575	21	1444	
	II – V*	6.7	500	12	1310.1	15.1
	I – I	7.7	540.1	54	1722.4	
	I – II	8.6	690	68	1598	27.6
E	I – III	8.4	475	29	1785.2	33.4
	II – I	7.9	450.5	26	1650.3	24.1
	II – II	7.5	605	48	1610.4	
	II – III*	9.3	680	55	1603.2	22.8
F	II – IV	8.5	575.3	20	1690	25.3
	II – V	7.9	510.8	16	1550.7	25.9

Table 1. Contd.

	II – VI	5.7	414.9	15	1555.1	
	III – I	6.6	665.5	14	1590.5	
	III – II	7.7	525.8	22	1551.1	
	III – III	8.2	560.3	18	1640	23.8
	III – IV**	7.4	571.2	26	1550.6	36.3
	I – I	8.6	622.8	60	1550.7	
	I – II	8.7	620.7	73	1753	25.3
	I – III	7.5	490.3	56	1555.2	
G	I - IV	7.8	520.1	62	1460.2	
	II – I**	8.7	582	30	1580.8	
	II – II	6.1	600.7	17	1550	
	II – III	6.8	590	14	1380.8	
	I – I	7.3	570.3	50	1521	
	I – II	8.8	610.9	58	1699	22.7
	II – I	6.5	503.1	8	1220.6	13.7
	II – II**	8.5	536.4	26	1595	
H	II – III	8	612.2	16	1475.4	
	II – IV	8.1	510.1	20	1473	
	II – V	6	625.6	44	1690.1	24.1
	II – VI	6.9	509.4	29	1561.4	
	II – VII	6.9	510	13	1551	16
	II – VIII	8.1	468	23	1765	
	I – I	6.6	490	32	1601	
	II – I	7.1	690	40	1691	
	II – II	9.4	660.6	44	1790	20.5
	II – III	7.2	495.5	30	1693.1	
I	II – IV	5.7	625	12	1355.3	
	II – V	7.1	610.4	16	1603.1	
	II – VI	7.8	506.6	18	1565.3	30.1
	III – I	6.2	625	18	1601.1	
	III – II	5.4	600.5	14	1370.9	
	III – III**	7.8	618	20	1650.2	

*Normal fragile X allele bearers; **Propositus.

Table 2. Composition of ridge breadth sample and height sample by sex and fragile X status.

Parameter	Normal	Fragile X	Total
Ridge Breadth			
Male	15	16	31
Female	17	30	47
Total	32	46	78
Height			
Male	15	16	31
Female	17	30	47
Total	32	46	78
Testicular volume			
Male	15	16	31

$\mu_{ridge\ breadth} = \{\square^{\mu adults'}/\alpha_{children} + \beta_{children}$ x palm width.

If age ≥=19 otherwise.

The parameters in this model were allowed to vary according to sex and fragile X status.

Modelling for height, the regression models are described as follows: $\mu_{height} = \{\square^{\mu adults'}/\mu_{children} + \theta$ age if age is greater than θ, otherwise, where again the parameters were allowed to vary with sex and fragile X status. It should be noted that in this model the parameter θ represents the age at which growth ends.

Modelling for testicular volume, the regression models are as follows: $\mu_{testicular\ volume} = \{\square^{\mu adults'}/\mu_{children} + \theta$ age) if age is greater than θ, otherwise, where again the parameters were allowed to vary with age and fragile X status.

Modelling the covariance

Two approaches were considered in modelling the covariance

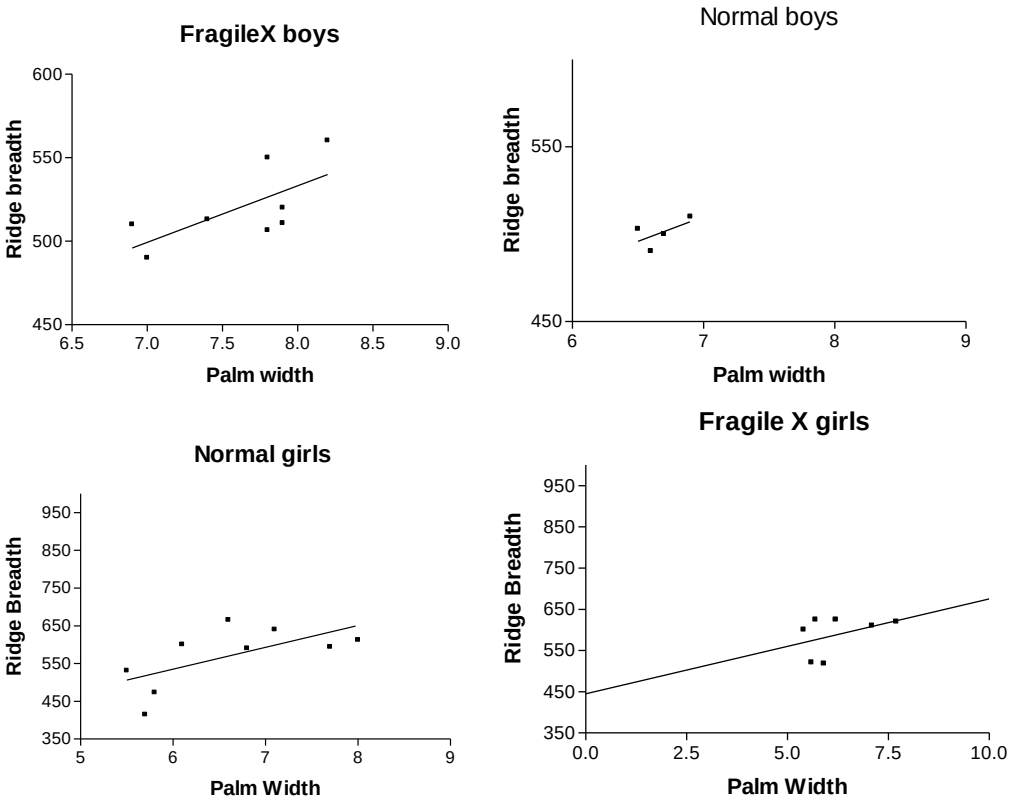

Figure 1. Scatter plots of ridge breadth against palm width in boys and girls.

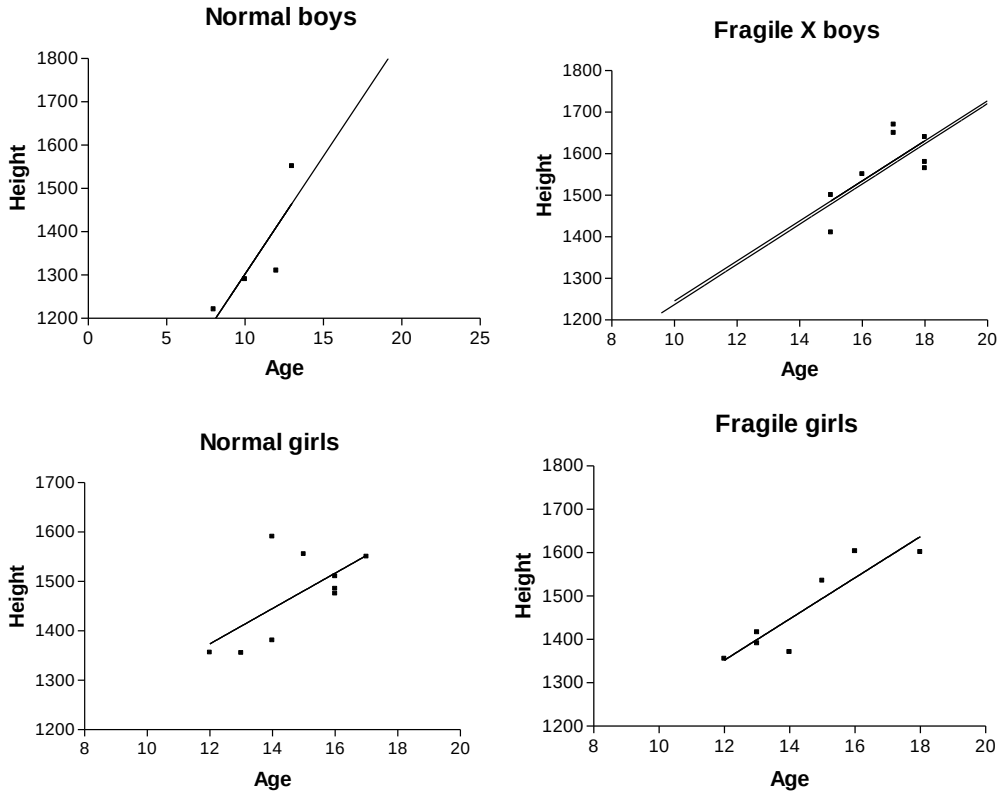

Figure 2. Scatter plots of height (mm) against age in boys and girls.

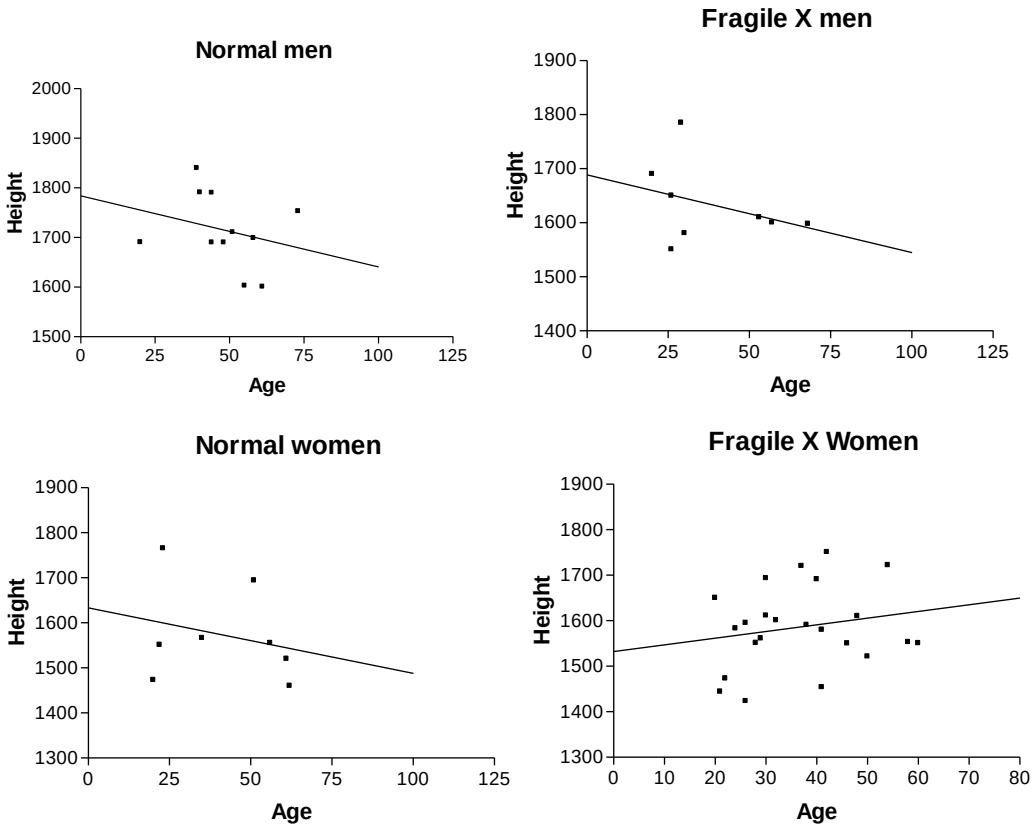

Figure 3. Scatter plots of height (mm) against age in men and women.

structures of the pedigrees according to Huggins and Loesch (1995). The first uses the models of Lange, (1978) and Hopper and Mathew (1982) which consider an additive genetic variance, a noon additive genetic or dominance variance, and the environmental variance. The second model considers phenotypic correlations between parent and offspring, between siblings, and between other relatives.

The basic model for the covariance matrix in the traits was $\Omega = 2\sigma^2_a\Phi + \sigma^2_d\Delta + \sigma^2_{ei}I$, where genetic variance included additive component, σ^2_a modelled using the kinship matrix denoted by $\Phi = (\phi_{i\ j})$ and dominance component, σ^2_d modelled using Jacquard's condensed coefficient of identity matrix, $\Delta = (\Delta i\ j)$. The environmental component in the covariance formula given above, σ^2_{ei}, represents individual environment. In order to take into account the common environment effects of siblings, which may be confounded with dominance variation, a dominance/common environment variance component σ^2_{dc} was considered rather than defining dominance as above, which replaced $\sigma^2_d\Delta_{i\ j}$ for siblings I and j.

A model for the covariance based on family relationships was also considered in order to examine possible deviations of this data from an additive model. In this model σ^2 denote the total variance, ρ_p denote the correlation between parent and offspring, ρ_s the correlation between siblings and ρ_o the correlation between other relatives. In order to take the extended family structure into account, ρ_o is taken to be the correlation between second degree relatives and the correlation between more distant relatives is taken to be $8 \times \rho_o \times \phi_{i\ j}$. The factor 8 was chosen as $\phi_{i\ j} = 1/8$ for second degree relatives such as grandparent and grandchild is ρ_o whilst that between third degree relatives such as cousins is $\rho_o/2$.

In this model, a difference between ρ_p and ρ_s suggest dominance deviation whilst a difference between ρ_p and $2 \times \rho_o$ suggest a correlation that is due to common family environment. Note that there could be many causes of observed difference between ρ_p and ρ_s , including non-genetic effects such as common sibling environment or a cohort effect. In order to establish if fragile X affects the values of correlations between relatives, the model was further extended by separating the correlations between normal pairs of relatives from pairs in which at least one individual is affected by fragile X.

The current data was analysed according to the application of these models and the resultant outcome is reported.

RESULTS

Ridge breadth

Based on the best fitting model, the robust estimates of parameters for the effect of fragile X and sex on the mean of ridge breadth are presented in Table 3. Tests involving intercepts and means are one sided whereas those concerning the slopes are two sided. It could be observed from the result in Table 3 that fragile X women have higher ridge breadth than normal and this similar trend exists for men although the difference is not statistically significant. Fragile X girls have higher intercepts than normal and fragile X boys show a contrast, there is no significant difference between fragile

Table 3. Robust estimate of the effect of age, sex and fragile X status on mean ridge breadth in adults and on the regression of mean ridge breadth on palm width (mm) on age in boys and girls.

Categories according to age, sex and fragile X status	Intercept (SE) $\alpha_{children}$	Regression (SE) $B_{children}$	Mean (SE) μ_{adults}
Normal men			586.2 (17.9)
Fragile X men			584.6 (31.4)
Normal boys	315.1 (184.1)	27.8 (27.6)	
Fragile X boys	262.4 (116.2)	33.9 (15.2)	
Normal women			512.5 (10.0)
Fragile X women			536.7 (13.3)
Normal girls	187.5 (176.1)	57.9 (26.5)	
Fragile X girls	445.3 (143.6)	23.0 (22.9)	

Table 4. Estimated variance component (a) and estimated total variance and correlations of ridge breadth between relatives with (bii) and without decomposition by fragile X status†.

a) Variance components		σ^2_e	σ^2_a	σ^2_{dc}
		3572.0 (59.8)	2767.0 (52.6)	3744 (61.2)
b) Pairs of relatives	Total variance σ^2	Parent-offspring ρ_p	Sibling-sibling ρ_s	Other ρ_o
bi) All	4309.0 (65.6)	0.32* (0.10)	0.004 (0.00)	0.35 (0.12)
bii) Normal-normal	4221.8 (65.0)	0.44 (0.19)	0.15 (0.02)	0.77**(0.59)
other	4541.0 (67.4)	0.27 (0.07)	0.17 (0.03)	0.24 (0.06)

† includes normal – normal, normal – fragile X and fragile X - fragile X siblings as other. *, ** P – values of comparisons are * < 0.01, ** <0.001

X and normal slopes for either sex.

The result of the covariance structure analysis showed that the genetic additive is significant (Table 4). This significance is explained by applying the simple variance component model to the pedigrees under study as shown in Table 4 by correlations between relatives. Equally significant correlations are observed in the parent-sibling pair and this is consistent with the model for additive inheritance (Table 4). In order to determine major fragile X gene influence, correlations were considered separately for normal-normal and for other pairs. Table 4 showed that, parent-offspring correlation is significantly greater than the value of sib – sib correlations and this is consistent with the additive inheritance model. The presence or absence of the fragile X cases in the pairings has minimal influence on parent-offspring and sib-sib correlations but a significant effect in other pairs of relatives in Tables. The value of normal other correlation is high in Table 4, indicating a significant contribution of the dominance component of covariance structure to the inheritance of ridge breadth in the pedigrees.

Height

The robust estimates of parameters for means of body height in fragile X individuals and their normal relatives are presented in Table 5. Fragile X men were shown to be significantly shorter than normal men. For women the reverse is the case, whereby fragile X women were taller than normal women, although the difference is not significant. The parameters of body height as a function of age showed that there is a statistically significant difference in the regression slopes between normal and fragile X boys although the cut-off age is clearly elevated in fragile X boys than in normal boys, growth in normal boys terminates about 4.2 years earlier than fragile X boys.

The results of fitting the covariance structure in Table 6 showed that genetic additive and environmental components of covariance are significant. The explanation for the presence of dominance in the covariance model for body height is sought by computing the correlations between relatives. As observed in the ridge breadth data, parent-offspring and sib-sib correlations are consistent with the additive model of inheritance, for all and normal pairs respectively. Therefore, it would appear from Table 6 that the additive effect of fragile X is the reduction of correlations observable when the pairings involve fragile X.

Testicular volume

The robust estimates of parameters for testicular volume in fragile X males and their normal male relatives presented in Table 7 show that testicular volume mean is

Table 5. Robust estimate of the effect of age, sex and fragile X status on mean height (in mm) in adults and on the regression of height (in mm) on age in boys and girls.

Categories according to age, sex and fragile X status	Regression (SE) $B_{children}$	Cut-off (SE) $\theta_{children}$	Adult mean (SE) $\mu_{children}$
Normal men			1714* (22.6)
Fragile X men			1633* (26.4)
Normal boys	54.5 (25.0)	14.6 (0.72)	
Fragile X boys	48.2* (19.2)	18.8 (0.44)	
Normal women			1573 (37.3)
Fragile X women			1581 (18.7)
Normal girls	35.6 (15.6)	18.0 (0.63)	
Fragile X girls	47.7** (9.98)	17.2 (0.37)	

*P < 0.05 for the comparison of the means and regression slopes. **P = 0.005.

Table 6. Estimated variance component (a) and Estimated Total Variance and Correlations of Height between Relatives With (bii) and Without Decomposition by Fragile X Status†.

a) Variance components		σ^2_e 16 642.9 (129.0)	σ^2_a 15682.8 (125.2)	σ^2_{dc} 14501.7 (120.4)
b) Pairs of relatives	Total variance σ^2	Parent-offspring ρ_p	Sibling-sibling ρ_s	Other ρ_o
bi) All	16029.6 (126.6)	0.40** (0.16)	0.59***(0.35)	0.18 (0.04)
bii) Normal-normal	25448.7 (159.5)	0.79***(0.62)	0.68** (0.46)	0.14 (0.02)
other	10265.5 (101.3)	0.36 (0.13)	0.40 (0.16)	0.14 (0.02)

† includes normal – normal, normal – fragile X and fragile X - fragile X siblings as other.*, ** P – values of comparisons are * < .01, ** <.001, *** < 0.0001

significantly greater in fragile X men than normal men. The parameters of testicular volume as a function of age showed that fragile X boys had higher intercepts than normal boys and this could be indicative of the differential observed in adults. This result is consistent with the clinical observation that orchidism is a frequent presentation in fragile X cases.

The results of fitting the covariance structure for the data presented in Table 8 showed contrast to the pattern observed in the ridge breadth and height data. In explaining the presence of significant dominance in the preferred model correlation computations among pairs of relatives reveal that parent-offspring correlations are significantly less than sib-sib correlations except in the normal pairings, thus producing deviation from a genetic additive model of inheritance. In order to examine if these observed effects are due to normal genes (or common sibling environment) or major fragile X gene, normal x normal and other pairs are considered separately. From the data in Table 7, it appears that for the normal pairs, parent offspring and sib-sib pairings are consistent with the additive model of inheritance, whereas fragile X causes the reduction of parent-offspring correlations.

DISCUSSION

The effect of fragile X on the mean values of one dermatoglyphic (ridge breadth), and two anthropometric (body height and testicular volume in males) measurements was demonstrated, where this effect is estimated against the background of the normal hereditary variations of these quantitative traits. The effectiveness of applying robustified likelihood function which simplifies the handling of outlying observations to the analysis of pedigrees was tested; particularly in this situation of small kindred, where sample size is not high.

The results of ridge breadth means and regressions confirmed the earlier findings of Huggins and Loesch (1995), based on simple comparisons between fragile X data and that of normal control samples which showed that fragile X individuals, especially female carriers have wider ridge breadth than the normal subjects (Loesch, 1986). The result of this analysis, which controlled for family factors and palm width, shows that fragile X has the effect of increasing ridge breadth. The effect of the expression of fragile X predominantly in females is at variance with the predicted model for the X-linked inheritance. It is possible that this observed increase in ridge breadth in females is due to the dosage effect of sex chromosomes on the value of this trait established in earlier studies (Penrose and Loesch, 1967), especially as the fragile X condition involves fluctuations in the magnitude of CGG repeats. On the other hand, the possibility of interplay of sex and genetic heterogeneity of the fragile X mutation cannot be exempted (Huggins and

Table 7. Robust estimate of the effect of age and fragile X status on mean testicular volume (in ml) in adults and on the regression of testicular volume (in ml) on age in boys.

Categories according to age, sex and fragile X status	Regression (SE) $B_{children}$	Cut-off (SE) $\theta_{children}$	Adult mean (SE) $\mu_{children}$
Normal men			24.0* (1.11)
Fragile X men			28.8* (1.60)
Normal boys	0.54 (0.30)	12.7 (0.88)	
Fragile X boys	0.47 (0.65)	23.7 (1.28)	

*P = 0.02.

Table 8. Estimated variance component (a) and estimated total variance and correlations of testicular volume between male relatives with (bii) and without decomposition by fragile X status†.

a) Variance components		σ^2_e	σ^2_a	σ^2_{dc}
		30.3 (5.50)	48.6 (7.00)	19.0 (4.36)
b) Pairs of relatives	Total variance σ^2	Parent-offspring ρ_p	Sibling-sibling ρ_s	Other ρ_o
bi) All	25.9 (5.09)	0.30 (0.09)	0.55* (0.30)	0.26 (0.07)
bii) Normal-normal	26.6 (5.16)	0.76**(0.58)	0.94**(0.89)	-0.74 (0.55)
other	11.7 (3.42	0.02 (0.00)	0.80* (0.63)	0.14 (0.02)

† Includes normal – normal, normal – fragile X and fragile X - fragile X siblings as other. *, ** P – values of comparisons are * < .01, ** <.001.

Loesch, 1995). In this case the mechanism of how the fragile X mutation leads to the specific characteristic of increase in dermal ridge breadth need to be fully understood if an acceptable explanation to be tenable. It is however inappropriate to draw any parallel between these two mechanisms from the existing data. In the height data, fragile X seem to have the effect of lowering body height in males. Similar trend observed in girls' height data is consistent with earlier studies. The reverse trend observed in adult females is not expected and may be attributable to cohort effect rather than a major indication. This is predicated on the observation of difference observed in the age cut-offs of girls, therefore implying that fragile X girls stop growing earlier than normal. It would appear from this data that boys grow at a lower, and the girls at a higher rate than their normal relatives and this is consistent with the earlier findings of Butler et al. (1992) and Huggins and Loesch (1995). The observation that growth in normal boys terminates about 4.2 years earlier than fragile X boys may not directly explain the observed differences in the means of adult mean. It could be concluded from this data that normal boys have a higher growth rate and therefore reach their peak body height earlier than fragile X boys. It was noted that even with 4.2 years extra growth the differential in mean height among adults giving an average increase of 4.2 × 54.7 = 228.9 mm is small compared to the adult mean differential of 81 mm. The observed significant difference in body height in adults may therefore be more related to growth rate rather than actual period of growth termination. Significant differences were observed in the slopes and cut-offs between normal and fragile X girls, which might be accountable for the differences observed in the adults.

However, to give more specific interpretation to these findings, the height as well bone age, need to be monitored longitudinally. And this would yield more accurate information on the growth pattern in relation to the onset, the rate, and the termination of skeletal maturity. An interesting aspect of the analysis applied in this study is that it allows for the estimation of the fragile X mutation on covariance between relatives as well as on the mean of the traits. Of interest is the observation that the fragile X alleles seem to lessen the contribution of the additive variance component in ridge breath, height and testicular volume, thus causing a deviation from the additive genetic model in contrast to the height and testicular volume data which tends toward an additive genetic model (Tables 6 and 8). Consequently the (narrow) heritability of height representing additive genetic effect based on the estimates of variance components is 0.50, which is appreciably lower than the values varying from 0.75 to 0.85 in other studies based on normal families (Tambs et al., 1992) and even lower than the narrow heritability of 0.58, deducible from the data of Huggins and Loesch (1995). Heritability for ridge breadth and testicular volumes are 0.55 and 0.43, 0.50 and 0.66 respectively. The author is not aware of any previous report on the heritability of testicular volume in fragile X pedigrees for comparison. Furthermore, by

separation of normal from other pairs of relatives, it was confirmed that the observed relative decline in the parent –offspring correlations may be largely attributed to a major fragile X gene in the three traits. It is probable that the effect of fragile X chromosome is caused by specific features of the abnormal gene containing the excessive number of the CGG triplet nucleotide repeats, which is further amplified in the offspring if transmitted trough the female (Glover-Lopez, 2006; Chiurazzi et al., 2003). This is what causes the anticipation phenomenon mentioned earlier whereby the severity of the fragile X increases in subsequent generations. Although the parent – offspring cohort effect may sufficiently explain the observed deviation from the perfectly additive model, it does not contradict the presence of male genetic dominance in body height postulated on the basis of the analysis of a large number of twins and their relatives (Tambs et al., 1992). However, using a relatively small samples as in the present study, and applying simple genetic models permitted the identification of large and obvious effects of such as those caused by abnormal genes. The results of this study emphasise the importance of identification of various types of effects in a family before drawing conclusions about the presence of genetic dominance in polygenic quantitative traits.

ACKNOWLEDGEMENTS

The author sincere thanks go to Dr. Hastings Ozwara of the Kenya National Museum for his contributions and support during the development of this manuscript. Same go to Tijmen Hilan for his accommodation and computer time at the initial part of data collation and analysis. Thanks to Edward, of Science journal (formally of the Biomedical primate research centre, Rijswijk, Netherlands, for the provision of graph pad prism software for scientific analysis.

REFERENCES

Beaty TH, Self SG, Liang KY, Connolly MA, Chase GA, Kwiterovich GO (1985). Use of robust variance component models to analyse triglyceride data in families. Ann. Hum. Genet. 49:315-328. http://dx.doi.org/10.1111/j.1469-1809.1985.tb01707.x

Butler MG, Brunschwig A, Miller LK, Hagerman RJ (1992) Standards for selected anthropometric measurements in males with the fragile X syndrome. Pediatr. 89:1059-1062.

Chiurazzi P, Neri G, Oostra BA (2003). Understanding the biological underpinnings of fragile X syndrome. Curr. Opin. Pediatr. 15(6):559-66. http://dx.doi.org/10.1097/00008480-200312000-00003

Garber KB, Visootsak J, Warren ST (2008). Fragile X syndrome. Eur. J. Hum. Genet. 16(6):666-72. http://dx.doi.org/10.1038/ejhg.2008.61

Glover-Lopez G, Guillen-Navarro E (2006). [Fragile X syndrome]. Rev Neurol. 42(Suppl 1):S51-4.

Heitz D, Devys D, Imbert G, Kretz C, Mandel JL (1992). Inheritance of the fragile X syndrome: size of the fragile X premutation is a major determinant of the transition to full mutation. J. Med. Genet. 29(11):794-801. http://dx.doi.org/10.1136/jmg.29.11.794

Hopper J, Mathews DL (1982). Extension to multivariate normal models for Pedigree analysis. Ann. Hum. Genet. 46:373-383. http://dx.doi.org/10.1111/j.1469-1809.1982.tb01588.x

Huggins RM (1993). On the robust analysis of pedigree data. Aust. J. Stat. 35:43-57. http://dx.doi.org/10.1111/j.1467-842X.1993.tb01311.x

Huggins RM, Loesch DZ (1995). Use of robust statistical methods to determine the effect of fragile X on means and variance components of a quantitative trait. Genet. Epidemiol. 12(3):279-90. http://dx.doi.org/10.1002/gepi.1370120305

Kabakus N, Aydin M, Akin H, Balci TA, Kurt A, Kekilli E (2006). Fragile X syndrome and cerebral perfusion abnormalities: Single-photon emission computed tomographic study. J. Child. Neurol. 21(12):1040-1046. http://dx.doi.org/10.1177/7010.2006.00230

Korneluk RG, Narang MA (1997). Anticipating anticipation. Nat. Genet. 15(2):119-120. http://dx.doi.org/10.1038/ng0297-119

Lange KL (1978). Central limit theorems for pedigrees. J. Math. Biol. 6:59-66. http://dx.doi.org/10.1007/BF02478517

Latunji CA (2008). Fragile X allelemorphism among the mentally retarded and in affected families. Sci. Res. Essays 4(10):1123-1131.

Loesch DZ (1986). Dermatoglyphic findings in fragile X syndrome: A causal hypothesis points to X-Y interchange. Ann Hum. Genet. 50(Pt 4):385-98. http://dx.doi.org/10.1111/j.1469-1809.1986.tb01759.x

Loesch DZ, Hay DA, Sheffield LJ (1992). Fragile X family with unusual digital and facial abnormalities, cleft lip and palate, and epilepsy. Am. J. Med. Genet. 44(5):543-50. http://dx.doi.org/10.1002/ajmg.1320440502

Loesch DZ, Huggins RM, Chin WF (1993). Effect of fragile X on physical and intellectual traits estimated by pedigree analysis. Am. J. Med. Genet. 46(4):415-422. http://dx.doi.org/10.1002/ajmg.1320460414

Loesch DZ, Lafranchi M, Scott D (1988). Anthropometry in Martin-Bell syndrome. Am. J. Med. Genet .30(1-2):149-164. http://dx.doi.org/10.1002/ajmg.1320300113

Mingroni-Netto RC, Rosenberg C, Vianna-Morgante AM, Pavanello Rde C (1990). Fragile X frequency in a mentally retarded population in Brazil. Am. J. Med. Genet. 35(1):22-27. http://dx.doi.org/10.1002/ajmg.1320350106

Penrose LS, Loesch DZ (1967). A study of dermal ridge width in the second (palmer) interdigital area with special reference to aneuploid states. J. Ment. Defic. Res. 11:36-42.

Royall RM (1986) Model robust confidence intervals using maximum likelihood estimators. Am. J. Hum. Genet. 50:1067-1076

Tambs K, Moum T, Eaves LJ, Neale MC, Midthjell K, Lund-Larsen PJ, Neass (1992). Genetic and environmental cotributions to the variance of the body height in a sample of first and second degree relatives. Am.J. Phys. Anthropol. 88:285-294. http://dx.doi.org/10.1002/ajpa.1330880303

Terracciano A, Chiurazzi P, Neri G (2005). Fragile X syndrome. Am. J. Med. Genet. C. Semin. Med. Genet. 137(1):32-37. http://dx.doi.org/10.1002/ajmg.c.30062

Van Esch H, Dom R, Bex D, Salden I, Caeckebeke J, Wibail A, Borghgraef M, Legius E, Fryns JP, Matthijs G (2005). Screening for FMR-1 premutations in 122 older Flemish males presenting with ataxia. Eur. J. Hum. Genet. 13(1):121-3. http://dx.doi.org/10.1038/sj.ejhg.5201312

Verkerk AJMH, Pieretti M, Sutcliffe JS, Fu Y-H, Kuhl DPA, Pizzuti A, Reiner O, Richards S, Victoria MF, Zhang F, Eussen BE, van Ommen G-JB, Blonden LAJ, Riggins GJ, Chastain JL, Kunst CB, Galjaard H, Caskey CT, Nelson DL, Oostra BA, Warren ST (1991). Identification of a gene (FMR-1) containing a CGG repeat coincident with a breakpoint cluster region exhibiting length variation in fragile X syndrome. Cell. 65(5):905-914. http://dx.doi.org/10.1016/0092-8674(91)90397-H

Warren ST, Nelson DL (1994). Advances in molecular analysis of fragile X syndrome. Jama 271(7):536-42. http://dx.doi.org/10.1001/jama.1994.03510310066040

White H (1982). Maximum likelihood estimation of misspecific models. Econometrica. 50:1-25. http://dx.doi.org/10.2307/1912526

academicJournals

Vol. 9(17), pp. 768-777, 15 September, 2014
DOI: 10.5897/SRE2013.5706
Article Number: FA29ACB47292
ISSN 1992-2248 © 2014

http://www.academicjournals.org/SRE

Scientific Research and Essays

Full Length Research Paper

Efficient tractor operation through satellite navigator

A. P. Magar[1], M. Singh[2], J. S. Mahal[3], P. K. Mishra[2]* , R. Kumar[2], K. Sharma[2] and A. Sharma[2]

[1]Central Institute of Agricultural Engineering, Bhopal, Madhya Pradesh, India.
[2]Department of Farm Machinery and Power Engineering, Punjab Agricultural University, Ludhiana-141004, India.
[3]Additional Director Research Engineering, Punjab Agricultural University, Ludhiana-141004, India.

Received 8 October, 2013; Accepted 8 September, 2014

A nine tyne tractor operated cultivator and spinner type fertilizer spreader were used to evaluate the efficiency of tractor. Tractor was operated without navigator and with navigator guidence to the operator to observe the missed area, overlapped area and actual productivity of the machines. Missing percentage was only 8.5% of total area cultivated in case of navigator assisted cultivator as comaperd to the 23.5% missed area without navigator guidence. For smaller field having area were 4.2 and 14% espectively of the total area under trials. But for larger area of 1.62 ha, on an average percentage missed area observed without and with navigator trials were 19.8 and 5.5% of the total area under trial. Overlapped area during cultivation without navigator was observed to be 0.042 or 18% as comaperd to the overlapped area of 0.006 ha or 3% by using navigator. Areas of overlap during fertilizer spreading for without and with navigator trials were observed to be 0.066 or 13.75% and 0.002 ha or 0.4% respectively for smaller fields. But for larger field, without navigator trial overlap of 0.027 ha which is 1.7% was obsereved and with navigator trial overlap was observed for area 0.048, which is 2.9% of total area of 1.62 ha. The actual productivity of the operation without navigator was 0.53 ha/h with 23.5% missing area as comapred to the actual productivity of cultivator with navigator i.e. 0.75 ha/h with 8.5% missing. It was concluded that actual productivity by using satellite navigator guided cultivator was 1.42 times more as compared to the actual productivity without navigator. During fertilizer spreading, the actual productivity of the spreader using navigator was 1.64 times more than the machine without naviagator. For larger field, satellite navigator guided fertilizer spreader was about having 1.37 times more productivity than spreader without navigator.

Key words: Satellite navigator, global positioning system (GPS), overlapped area, missed area, machine productivity, precision farming.

INTRODUCTION

Farm mechanization at every stage of crop production is playing a vital role in agriculture. Due to which, there is increase in yield and labour productivity over traditional agriculture. Skilled drivers are needed to operate tractor or combines efficiently. The requirement placed on farm equipment operators have changed drastically with increase in equipment size, power, multiple equipment functions, and speeds well as monitors reporting on

*Corresponding author. E-mail: pramod.btag@gmail.com, Tel: 7837243594.

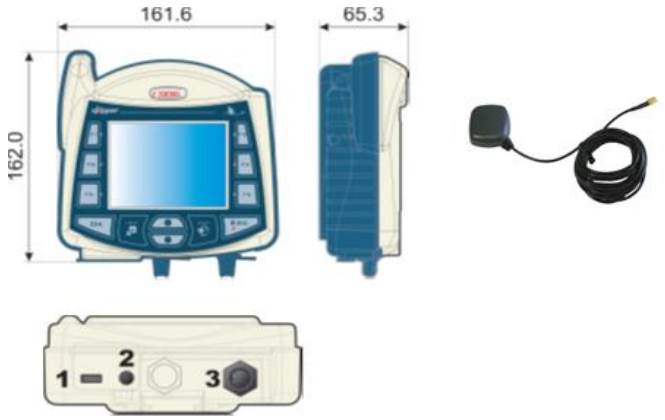

Figure 1. Satellite Navigator and GPS antenna (all the dimentions are in cm); Legends: 1-USB host port (pen drive etc.) ; 2-GPS antenna; 3-Power supply.

specific system performance. These increasing demands on the operator can result in increased errors in function, costs, environmental problems, and operator fatigue (Robert et al., 2009). Missed area after completion of work or repeat operation over the work already done that is, overlap decides work quality. Which is difficult to predict visually. To maintain the work quality one has to repeat the operation over the whole field. These causes an additional expenditure for the same quality of work over unit area. If these overlapping oprations are carried over the missing oprations rather than repeating the whole operation, so many inputs of the agriculture like fuel, labour, time etc. would be saved. Which mainly includes time-for which we are paying more than any other agricultural input. Also in farming work using agricultural vehicles such as tractors, it is important to minimize the area of unworked and double-worked land by driving the vehicle straight and at a constant interval in the field in order to achieve high efficiency and the optimum use of inputs such as fertilizers and chemicals (Yasuyuki et al., 2009).

In India, operator drives the tractor or combine harvester simply by their judgment. Due to which there may have missing or overlapped areas in the fields, resulting lesser productivity. Jatin et al. (2012) studied the Global Positioning System (GPS) for precise area measurement in the field. The author found GPS is very useful for the geo-referencing and to calculate the area harvested by combine harvester. In agriculture, better positioning combined with other spatial information permit significant reductions in use of fertilizer, pesticides and other environmentally sensitive chemicals. The error in area measured by GPS and actual ranged from 5.0 to 7.0%.

Tractors are sometimes fitted with navigator to increase the productivity of the machine. These navigator fitted tractor can be used for any operation performed by the tractor. Fulton et al. (1999) analysed a variable-rate spinner spreader, equipped with Differential Global Positioning System (DGPS) and a variable rate control system to assess its distribution accuracy. The authors found that the quality of the fertiliser application depends upon the accuracy of the guidance system used. Ehsani et al. (2002) studied important issues related to testing and comparing the guidance systems which they defined and explained, and a method of evaluating GPS guidance systems while following a straight line was introduced. According to their results, comparing the performance of the guidance systems with a real-time kinematic (RTK) GPS is the easiest method and probably the most accurate way of field-evaluating guidance systems. The advantage of this method is that it reflects the overall performance of a guidance system on the farm and the results can be used directly by the end user. According to Griffin (2009), the use of the guidance systems to guide the farm machines during their work on the field brings several benefits including the reduction in overlap, increased working speed during the field operations, workday expansion, and appropriate placement of spatially sensitive inputs. During recent years, many researchers studied different effects of using the guidance systems in view of accuracy, economical efficiency, etc. The use of the field guidance systems has some specific economical consequences, and therefore Griffin et al. (2008) and Griffin (2009) used a linear programming model to compare 5 types of the guidance system:

(1) A baseline scenario with foam, disk, or other visual marker reference,
(2) Lightbar navigation with basic GPS availability (+/–0.3 m accuracy),
(3) Lightbar with satellite subscription correction GPS (+/–0.1 m),
(4) Automated guidance with satellite subscription (+/–0.1 m),
(5) Automated guidance with a base station RTK GPS (+/–0.01 m).

The results obtained indicated that RTK automated guidance becomes the most profitable alternative when farm size is increased while maintaining the same equipment set. Owing to these facts, to save the operational time by avoiding repeat operation over the single pass, GPS Navigator was used to guide the tractor and analyzed the effect on seedbed preparation with nine tyne tractor drawn cultivator and fertilizer application using spinner type applicator.

METHODOLOGY

Satellite navigator

SKIPPER LT satellite navigator of ARAG, Italy (Figure 1) was used for navigation applications when connected to the external GPS antenna. As per the manufacturer, satellite navigator was designed and built in compliance with EN ISO 14982 standard

Figure 2. Satellite navigator fitted the tractor for without navigator and with navigator trial.

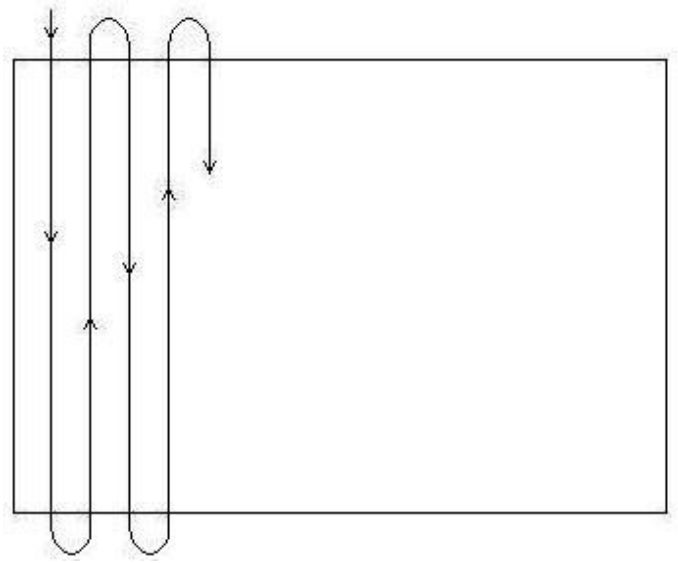

Figure 3. Straight parallel guidence pattern for Satellite navigator operation.

(Electromagnetic compatibility - Forestry and farming machines), harmonized with 2004/108/EC Directive. Satellite navigator mainly consists of navigator screen, of mounting bracket kit, power supply cable and GPS Antenna. Skipper LT navigator has the provision to save the various machine a configurations. After completion of job/desired operation, navigator saves the job automatically, the alternate name may be given manually if necessary. Machine setup mainly includes overall width of machine in operation and position of GPS antenna (antenna distance from the work point). To manage the saved data files in the navigator, satellite navigator manager software was provided by the firm.

Satellite navigator installation and connections

Installation of the satellite navigator was very simple. The navigator was supposed to fit on the body of tractors having low vibrations and shocks or away from moving parts of the tractors. The remote control unit should be in a visible position, without obstructing the operator's view, and within easy reach of the operator. Hence considering all these points satellite navigator was placed as shown in Figure 2. GPS antenna, as per the information manual of the firm, was to be installed on the highest point of the tractor. The roll over protective structure's frame served the base for the antenna. Having magnetic base, GPS antenna was easily get stuck to the place to receive the signals from satellite without much interruptions.

Connectons mainly include connection of the GPS antenna to navigator and battery connection of navigator with tractor battery for power supply. The electric power supply for satellite navigator was given from the tractor battery (12 Vdc). Positive and negative connections of the navigator were made as per the sign conventions given in information brochure of the GPS navigator. There are two available modes of guidence pattern in the satellite navigator i.e. one is in straight parallel (A-B pattern) and another in curved parallel. Because the plots were rectangular in shape, hence straight parallel (A-B pattern) guidence pattern was chosen for the operation (Figure 3). Observational data for without navigator and with navigator trials were simplified by using SKIPPER NAVIGATOR MANAGER software.

Field planning

Tillage

The seed bed preparation was done by using a conventional cultivator of width 9 x 30 cm in single pass operation by mlounting it with Massey Ferguson 5245 DI make tractor. To conduct experimental trails, the plots having dimention 55 x 36.4 m (Area 0.20 ha) were selected at the experimental farm of Punjab Agricultural University, Ludhiana, Punjab. Trails were conducted without navigator and with navigator guidance. Without navigator position, satellite navigator's display was kept out of eyesight of tractor opreator and operator was cultivating by traditional practice using cultivator. But with navigator, the machine operator was guided by the sattelite navigator. The satellite navigator was placed and fitted in front of trator operator, from where satellite navigator's functional keys were easily accessed by the operator. The operator had been oriented and trained the use of the navigator to drive the tractor along and over the reference lines displayed on the navigator's display. Operator was told to activate and deactivate working of cultivator by pressing the user option key of the satellite navigator while coming inside and going outside field boundries.

Fertilizer application

Multi-utility high clearance tractor (Singh et al., 2013) used for

Figure 4. High clearence tractor (HCT) with fertilizer spreader used for urea spreading.

Table 1. Observational data during seedbed preparation without navigator and with navigator.

Parameter	Without navigator	With navigator
Location of research plot	30.908464°N 75.817375°E	30.908489°N 75.817566°E
Area to be cultivated (ha)	0.20	0.20
Operating width of machine (m)	2.7	2.7
Position of GPS antenna from cultivator (m)	1.7	1.7
Visibility of navigator to operator	Not visible	Visible
Actual operation time, HH:MM:SS	00:22:43	00:16:01
Perimeter of the field (m)	175	175
Missed area of the field, ha (%)	0.047 (23.5%)	0.017 (8.5%)
Overlapped area, ha (%)	0.042 (21%)	0.006 (3%)
Actual productivity (ha/h)	0.53	0.75

% area's in the bracket were calculated with respect to the area to be worked that is, 0.20 ha.

mounting the fertilizer spreader to apply the fertilizer urea to paddy crop. Test trials were conducted for two fields of 0.48 and 1.62 ha areas having dimensions 60 x 80 m and 108 x 150 m respectively. Trails were conducted without guidence of satellite navigator and with navigator. Spinner type fertilizer spreader of Make Swan Agro Iindustry, Ludhiana was used for the trials. The fertilizer spreader having heavy duty gear box with combination of gears to absorb possible changes in power. There is a slitter lever, which allow to scatter only at left or right as per requirement. It distribute fertilizer evenly on each vane. Necessary setting of the control lever of spreader was done before the trials. Machine parameter includes mainly width of spread that is,12 m of fertilizer spreader (Figure 4) with fixed position of lever and constant rpm of tractor engine.

Selection of parametres

Three main parametres were selected to determine the efficiency of the navigator. These parameters were missed area, overlapped area and actual productivity of the tractor with machine. Missed area is the area, which was left without actual work done by the machine. Overlapped area was the area where more than once the desired operation was done by the machine. Actual productivity of the machine was effective work done per unit time, which was affected by the overlapped area and missed area. With more overlap area, productivity will be losses but with more missed area, productivity will also be more.

RESULTS AND DISCUSSION

Field observations without navigator and with navigator trial, for the nine tyne cultivator and fertilizer applicator are tabulated in Tables 1, 2 and 3. Actual field conditions showing missed area, overlapped area and headland area during cultivation and fertilizer application with and

Table 2. Observational data during ferilizer spreading without and with navigator for field 1.

Experimental parameter	Without navigator	With navigator
Location of research plot	30.900816°N 75.815544°E	30.908442°N 75.817215°E
Area to be fertilized (ha)	0.48	0.48
Spread width of machine (m)	12	12
Position of GPS from delivery of spreader (m)	2.5	2.5
Visibility of navigator to operator	Not visible	Visible
Fertilizer spreader delivery setting to maintain recommended Urea rate of 112 kg/ha	2	2
Spreading time, HH:MM:SS	00:07:11	00:04:23
Missed area of the field (ha)	0.020 (4.2%)	0.067 (14%)
Overlapped area (ha)	0.066 (13.75%)	0.002 (0.42%)
Actual productivity (ha/h)	4.01	6.57

Table 3. Observational data during ferilizer application without and with navigator field 2.

Experimental parameter	Without navigator		With navigator	
	R1	R2	R1	R2
Location of research plot: Latitude; Longitude	30.900078°N 75.816559°E	30.900690°N 75.815010°E	30.900690°N 75.815010°E	30.900743°N 75.815025°E
Area to be fertilized (ha)	1.62	1.62	1.62	1.62
Spread width of machine (m)	12	12	12	12
Position of GPS from delivery of spreader (m)	2.5	2.5	2.5	2.5
Visibility of navigator to operator	Not visible	Not visible	Visible	Visible
Fertilizer spreader delivery setting to maintain recommended urea rate of 112 kg/ha	2	2	2	2
Spreading time, HH:MM:SS	00:21:27	00:13:29	00:10:48	00:13:53
Missed area of the field, ha (%)	0.275 (16.97%)	0.366 (22.59%)	0.084 (5.18%)	0.094 (5.8%)
Overlapped area, ha (%)	0.027 (1.7%)	00	0.046 (2.8%)	0.050(3.1%)
Actual productivity (ha/h)	4.5	7.2	9	7

without navigator are shown in Figures 5 to 12. Next is a detail discussion of these areas.

Missed area

Tillage

Missed area is the sum of all the missed areas observed during the cultivator operation. Figure 6 shows missed area in both the cases and data values are tabulated in Table 1. Out of the targeted area that is, 0.20 ha to be cultivated 0.047 and 0.017 ha area were missed or not cultivated without navigator and with navigator trials. It is clear that missing percentage is only 8.5% of total area cultivated in case of navigator assisted machinery as compared to the 23.5% missed area without navigator guidence. Tractor operator/driver also got physical relief assisted by the use of navigator to some extent which would be helpful to do more work per unit time.

Fertilizer application

Tables 2 and 3 shows the missing areas without and with navigator trials. Out of the targeted area that is, 0.48 ha for field no.1, about 0.020 and 0.067 ha areas were missed or no urea was spreaded without navigator and with navigator trials, which was 4.2 and 14% espectively of the total area under trials (Figure 7). More missing in crop with navigator may be due to the ignorance of operator to navigator signal. For field no. 2 having total area of 1.62 ha, 0.320 ha area was missed without navigator as compared to only 0.089 ha missed area with the use of navigator. On an average percentage missed area observed without navigator and with navigator trials were 19.8 and 5.5% of the total area under trials. About 20% area, where there is no fertilizer spreaded is

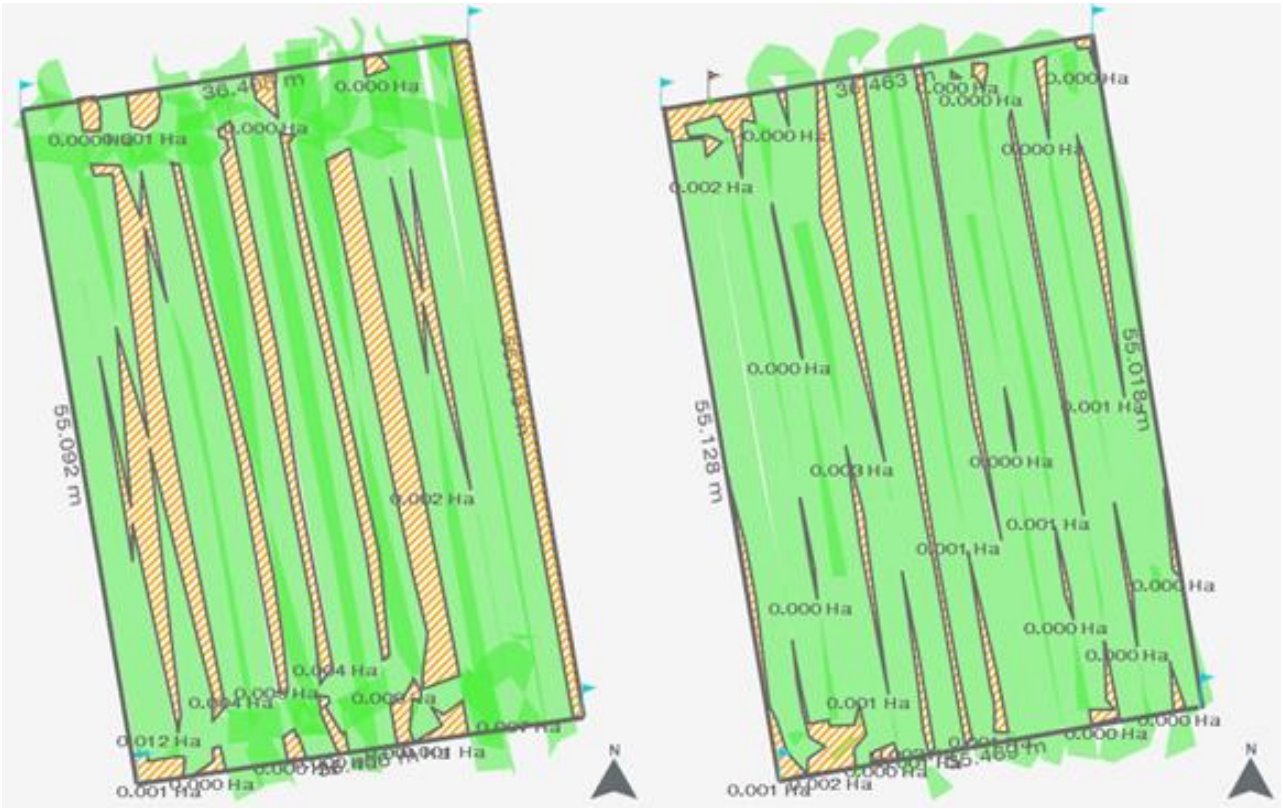

Figure 5. Missed area in cultivator working: (a) Without navigator (b) With navigator.

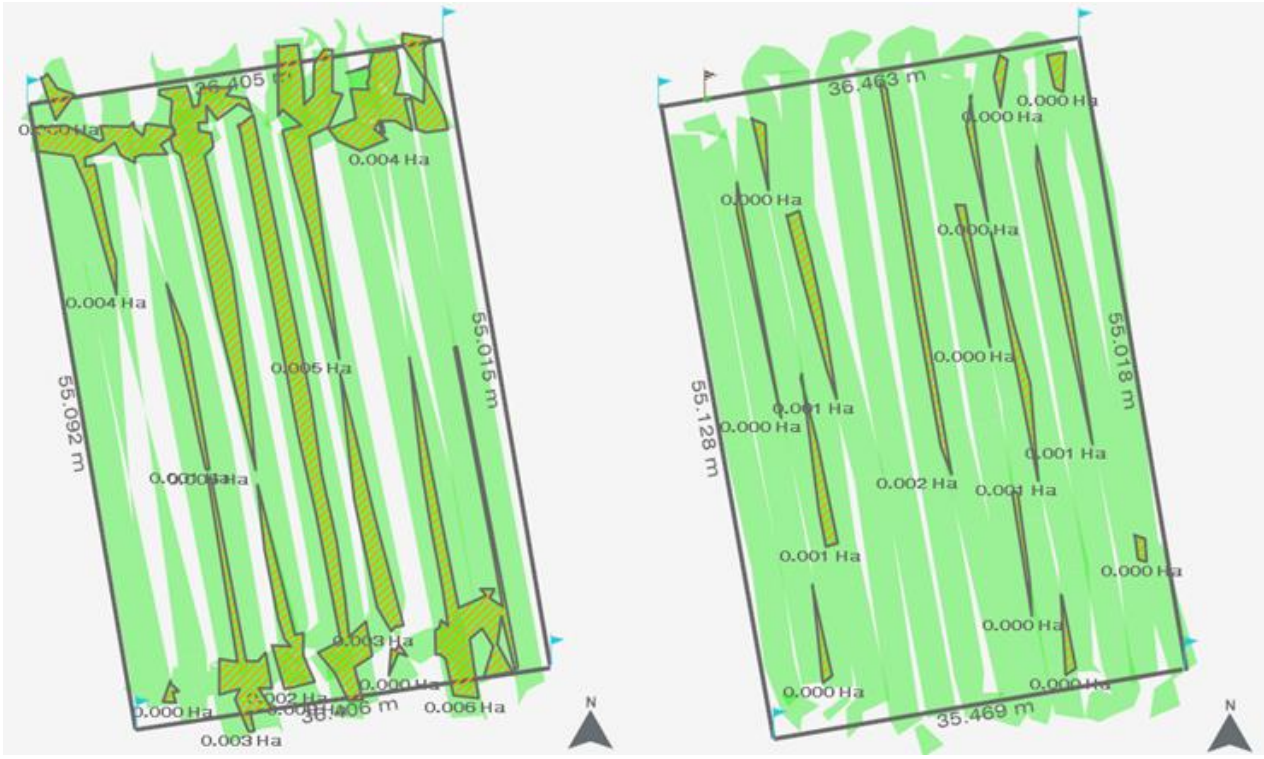

Figure 6. Overlapped area in cultivator working: (a) Without navigator (b)With navigator.

Figure 7. Missed area in fertilizer spreader for Field No. 1 (a) Without navigator (b) With navigaor.

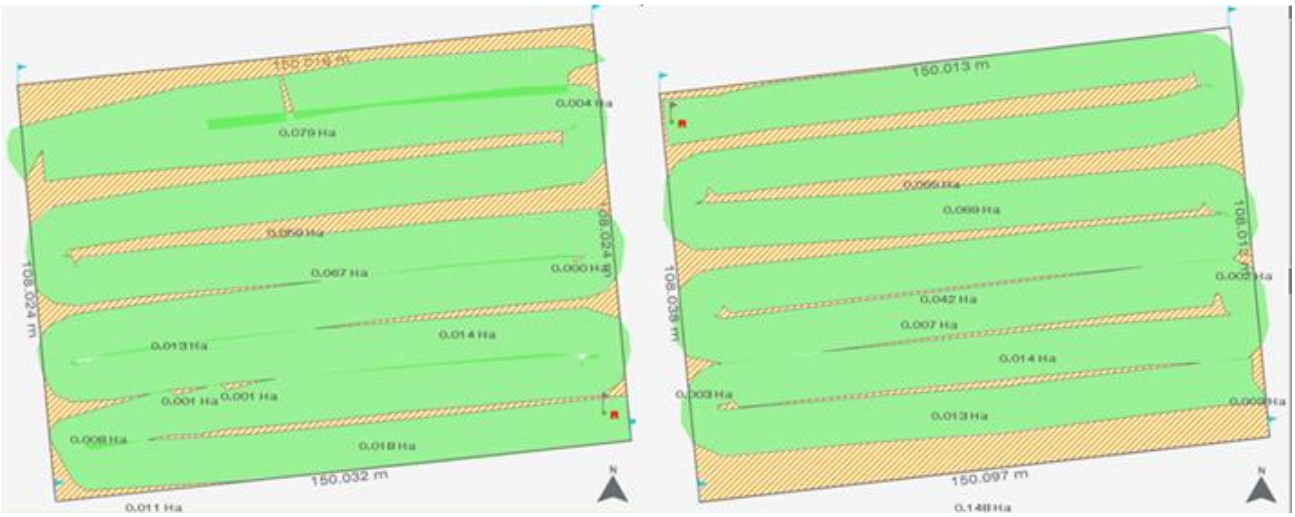

R1 **R2**

Figure 8. Missed area without navigator fertilizer spreader for field no. 2.

considerable area that may affect the yield of crop significantly.

Overlappped area

Tillage

Same operation performed more than once over the same area is termed as overlap. Figure 6 shows the field view showing overlapped area for both the cases of seedbed preparation. Gross values of overlap area without navigator and with navigator trial were observed to be 0.042 and 0.006 ha respectively. It means the overlapped area was only 3% by using navigator as compared to the 18% area overlapped without using navigator.

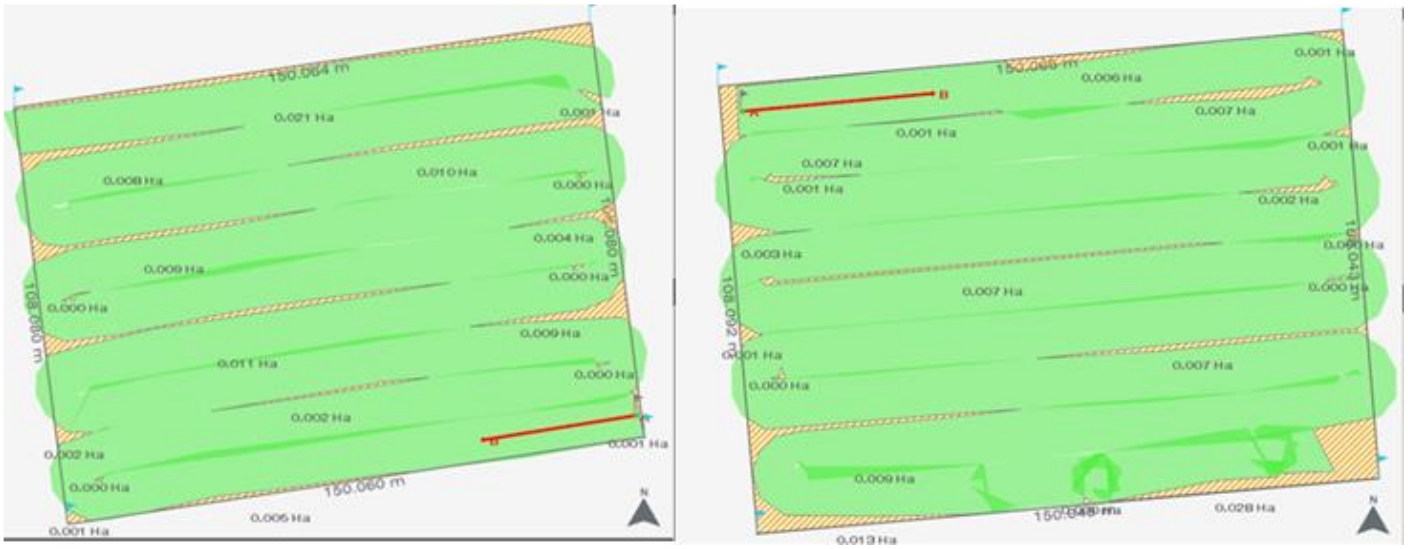

Figure 9. Missed area with navigator fertilizer spreader in field no. 2.

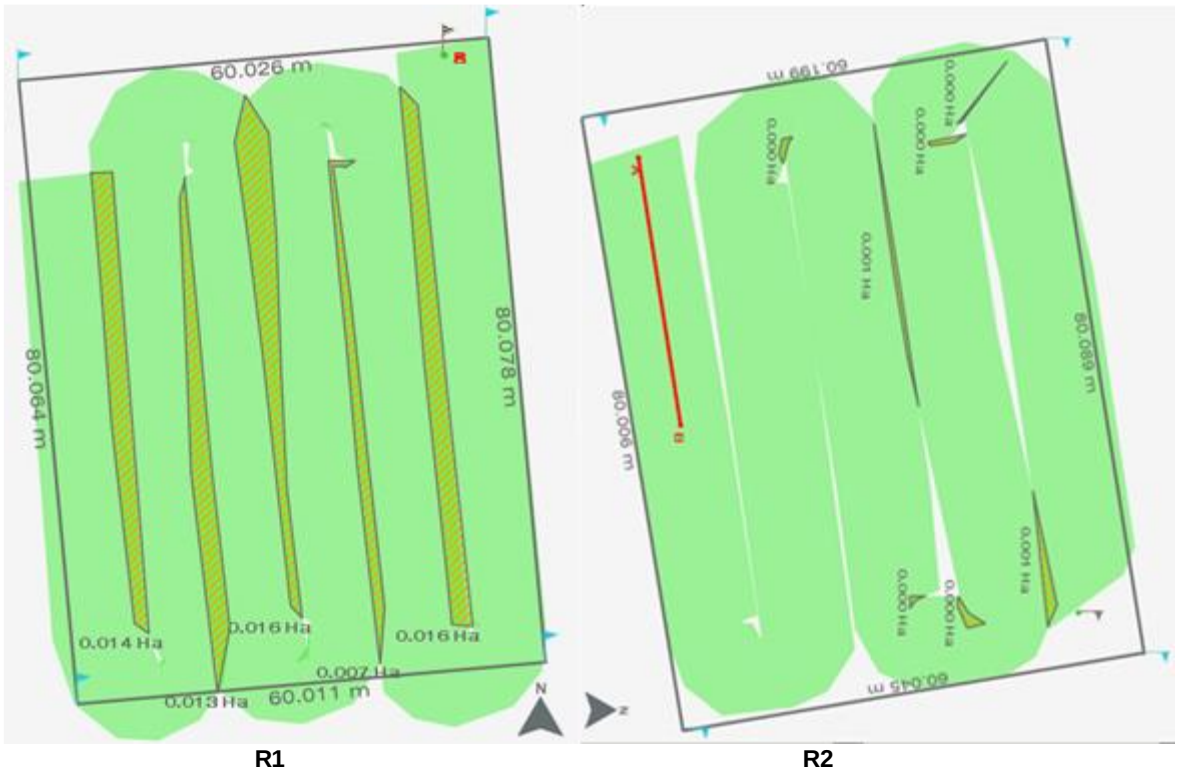

Figure 10. Overlapped areaby fertilizer spreader in field no. 1 (a) Without navigator (b) Without naviagator.

Fertilizer application

To cover the width of 60 m, machine without navigator made 6 strips instead of 5 strips. Hence, areas of overlap without navigator and with navigator trials were observed to be 0.066 or 13.75% and 0.002 ha or 0.4% respectively. It means, about 14% of the fertilizer may be saved by using navigator. The overdose of fertilizer may lead unacceptable long-term retention of chemical components results in environment degradation. Overlap

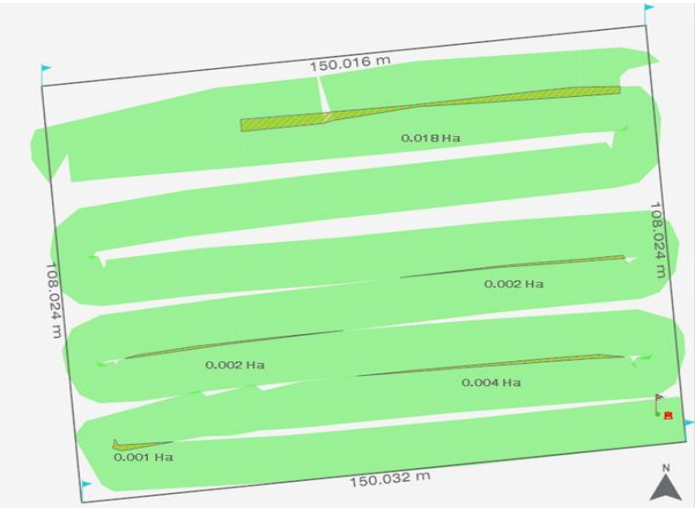

Figure 11. Overlapped area without navigator fertilizer spreader in field no. 1.

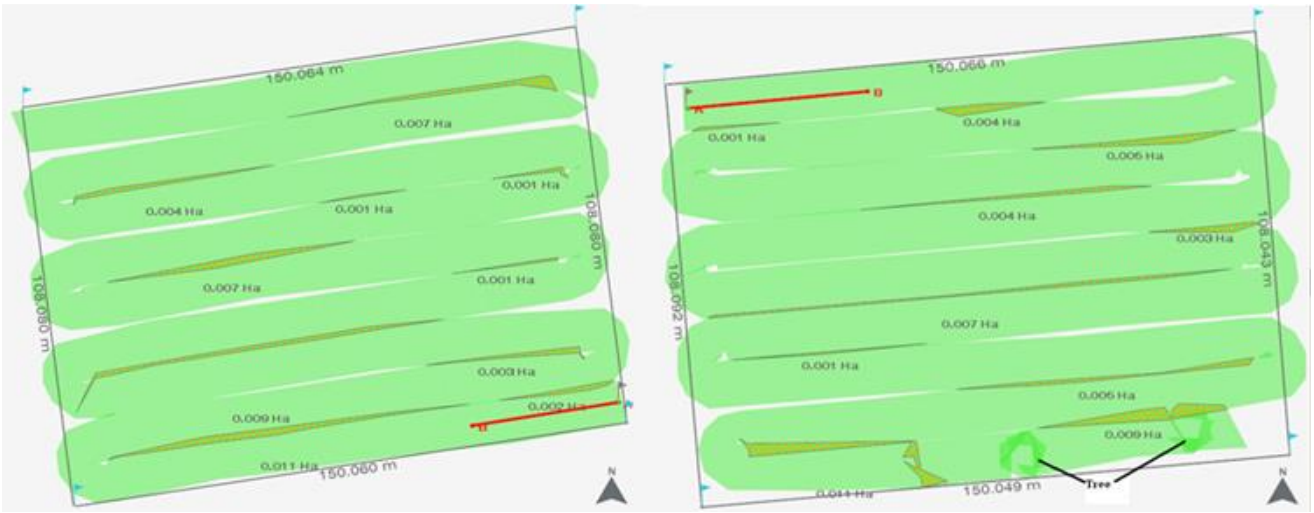

R1 **R2**

Figure 12. Overlapped area with navigator fertilizer spreader in field no. 2.

of 0.027 ha was obsereved without navigator trial for field no. 2 having area of 1.62 ha. In case of with navigator trial overlaps were observed for area 0.048 ha, which is 2.9% of targeted area of 1.62 ha. All the areas of overlaps were almost along the strips and also distributed over entire field uniformly.

Actual productivity

Tillage

Actual productivity is the effective worked area per unit time. Effective worked area is the cultivated area within the predefined boundry of the field. To calculate effective worked area, missed area was deducted from the targeted area that is, 0.2 ha. Without navigator and with navigator trials, effective worked areas were 0.158 and 0.183 ha respectively. Time taken to complete these trials were 22:43 and 16:01 min without navigator and with navigator, in which considerable time that is, 06:42 min (33.75 min per ha) were saved with navigator as comapred to without navigator trial. These effective worked areas per unit time are actual field capacities of the machine in both the cases which includes 23.5 and 8.5% missed area. Hence, various time based agricultural inputs like fuel, labor etc required to cultivate

the field can be calculated which were saved by using navigator. The actual productivity of the machine without navigator was 0.53 ha/h, whereas actual productivity of the machine with navigator was 0.75 ha/h. Hence, it can be concluded that actual productivity by using satellite navigator guided cultivator was 1.42 times more as compared to the actual productivity without navigator.

Fertilizer application

For field no. 1, 07:11 and 04:23 min were required to apply the urea over 0.48 ha without and with navigator. The actual productivity was 4.01 and 6.58 ha/h without navigator and with navigator respectively. The actual productivity of the spreader using navigator was 1.64 times more than the machine without naviagator. For field no. 2, average time required without navigator and with navigator trials were 17:28 and 12:20 min to spread urea over an average effective areas of 1.3 and 1.53 ha respectively. On an average actual productivities without navigator and with navigator were calculated to be 5.85 and 8 ha/h respectivitly. Satellite navigator guided fertilizer spreader was having 1.37 times more productivity than spreader without navigator.

Conclusions

(1) Missing percentage was only 8.5% of total area cultivated in case of navigator assisted machinery as comaperd to the 23.5% missed area without navigator guidence.
(2) For smaller field having area of 0.48 ha, the missed area or where no urea was spreaded without navigator and with navigator trials were 4.2 and 14% espectively of the total area under trials. But for larger arae of 1.62 ha, on an average percentage missed area observed without navigator and with navigator trials were 19.8 and 5.5 per cent of the total area under trial.
(3) Overlapped area during cultivation without navigator was observed to be 0.042 or 18% as comaperd to the area of 0.006 ha or 3% by using navigator.
(4) Areas of overlap during fertilizer application without navigator and with navigator trials were observed to be 0.066 or 13.75% and 0.002 ha or 0.4% respectively for smaller fields. But for larger field, without navigator trial overlap of 0.027 ha was obsereved and with navigator trial overlaps were observed for area 0.048, which is 2.9% of total area of 1.62 ha.
(5) The actual productivity of the cultivator without navigator was 0.53 ha/h whereas actual productivity of the machine with navigator was 0.75 ha/h. Hence, it can be concluded that actual productivity by using satellite navigator guided cultivator was 1.42 times more and 15% lesser missing as compared to the actual productivity without navigator.
(6) For smaller field, actual productivity was 4.01 and 6.58 ha/h without navigator and with navigator respectively. The actual productivity of the spreader using navigator was 1.64 times more but also with more missing than the machine without naviagator.
(7) For larger field, on an average actual productivities without navigator and with navigator were calculated to be 5.85 and 8 ha/h. Satellite navigator guided fertilizer spreader was having 1.37 times more productivity than spreader without navigator.

Conflict of Interest

The authors have not declared any conflict of interest.

REFERENCES

Ehsani MR, Sullivan M, Walker JT, Zimmerman TL (2002). A Method of Evaluating Different Guidance Systems. St. Joseph, ASAE Paper No. 021155.
Fulton JP, Shearer SA, Chabra G, Higgins SG (1999). Field Evaluation of a Spinner Disc Variable-Rate Fertilizer Applicator. Toronto, ASAE Paper No. 991101.
Griffin T (2009). Whole-farm Benefits of GPS-enabled Navigation Technologies. St. Joseph, ASABE.
Griffin TW, Lambert DM, Lowenberg J, Deboer (2008). Economics of GPS-enabled navigation technologies. In: Proceedings of the 9th International Conference on Preci¬sion Agriculture, July 21–23, 2008. Denver, USA.
Jatin, Singh M, Sharma A (2012). Global Positioning System for Precise Area Measurement in the Field. AET 36(1):1- 4.
Robert G, Alley M, Wysorand WG, Groover G (2009). Precision Farming Tools: GPS Navigation. Publication 442-501, Produced by Communications and Marketing, College of Agriculture and Life Sciences, Virginia Polytechnic Institute and State University.
Singh M, Das G, Sharma A, Patil RN (2013). A Technical and Analytical Report on Development of Multi-Utility Tractor prepared under NAIP, Operational in Department of Farm Machinery and Power Engineering, PAU, Ludhiana.
Yasuyuki H, Yosuke M, Takashi Y (2009). Agricultural Vehicle Navigation System: Development of a Guidance Information Display. JARQ 43(3):187-192. http://dx.doi.org/10.6090/jarq.43.187

academicJournals

Vol. 9(17), pp. 778-784, 15 September, 2014
DOI: 10.5897/SRE2013.5528
Article Number: 789811047294
ISSN 1992-2248 © 2014

http://www.academicjournals.org/SRE

Scientific Research and Essays

Full Length Research Paper

Hydrocarbon exploration in Odo Field in the Niger Delta Basin Nigeria, using a three-dimensional seismic reflection survey

T. N. Obiekezie

Department of Physics and Industrial Physics, Nnamdi Azikiwe University, Awka Nigeria.

Received 13 May, 2013; Accepted 24 July, 2014

A three-dimensional seismic reflection survey carried out in Odo Field in the central swamp of the Niger Delta Basin has been interpreted with respect to exploration for hydrocarbons. The Odo Field is marked by a large southwest heading listric growth fault with numerous synthetic and antithetic faults. The two picked seismic events, horizons 1 and 2 indicate four closures each, which are hydrocarbon bearing. The faults in the field thus support hydrocarbon accumulations which are seen to be mainly fault/dip closures. The expectations calculated for the observed fault closures suggest that several in-field appraisal prospects exist. The seismic attributes (amplitude maps) furthermore suggest that horizon 1 is mainly gas bearing.

Key words: Field, faults, Niger Delta, seismic, hydrocarbon

INTRODUCTION

Hydrocarbons such as oil and gas are found in geologic traps, which can either be structural or stratigraphic (Doust and Omatsola, 1990). Hydrocarbon exploration aims at identifying and delineating these structural and stratigraphic traps suitable for economically exploitable accumulations in a field. It also helps in delineating the extent of discoveries in field appraisals and development. These traps could be very multifaceted and subtle, thus mapping it accurately becomes difficult. The geophysicist works with a set of seismic sections and the primary product of the geophysical interpretation is a series of annotated maps indicating presence of prospective highs or other potential trap structures (McQuillin et al., 1984). Petroleum reserves are contained in three-dimensional traps but the seismic method in its attempt to image the subsurface has traditionally taken a two-dimensional (2D) approach (Brown, 2004). The use of 3D interpretation has been reported to yield better results; they have better resolution and have increased fault details as compared to the old 2D surveys.

The Niger Delta Basin is a major geological feature of significant petroleum exploration and production in Nigeria (Whiteman, 1982), now it is Africa's leading oil province (Reijers, 2011). The Niger Delta Basin (Figure 1) accounts for the entire hydrocarbon production at present-day Nigeria and is situated on the continental margin of the Gulf of Guinea in equatorial West Africa between latitude 3°N and 6°N and longitude 5°E and 8°E

Email: as27ro@yahoo.com

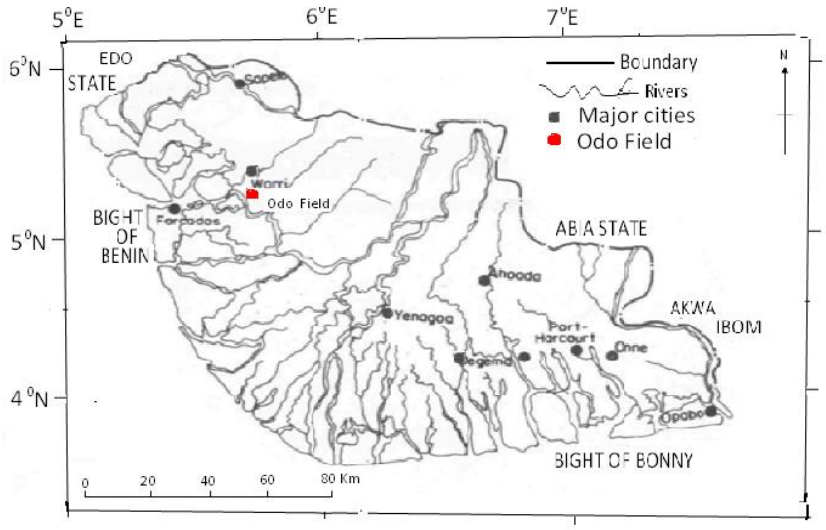

Figure 1. Map of the Niger Delta Basin.

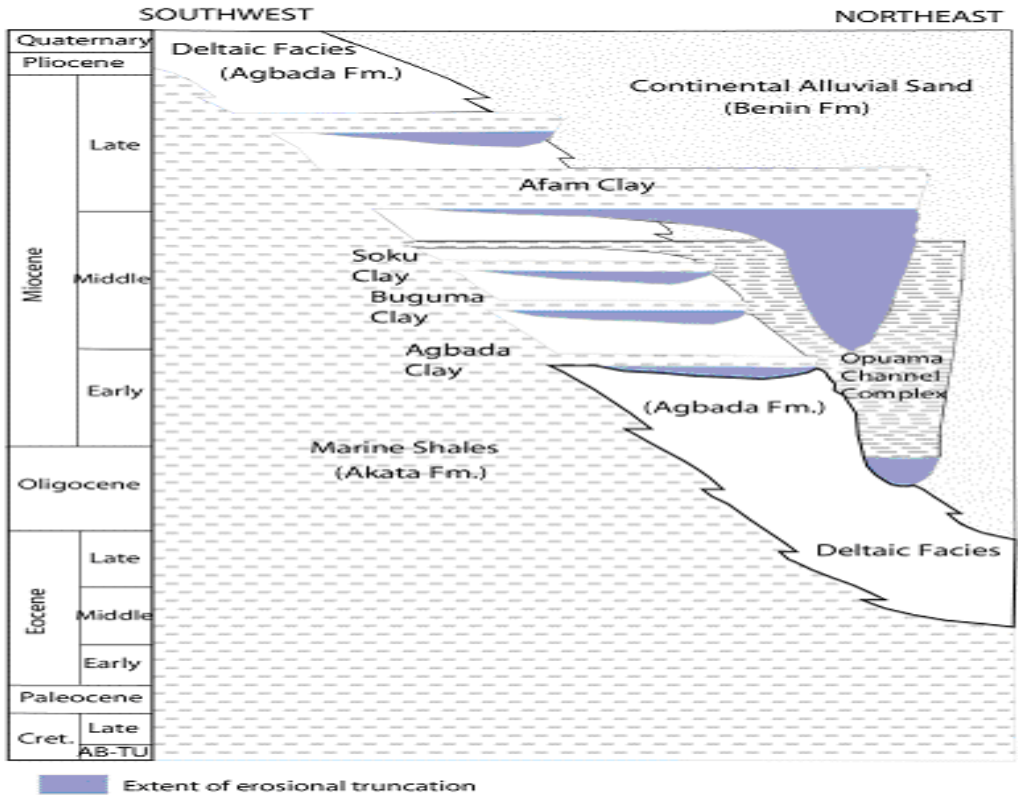

Figure 2. Stratigraphic column showing the three Formations of the Niger Delta, the continental *Benin* sandstone, the paralic Agbada formation and the Marine Akata shale. Modified from Doust and Omatsola (1990).

(Reijers, 1996). The Niger Delta sediments comprise three broad Formations, the Benin, Agbada and Akata Formations (Figure 2). The upper Benin Formation consists predominantly of fresh water bearing continental sands and gravels. The middle Agbada Formation consists primarily of sand and shale and is of fluviomarine origin. The lower Akata Formation is composed of shales, clays and silts (Short and Stauble,

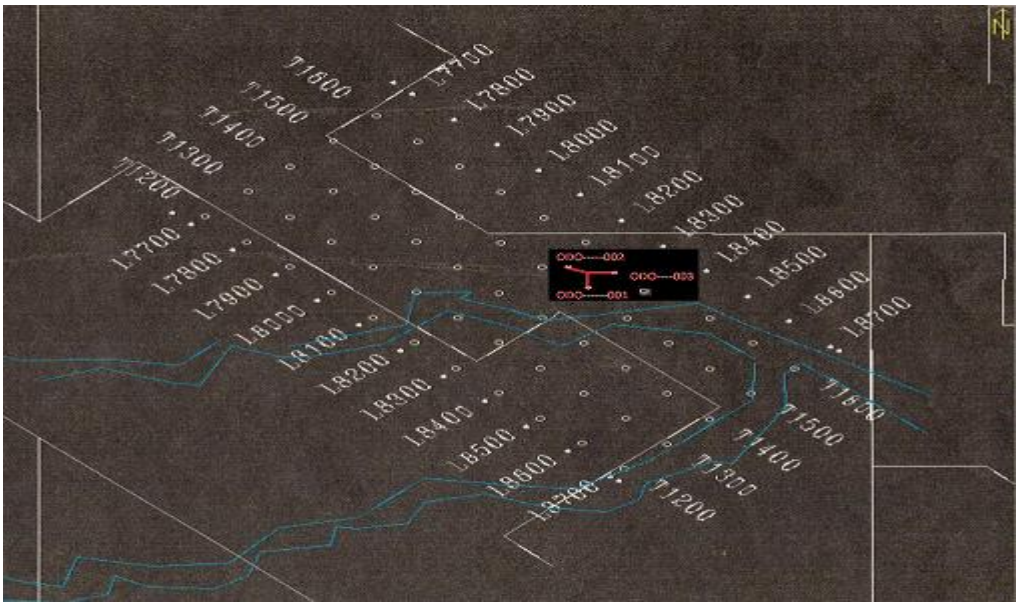

Figure 3. Base map of Odo Field showing the transition areas in blue, the land areas in white and the three existing wells in red.

1967; Magbagbeoloa and Willis, 2007; Owoyemi and Willis, 2006).

The distribution of hydrocarbon in the Niger Delta is complex with gas-to-oil ratio generally increasing southward away from the depocentre within a depobelt (Evamy et al., 1978). The distribution is found to be principally controlled by the quality and thermal history of source rocks, migration, fault sealing quality and the timing of traps formation (Chukwueke, 1997). The source rock for petroleum in the Niger Delta basin is assumed to arise from the marine interbedded shale in the Agbada Formation, the marine shale in the Akata formation and the Cretaceous shale (Doust and Omatsola, 1990; Short and Stauble, 1967; Ejedawe, 1981; Ekweozor and Okoye, 1980; Lambert-Aikhionbare and Ibe, 1984). Intervals with total organic-carbon contents sufficient to be considered as good source rocks exist in the Agbada Formation. These intervals are immature in various parts of the Niger Delta and rarely reach the thickness that is sufficient to produce a world-class oil province. The Akata Formation which is below the Agbada Formation shale is volumetrically sufficient to generate enough oil for a world class oil region such as the Niger Delta. The source-rock potential of the Cretaceous shale has not been ascertained because the Cretaceous shale is at present very deeply buried and has never been drilled (Evamy et al., 1978).

The majority of the traps found in the Niger Delta are structural in nature though stratigraphic traps are not unusual (Doust and Omatsola, 1990). The structural traps developed during syn-sedimentary deformation of the Agbada paralic sequence (Evamy et al., 1978). The syn-sedimentary structures which deform the delta largely beneath the Benin sand facies are the most striking structural features of the Niger Delta complex. These structures are believed to arise from gravity sliding during the course of deltaic sedimentation. They are polygenic in origin and their complexity increases generally in a down delta direction (Merki, 1972). The syn-sedimentary structures which are named growth faults are predominantly trending northeast to southwest and northwest to southeast (Hosper, 1971). They are usually associated with rollover anticlines, shale ridges, and sand-shale diapirs which are caused by shale upheaval ridges. Most of the faults are listric normal; others include structure building growth faults, crestal faults, flank faults, counter regional faults and antithetic faults.

Odo Field is located in the central swamp of the Niger Delta Basin. The field was discovered in 1978. The 3D seismic data were acquired in 1992 and covers 277.11 km^2 of subsurface full fold coverage. Subsurface sampling was 15 fold with a 25 m × 25 m bin size.

The base map or survey block of the field can be seen in Figure 3, the region bounded by the white lines indicates very dry land while the region bounded by the blue lines indicates transition zones. The 3D data were acquired using the usual methods for land and transition zones. The field is partly appraised having three already drilled wells.

The aim of this work is to interpret an already processed seismic reflection data from Odo Field in the Niger Delta Basin in order to explore for hydrocarbons. The seismic data had been processed to zero phase reflectivity and loaded to Halliburton land mark work station. The processed data quality was good but deteriorates below 3 s behind the major faults and within

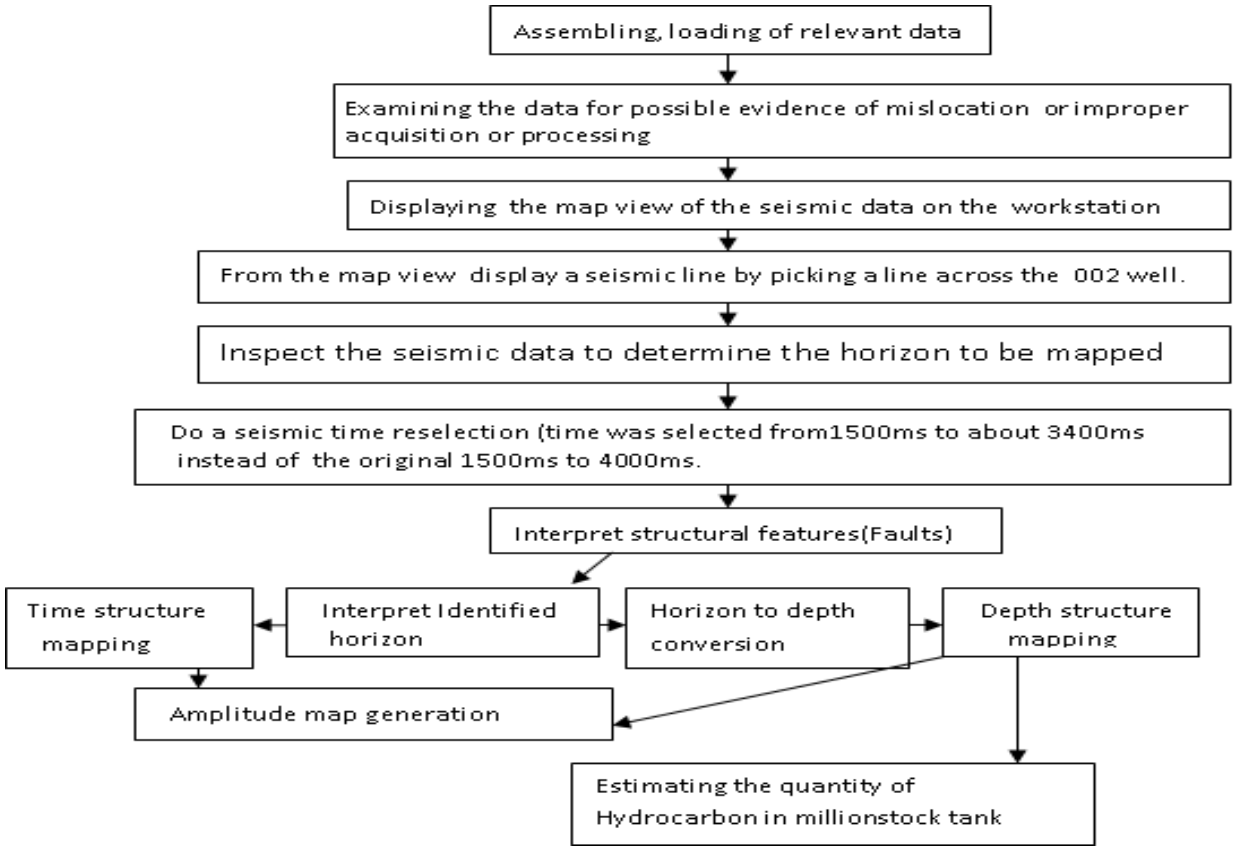

Figure 4. Flow chart of the analytic procedure.

narrow fault blocks. Recommendation for favourable drilling sites is expected to be made if the data suggests economically exploitable accumulations of hydrocarbon.

METHOD OF ANALYSIS

The analysis method followed the flow chart in Figure 4. Faults were interpreted as structures on every eight in line while the seismic events were interpreted on every eight in-lines and sixteenth cross-lines thereby generating an 8 × 16 grid. Several arbitrary lines were also generated to check the correlation. The horizons were identified as horizon 1 (red) and horizon 2 (blue) in Figure 5.

The quantity of hydrocarbon is estimated in million stock tank barrel using

$$STOIIP = \frac{GRV \times 43560 \times \Phi \times \frac{N}{G} \times (1 - S_w)}{5.615 \times FVF \times 1000000} \quad (1)$$

Where
STOIIP =Stock Tank Oil in Place (in million stock tank barrels),
GRV= Gross Rock Volume (in acrefeet),
N/G= Ratio of clean sand to the total sand, Φ =porosity.
$(1 - S_w)$ = Hydrocarbon saturation,
FVF = Formation Volume Factor.

INTERPRETATION OF RESULTS

The structure shows that the area is an elongated rollover anticline with a collapsed crest. The field is marked by a large southwest heading listric growth fault with numerous but closely spaced northwest to southeast antithetic and synthetic faults which are seen to be discontinuous across the field forming semi-parallel fault blocks (Figure 5). The depth maps (Figure 6) show structural highs against faults, which represent potential traps for hydrocarbons. The synthetic and antithetic faults form the footwall closures of the field. Four closures were identified on both horizons 1 and 2.

The hydrocarbon estimates calculated in million stock tank barrels for the fault closures in horizons 1 and 2 (Table 1) indicates that closures 1, 2, 3, 4 are hydrocarbon bearing. This suggests that several in field appraisals prospects exist in the field. The result shows that more hydrocarbon accumulation can be seen in closure 3 in horizon 2.

3D seismic has made the use of amplitudes an integral part of seismic interpretation. Amplitude related seismic attributes have robust physical relationships to lithology and porosity (Banchs and Michelena, 2002; Dorrington and Link, 2004; Calderon and Castagna, 2005).

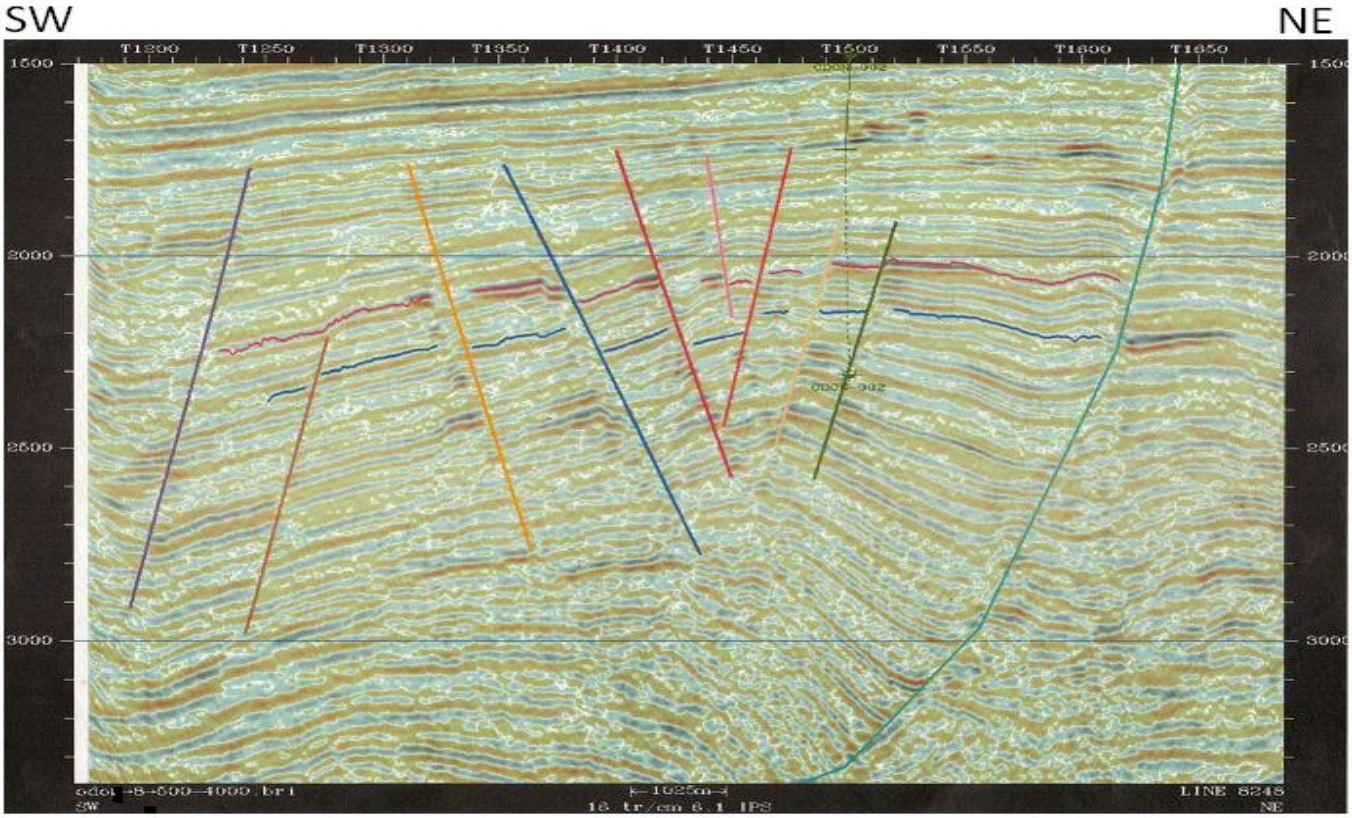

(a)

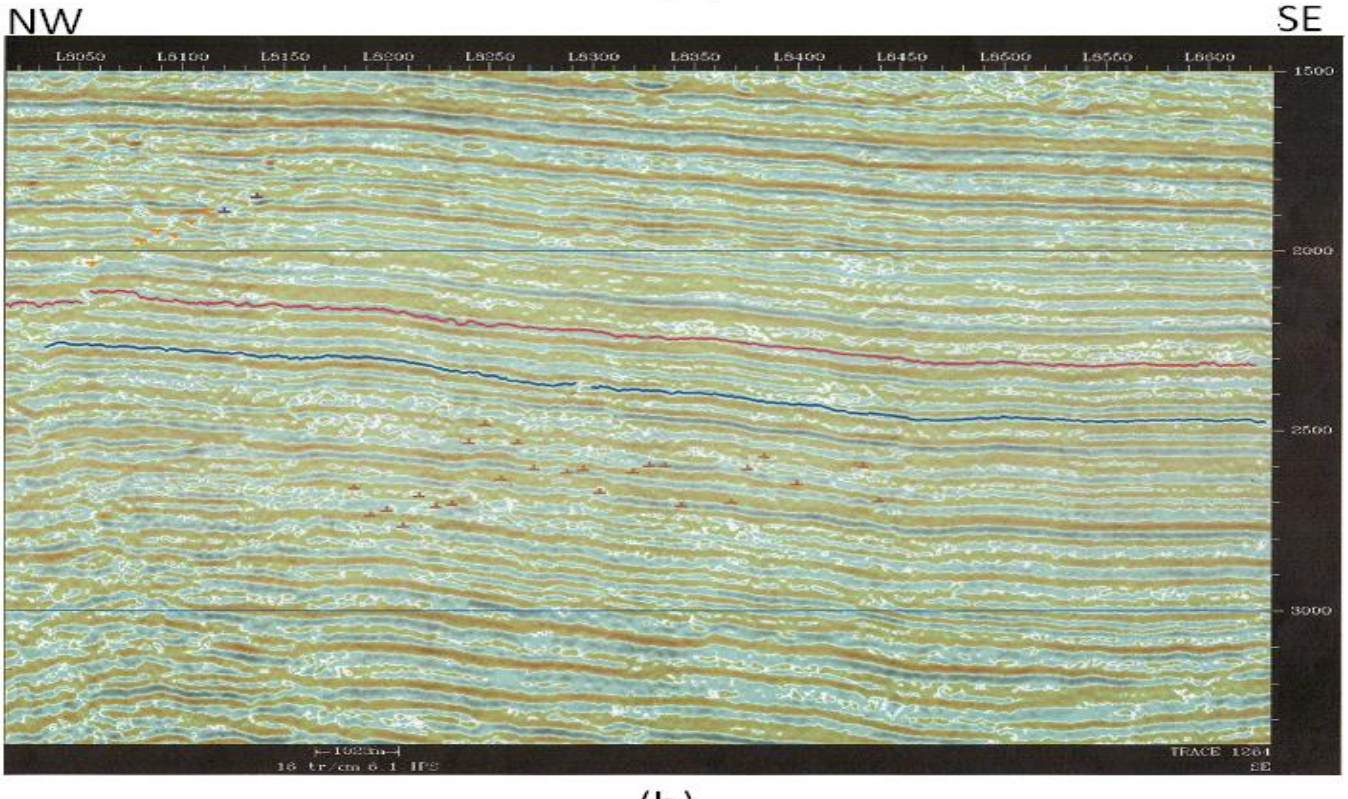

(b)

Figure 5. (a) Interpreted seismic in-line showing the faults and two horizons and (b) Interpreted cross line showing the two horizons and the cross posted fault.

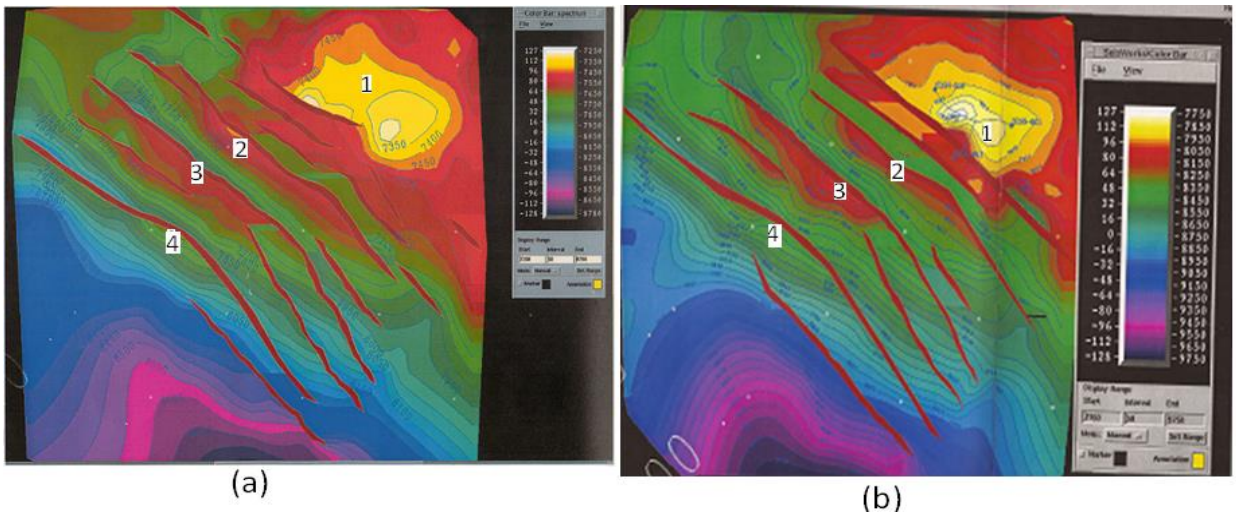

Figure 6. Depth contour map for (a) horizon 1, and (b) Depth contour map for horizon 2, showing the four closures.

Table 1. Estimated quantity of hydrocarbons from the closures.

Closures	Quantity of hydrocarbon in million stock tank barrel	
	Horizon 1	Horizon 2
1	18.871	35.082
2	111.293	43.922
3	30.861	129.665
4	11.661	1.186

The presence of gas in a reservior has often the property of a significant reduction in seismic velocity. The presence of oil does not have such significant effect. More usually the only detectable effect is the production of amplitude anomalies, these being due to the large negative reflection coefficient at the interface between gas-filled reservoirs and the overlying cap rock. Such amplitude anomalies are often termed 'bright spots' (McQuillin et al., 1984). Thus bright spots are seen as an indication of hydrocarbon presence; Figure 7 shows the amplitude maps for horizons 1 and 2. It is noted that gas shows clearly where the hydrocarbon is trapped. Thus from Figure 7 it is assumed that horizon 1 is mainly gas bearing.

Conclusions

The results from the hydrocarbon exploration in Odo Field in the Niger Delta Basin Nigeria, using a three-dimensional seismic reflection survey indicates that; Odo Field is an elongated rollover anticline with a collapsed crest which is associated with a growth fault. The picked seismic events (horizons) has four identified structural closures which were mainly fault /dip closures and were found to be hydrocarbon bearing. These hydrocarbon accumulations were seen to be supported by the faults within the field. Following the calculated estimations, several infield appraisal prospects exist. Finally, from the amplitude maps, horizon 1 is assumed to be mainly gas bearing.

It is suggested that drilling should not be carried out now but after a 3D time lapse (4D) has been carried out in the field to determine changes in rock properties to enable qualification and quantification of the hydrocarbons for production planning and well drilling.

Conflict of Interests

The author(s) have not declared any conflict of interests.

ACKNOWLEDGEMENTS

This research was carried out under sponsorship from Shell Petroleum Development Company (SPDC) Nigeria and the Nigerian Government. The Department of Petroleum Resources (DPR) Nigeria gave the necessary permissions. The author is sincerely greatly to the managements of SPDC, DPR and the Nigerian Government.

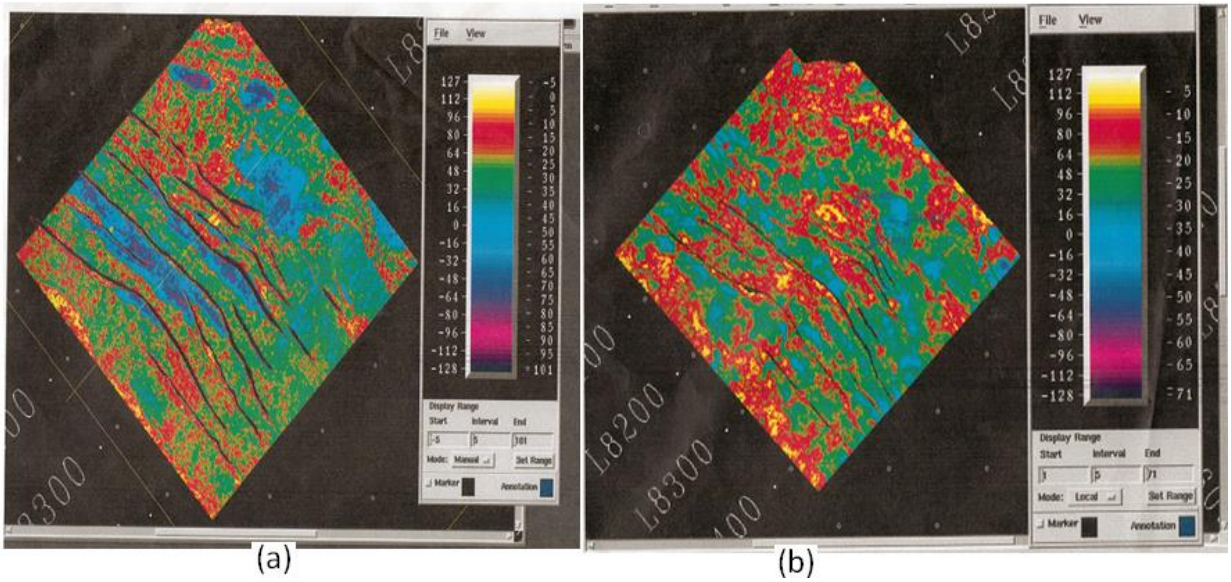

Figure 7. Amplitude map for (a) horizon 1 (b) horizon 2.

REFERENCES

Banchs RE, Michelena RJ (2002). From 3D seismic attributes to pseudowell-log volumes using neural networks: Practical considerations. The Leading Edge 21(10):996-1001. http://dx.doi.org/10.1190/1.1518436

Brown AR (2004). Interpretation of three dimensional seismic data. Society of exploration Geophysiscist, Tulsa. 560 pp.

Calderon JE, Castagna J (2005). Porosity and Lithologic Estimation Using Rock Physics and Multiattribute Transforms In the Balcon Field, Columbia-South America. Expanded Abstracts, 75th SEG Annual International Meeting, pp. 444-447.

Chukwueke CC (1997). Factors controlling hydrocarbon distribution in the central swamp deposit of the Niger Delta. Nig. Assoc. Petrol. Explorat. Bull. 12:41-45.

Dorrington KP, Link CA. (2004). Genetic-algorithm/ neural network approach to seismic attribute selection for well-log prediction. Geophysics 69(1):212-221. http://dx.doi.org/10.1190/1.1649389

Doust H, Omatsola E (1990) Niger Delta, in, Edwards, JD., and Santogrossi PA, eds Divergent/passive Margin Basins, AAPG Memoir 48: Tulsa, American Association of Petroleum Geologists, pp. 239-248.

Ejedawe JE (1981). Patterns of incidence of oil reserves in Niger Delta Basin. Am. Assoc. Petrol. Geol. Bull. 65:1574-1585.

Ekweozor CM, Okoye NV (1980). Petroleum source-bed evaluation of Tertiary Niger Delta. Am. Assoc. Petrol. Geol. Bull. 64:1251-1259.

Evamy BD, Haremboure J, Kamerling P, Knaap WA, Molloy FA, Rowlands PH (1978). Hydrocarbon habitat of Tertiary Niger Delta. Am. Assoc. Petrol. Geol. Bull. 62:277-298.

Hosper J (1971). The geology of the Niger Delta area, in the Geology of the East Atlantic continental margin, Great Britain. Inst. Geol. Sci. Report 70(16):121-141.

Lambert-Aikhionbare DO, Ibe AC (1984). Petroleum source-bed evaluation of the Tertiary Niger Delta: discussion. Am. Assoc. Petrol. Geol. Bull. 68:387-394.

Magbagbeoloa O, Willis BJ (2007). Sequence stratigra¬phy and syndepositional deformation of the Agbada Formation, Robertkiri field, Niger Delta, Nigeria. Am. Assoc. Petrol. Geol. Bull. 91:945–958.

McQuillin R, Bacon M, Barclay W (1984). An Introduction to Seismic Interpretation. Graham and Trotman, London, 287 pp.

Merki PJ (1972). Structural geology of the Cenozoic Niger Delta: 1st Conference on African Geology Proceedings, Ibadan University Press, pp. 635-646.

Owoyemi AO, Willis BJ (2006). Depositional patterns across syndepositional normal faults, Niger delta, Ni¬geria. J. Sediment. Res. 76:346-363. http://dx.doi.org/10.2110/jsr.2006.025

Reijers TJA (1996). Selected chapters on geology. SPDC Corporate Reprographic Service, Warri, Nigeria, 194 pp.

Reijers TJA (2011). Stratigraphy and sedimentology of the Niger Delta. Geologos 17(3):133-162. http://dx.doi.org/10.2478/v10118-011-0008-3

Short S and Stauble G (1967). Outline of Geology of Niger Delta. Am. Assoc. Petrol. Geol. Bull. 51:761-779.

Whiteman AJ (1982). Nigeria: Its Petroleum Geology, Resources and Potentials. Graham and Trotman, London, 394 pp.

academicJournals

Vol. 9(17), pp. 785-793, 15 September, 2014
DOI: 10.5897/SRE2014.5892
Article Number: 23A28F347296
ISSN 1992-2248 © 2014

http://www.academicjournals.org/SRE

Scientific Research and Essays

Full Length Research Paper

Fractional order chaos in Josephson junction

Yoothana Suansook[1]* and Kitti Paithoonwattanakij[2]

Faculty of Engineering, King Mongkut's Institute of Technology Ladkrabang, Chalongkrung Rd., Ladkrabang, Bangkok, Thailand 10520, Thailand.

Received 26 March, 2014; Accepted 3 July, 2014

This paper studies the fractional-order chaotic dynamics of Josephson junction based on resistor and capacitor shunted junction (RCSJ) model proposed by W. C. Stewart and D. E. McCumber. The fractional-order numerical integration is carried out with modified trapezoidal rule. Fractional-order chaotic behaviors of the model are explained by bifurcation diagram. Numerical results confirm that there exists chaos at fractional-order in this model.

Key words: Fractional calculus, Josephson junction, chaotic dynamical system, numerical method.

INTRODUCTION

The theory of fractional calculus is 300 years old mathematical topic. This theory originated from Leibnitz's note in the 17th century. This mathematical theory has long history that dates back to the day that Leibnitz replied query from L'Hospital about the meaning of half order derivative (Oldham and Spanier, 1974). The theory is not known to scientist and engineers that much because there are few solutions for solving the fractional differential equation (Oldham and Spanier, 1974). Recently, the study in this theory has gained more applications such as viscoelasticity, mechanics and nonlinear dynamic and anomalous phenomena (Zaslavsky, 2002). The comprehensive discussions of this theory are presented by Oldham and Spanier (1974), Miller and Ross (1993), and Podlubny (1999) and applications in physics and engineer are presented by Sabatier and Machado (Sabatier et al., 2007).

In general, the non-linear dynamical system can be described by simple rules as well as different physical systems. In certain dynamical system, there exists the irregular behavior that is sensitive to small changes in the initial condition known as chaos (Strogatz, 1994). Many non-linear systems in nature exhibit irregular pattern or chaotic property by being sensitive to initial condition. Examples include the models that describe the planetary motion, oscillation in electric circuit, swinging of pendulum, the flow of liquid, chemical reaction, fermentation process (Strogatz, 1994), dripping faucet (Dreyer and Hickey, 1991) and population of some species in ecological system (May, 1976).

Chaos is an irregularity behavior which arises in nonlinear dynamical systems. The first discovery of chaos in atmospheric convection model by Lorenz is the beginning of research in this area (Lorenz, 1963). The equations that described the dynamical system are differential equations which yield different type of solutions, such as limit cycle, periodic, periodic doubling, non-periodic and chaotic (Strogatz, 1994).

The fundamental results in fractional order differential equation that are useful for the applications are stable. The studies of fractional-order stability include the fractional Duffing oscillator, fractional predator-prey and

*Corresponding author. E-mail: yoothana@gmail.com

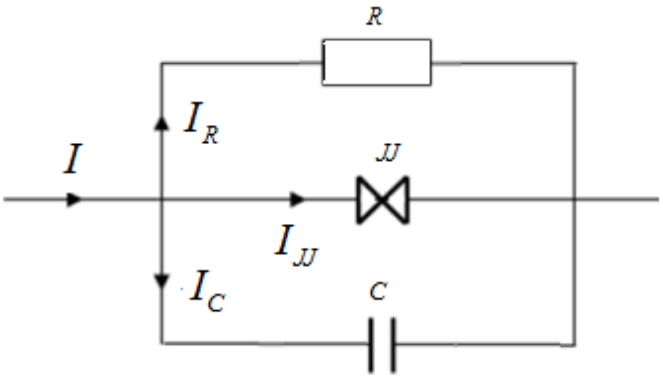

Figure 1. Simple circuit model of Josephson junction.

rabies models. In control theory, the fractional-order control systems have many interesting problems related to stability theory such as robust stability, bounded input – bounded output stability, internal stability, root-locus, robust controllability, robust observability, etc (Li and Zhang, 2011). The stability of fractional order often refers to Matignon's theorem for commensurate order. The theorem analyzes the system stability by locating the eigenvalues of the dynamical system in complex plane. Xiang-Jun et al. (2008) have proven the stability theorem of nonlinear fractional-order differential equation by using the Gronwall-Bellman lemma (Li and Zhang, 2011). Petras provided a survey on the methods for stability investigation of certain class of fractional differential systems with rational orders (Petras, 2009).

The theory of Poincare Bendixson explains that chaos can exist in continuous dynamical system with at least three degrees (Li and Yorke, 1975). The study of nonlinear dynamical systems with theory of fractional calculus provided novel conclusion; for example, chaotic dynamics of fractional-order Arneodo's systems (Lu, 2005), fractional Chen system (Lu et al., 2006), chaos in the Newton–Leipnik system with fractional order (Wang and Tian, 2006), chaos in a fractional order modified Duffing system (Ge and Ou, 2007), fractional order Chua's system (Radwan et al., 2011; Hartley et al., 1995; Petras, 2008), fractional-order Volta's system (Petras, 2009), chaos in a fractional-order Rössler system (Li and Chen, 2004, Zhang et al., 2009), fractional-order Lorenz chaos (Yu et al., 2009).

Nonlinear physical phenomena are often described by integer order differential equations. With the development of fractional calculus, it has been found that the behavior of many systems can be described by using the fractional differential systems fractional order damping of duffing system (Cao et al., 2010). Josephson junction is a nonlinear device that has many applications in high frequency, ultra-low noise and low power consumption (Chen et al., 2012). In this paper, we study further the fractional dynamic of Josephson junction circuit from the well-known. The Resistively and Capacitively Shunted Junction-model (RCSJ) proposed by Stewart McCumber. This device is a good candidate for studying the fractional-order chaotic patterns. The chaotic behaviors of fractional order have been investigated by the bifurcation diagram and phase space. Numerical algorithm was carried out using modified trapezoidal rule proposed by Odibat and Momani, (2008b). The aim of this study is to examine the intermediate state of the bifurcation patterns.

METHODOLOGY

Mathematical model of Josephson junction

A simple model of the Josephson junction (JJ) can be considered with a resistor and capacitor shunted junction (RCSJ) circuit as represented in Figure 1. The model was proposed by W. C. Stewart and D. E. McCumber (Clarke and Braginski, 2006). The current through the circuit is determined with the Kirchoffs law as follows (Chen et al., 2012):

$$I = I_{JJ} + I_C + I_R = I_c \sin\varphi + C\frac{dV}{dt} + \frac{V}{R} \quad (1)$$

A standard form of the RCLSJ model is proposed as:

$$\frac{h}{4\pi e}\frac{d\varphi}{dt} = V, \quad (2)$$

$$C\frac{dV}{dt} + \frac{V}{R_V} + I_c \sin(\varphi) + I_s = I, \quad (3)$$

$$L\frac{dI_s}{dt} + I_s R_s = V, \quad (4)$$

Let $x = \varphi, y = \frac{V}{I_c R_s}, z = \frac{I_s}{I_c}$ and

$$\beta_c = 4\pi I_c R_s^2 C / h, \beta_L = 4\pi e I_c L / h, g = R_s / R_V$$

where β_c and β_L are simplified capacitance and inductance. We can rewrite the above relation into three differential equations as follows (Feng and Shen, 2008):

$$x' = y \quad (5)$$

$$y' = \frac{1}{\beta_c}(i - gy - \sin(x) - z) \quad (6)$$

$$z' = \frac{1}{\beta_L}(y - z) \quad (7)$$

By replacing the derivative with fractional derivative, we have the fractional-order differential equations of RCSJ model as follows:

$$D^q x = y \quad (8)$$

$$D^q y = \frac{1}{\beta_c}(i - gy - \sin(x) - z) \quad (9)$$

$$D^q z = \frac{1}{\beta_L}(y - z) \quad (10)$$

Normalized time $\tau = \omega_c t$, $\omega_c = 4\pi I_c R_s / h$

Normalized current $i = I / I_c$

Normalized voltage $v = V / I_c R_s$ (Feng and Shen, 2008).

Fractional calculus

In fractional calculus, there are many definitions proposed. Two mostly use definitions are Riemann-Liouville and Grunwald-Letnikov. The definition that is suitable for studying the analytic solution is Riemann-Liouville definition while the definition that is more appropriate for numerical calculation is Grunwald-Letnikov definition (Podlubny, 1999).

Definition 1: The Riemann-Liouville fractional integral of order $q > 0$ of a function $f : R^+ \to R$ is given by Podlubny (1999):

$$I^q f(x) = \frac{1}{\Gamma(q)} \int_0^x (x-t)^{q-1} f(t) dt \quad (11)$$

Podlubny (1999) provided the right side point-wise defined on R^+ where $\Gamma(\cdot)$ is Gamma function defined by:

$$\Gamma(x) = \int_0^\infty e^{-u} u^{x-1} du \quad (12)$$

Definition 2: The Caputo fractional derivative of order $q \in (n-1, n)$ of a continuous function $f : R^+ \to R$ is given by Podlubny (1999):

$$D^q f(x) = I^{n-q} D^n f(x), D = \frac{d}{dt} \quad (13)$$

Definition 3: Grunwald–Letnikov definition for fractional derivative of order q is given by Podlubny (1999):

$${}_a D_t^q f(t) = \lim_{h \to 0} h^{-q} \sum_{j=0}^{[t-a/h]} (-1) \binom{q}{j} f(t - jh) \quad (14)$$

Where,

$$\binom{n}{r} = \frac{n!}{r!(n-r)!} = \frac{n(n-1)(n-2)...(n-r+1)}{r!}$$

$$\binom{n}{r} = \frac{n!}{r!(n-r)!}$$

$$= \frac{\Gamma(n+1)}{\Gamma(r+1)\Gamma(n-r+1)} \quad (15)$$

In classical calculus, the meaning of integer order derivative is the rate of change, direction of decline or slope in the geometric interpretation. The meaning of fractional-order derivative is different. It has no conventional geometric meaning and physical interpretation of fractional integration and differentiation. Recently, Podlubny has proposed a new physical interpretation based on general convolution integrals of the Volterra type (Podlubny, 1999). Machado gives a geometric and probabilistic interpretation based on Grunwald-Letnikov definition of the fractional derivative (Machado et al., 2009). Fractional derivative and integration have many forms and definitions. The operators in this mathematical theory are fascinating. The fractional derivative of the constant value is not zero (Podlubny, 1999). For three centuries, the theory of fractional derivatives is developed only for mathematicians.

There are many approaches for solving the fractional order differential equation which include numerical approximation, series expansion, method of decomposition, predictor corrector scheme (Petras, 2008), Adam Moulton algorithm, Laplace transform (Tavazoei et al., 2008), differential transform (Odibat et al., 2010), (Odibat and Momani, 2008a), (Odibat et al., 2008c) and numerical calculation of nonlinear fractional partial differential equations (Momani et al., 2008). Solutions are written in the compact form of mathematical function mathematicalfunction (Erturk et al. 2012; Erturk et al., 2008; Baleanuet al., 2009; Li and Deng, 2007). The applications of fractional calculus in physics are better for describing the diffusion phenomena in homogeneous media with non-integer derivative; the fractional derivatives model of viscoelastic material (Bagley and Calico, 1991); fractional order impedance in electric circuit; dynamical process of heat conduction and chaotic dynamical system (Podlubny, 1999).

The advantage of fractional derivatives compared to classical integer-order calculus is the description of memory and hereditary properties of various materials and processes. In the last few decades, many authors show that derivatives and integral of non-integer order are very suitable for describing properties of various real materials e.g. polymers. It has been shown that fractional-order models are more adequate than integer-order models (Bagley and Torvik, 1983). Recently, this mathematical theory has gained more attention due to their vast applications in Applied Sciences (Podlubny, 1999).

Numerical method

There are many approaches in fractional order numerical calculation. Two main approaches for numerical calculation are the frequency domain and time domain. From the study of Tavazoei, the frequency domain approach can lead to the fake chaotic results (Tavazoei et al., 2008). The numerical method that we utilized in this paper is the modified trapezoidal rule proposed by Odibat and Momani, (2008b). This method is simple calculation scheme that was derived from the area of trapezoidal shape.

Consider $y = f(x)$ over $[a,b]$ suppose that the interval $[a,b]$ is subdivided into m subintervals $\{[x_{k-1}, x_k]\}_{k=1}^m$ of equal width $h = \frac{b-a}{m}$ by using the equally spaced nodes $x_k = x_0 + kh$ for $k = 1, 2, ..., m$.

The composite trapezoidal rule for m subinterval is:

$$T(f,h) = \frac{h}{2}(f(a) + f(b)) + h\sum_{k=1}^{m} f(x_k) \quad (16)$$

The formula can be extended by using fractional order differential as follows (Odibat and Momani, 2008b):

$$T(f,h,q)=((k-1)^{q+1}-(k-q-1)k^{q})\frac{h^{q}f(0)}{\Gamma(q+2)}+\sum_{j=1}^{k-1}((k-j+1)^{q+1}-2(k-j)^{q+1}+(k-j-1)^{q+1})\frac{h^{q}f(x_j)}{\Gamma(q+2)} \quad (17)$$

The formula in Equation (17) is used to approximate the integral function of arbitrary order. According to the classical theory of ordinary differential equations, we need to specify initial conditions to produce a unique solution for the problem (Odibat and Momani, 2008b).

Equation (18) is an approximation to fractional integral at order q:

$$(I^{q}f(x)(a))=T(f,h,q)-E(f,h,q) \quad (18)$$

where $a>0, q>0$

Odibat and Momani (2008b) shows that the error is a function of parameter h

$$|E(f,h,q)|=O(h^{2}) \quad (19)$$

It is obviously that if the order $q=1$, then the modified trapezoidal rule is reduced to the classical trapezoidal rule:

$$\lim_{q\to 1}D^{q}f(x)=\frac{df(x)}{dx} \quad (20)$$

Stability of fractional-order chaos

Here we discuss the stability condition for fractional-order systems and a necessary condition for chaos to exist. Consider the following fractional differential equations (Petras, 2009; Podlubny, 1999; Li et al., 2011; Odibat et al., 2008c).

$$D^{q}x_i=f_i(x_1,x_2,x_3),\qquad i=1,2,3 \quad (21)$$

The equilibrium points x_i^{eq} of the fractional-order differential system can be obtained by solving the following equations:

$$D^{q}x_i=0 \quad (22)$$

and δ_i is a small deviation from the equilibrium.

$$f_i(x_1^{eq}+\delta_1(t),x_2^{eq}+\delta_2(t),x_3^{eq}+\delta_3(t))=f_1(x_1^{eq},x_2^{eq},x_3^{eq})+\left.\frac{\partial f_1}{\partial x_1}\right|_{eq}\delta_1+\left.\frac{\partial f_1}{\partial x_2}\right|_{eq}\delta_2+\left.\frac{\partial f_1}{\partial x_3}\right|_{eq}\delta_3 \quad (23)$$

Then

$$D^{q}(\delta_i)\cong+\left.\frac{\partial f_1}{\partial x_1}\right|_{eq}\delta_1+\left.\frac{\partial f_1}{\partial x_2}\right|_{eq}\delta_2+\left.\frac{\partial f_1}{\partial x_3}\right|_{eq}\delta_3 \quad (24)$$

Therefore, we will have a linear system:

$$D^{q}(\delta_i)=\mathrm{A}\delta \quad (25)$$

Where:

$$\mathrm{A}=\begin{bmatrix}\frac{\partial f_1}{\partial x_1} & \frac{\partial f_1}{\partial x_2} & \frac{\partial f_1}{\partial x_3}\\ \frac{\partial f_2}{\partial x_1} & \frac{\partial f_2}{\partial x_2} & \frac{\partial f_2}{\partial x_3}\\ \frac{\partial f_3}{\partial x_1} & \frac{\partial f_3}{\partial x_2} & \frac{\partial f_3}{\partial x_3}\end{bmatrix} \quad (26)$$

The following autonomous system is:

$$D^{q}x=Ax,\ x(0)=x_0 \quad (27)$$

where $0<q<1, x\in R^{n}, A\in R^{nxn}$ is asymptotically stable if and only if $|\arg(\lambda_i(A))|>q\pi/2$. In this case, each component of the states decays towards 0 like t^{-q}. Also, this system is stable if and only if $|\arg(\lambda_i(A))|\geq q\pi/2$ and those critical eigenvalues that satisfy $|\arg(\lambda_i(A))|=q\pi/2$ have geometric multiplicity one (Matignon, 1996).

Given the parameters as follows $i=1.11, \beta_c=0.707, \beta_L=2.68, g=0.0478$, then we can have the asymptotically stable condition $q<\frac{2}{\pi}(2.53892)\approx 1.62$.

NUMERICAL RESULTS

Lyapunov exponent

Nonlinear dynamical system is often defined by the differential equation. The dynamical system may have attracting limit set. The different attracting limit set with different basin of attraction is determined by the initial condition. The limit set can be characterized by four fundamental types of limit sets: fixed points, periodic, quasi-periodic and chaos. The dynamical system can be used to measure the rate of divergence of nearby trajectories using the Lyapunov exponents. These quantities can characterize the solutions of the differential equations (Sandri, 1996). The Lyapunov exponents of the Josephson junction model for $i=1.11, i=1.56$ and $\beta_c=0.707, \beta_L=2.68, g=0.0478$ are shown in Figure 2.

Fractional-order phase space

The study of dynamical system behavior entails studying the behavior of the trajectories in the phase space. The

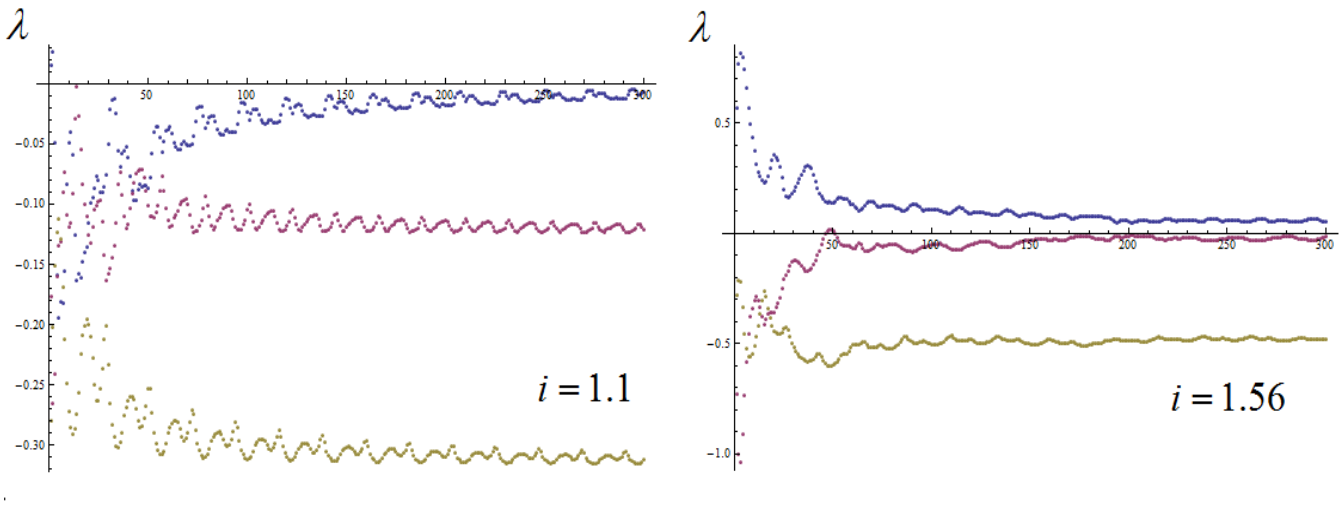

Figure 2. The Lyapunov spectrum for the Josephson junction model.

phase space in the structural form of trajectories is examined. The structures of the trajectories are diagram of phase space of the dynamical systems. From a geometrical point of view, this structure is the geometrical pattern of the relative positions of trajectories in the phase space. The study of phase space by fractional calculus helps in understanding the small deviation of the dynamical systems. The behavior of chaotic dynamical system can be understood by construction viewed from a phasespace perspective. In Josephson junction circuit, the chaotic behavior is often viewed from the phase space of the voltage and current of the dimensionless variables. The geometric meaning of the single close loop of phase space presents the periodic system and two close loops of phase space represent the periodic doubling and so on. The chaotic system of the phase space appears as a messy loop.

The numerical results of fractional-order phase space of the variable y and z are shown in Figure 3. According to the numerical results, the change in integration-order results as bent curve or distorted trajectories.

Memory effect with Bifurcation theory

The behaviors of nonlinear system are intrigue because they range from simple to complex and periodic to non-periodic. In certain nonlinear system, chaotic behavior is exhibited at certain range. Two different nonlinear systems can be described by similar set of equations. The study of sensitivity in nonlinear dynamical system helps in understanding how systems behave at certain parameters. The behaviors of nonlinear dynamical system are studied by bifurcation theory. Bifurcation theory is mathematical theory that study changes in qualitative or topological structure of the dynamical system. The theory explains the behavior of the integral curves of the vector fields and the solution of differential equation (Strogatz 1994). The combination of fractional calculus and this mathematical theory help us in understanding how system change upon the order.

Integer-order Bifurcation diagram

Bifurcation pattern can be obtained by varying certain parameters. In this case we use β_L. In the diagrams (Figure 4), the values of i vary from 1.12 to 1.15 results in bifurcation diagram (Figure 3). Numerical results show different bifurcation patterns start from periodic and become chaotic; they disappear when β_L increases. The dot bands are the chaotic regions. There is periodic doubling and quadrupling of the value of $i = 1.14$; it disappears when $i = 1.15$. According to the pattern, we may conclude that different values of parameters provide different bifurcation patterns.

Fractional order Bifurcation diagram

The numerical integration of fractional order is calculated by applying the modified trapezoidal rule to the differential equation of the RCSJ model. In order to reduce numerical errors, the time-step of the fractional-order numerical integration is set to $h = 2000$.The diagrams are obtained by varying the fractional integration order with the fixed values of the parameters. In this calculation, we use $i = 1.59, i = 1.11$; while the other variables are $\beta_c = 0.707, \beta_L = 2.68, g = 0.0478$.

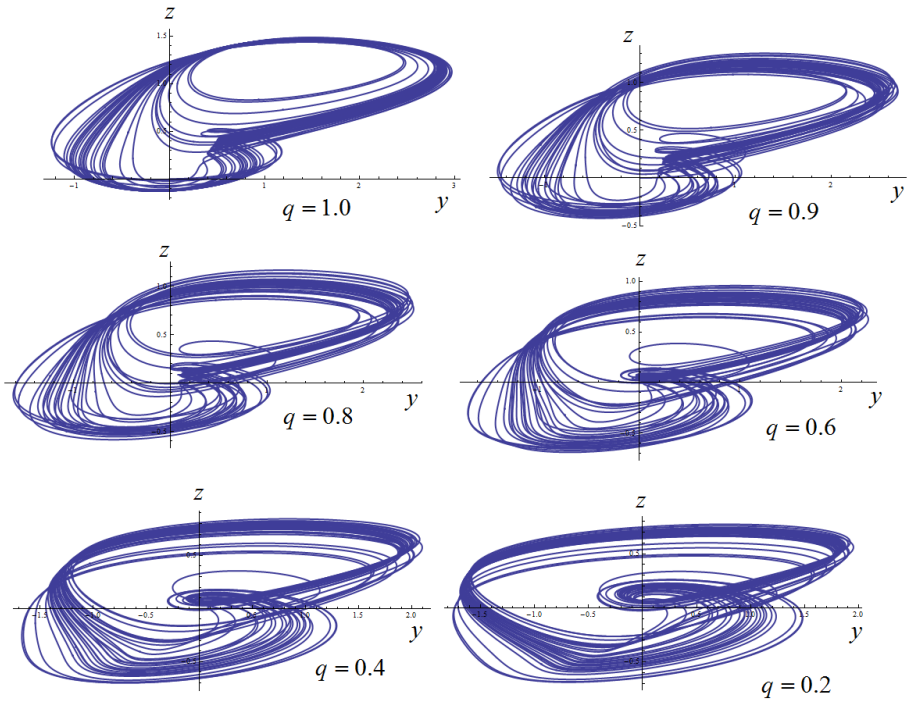

Figure 3. Fractional-order phase space of RCSJ model for following parameters $i = 1.11, \beta_c = 0.707, \beta_L = 2.68, g = 0.0478$.

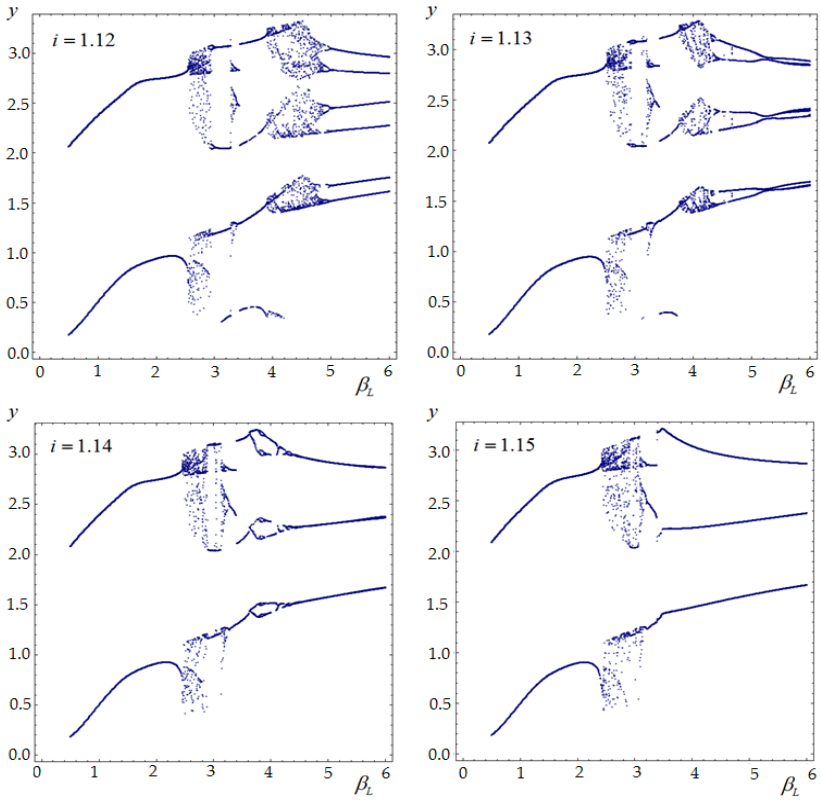

Figure 4. Integer-order Bifurcation diagram for the following parameters $i = 1.12 - 1.15, \beta_c = 0.707, \beta_L = 2.68, g = 0.0478$.

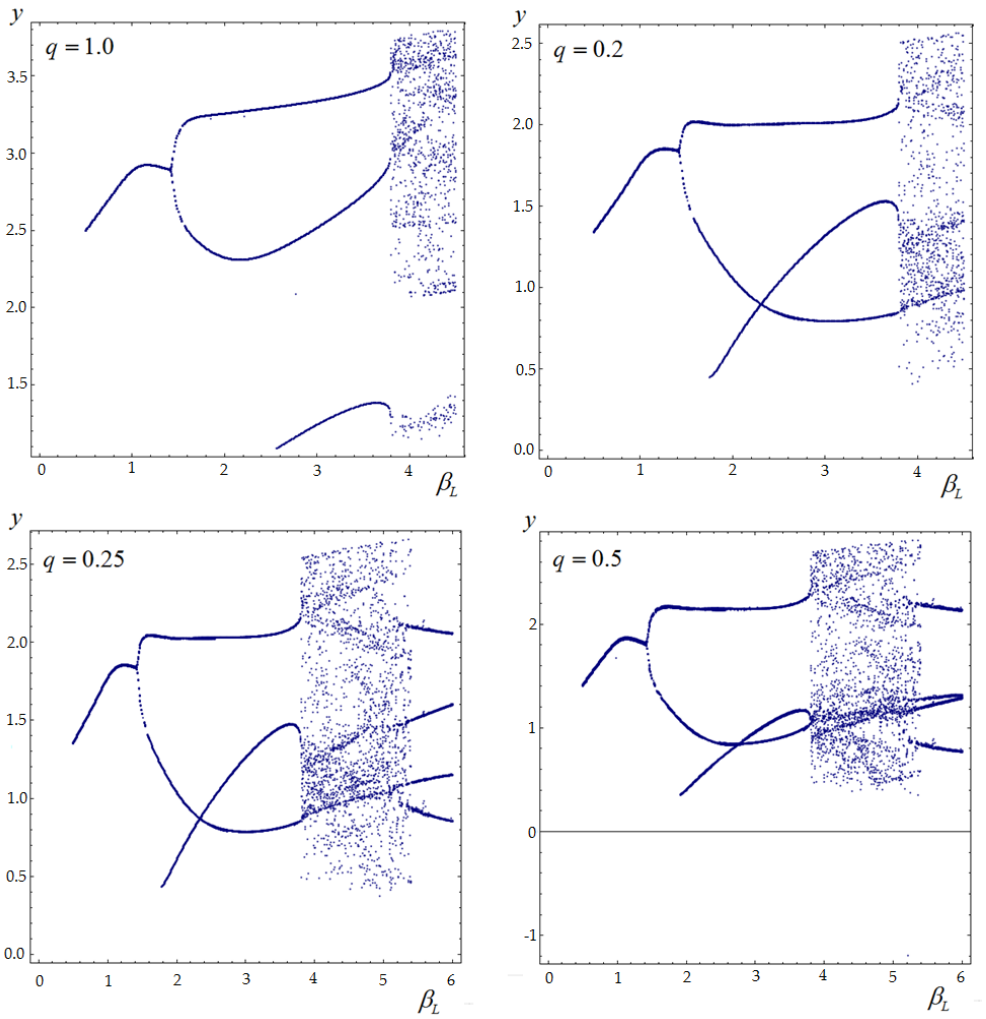

Figure 5. Fractional-order Bifurcation diagram of the following parameter $i = 1.59, \beta_c = 0.707, \beta_L = 2.68, g = 0.0478$.

For the values $i = 1.59$, the chaotic region begins with $\beta_L \approx 4$. For the values $i = 1.11$, the chaotic region begins with $\beta_L \approx 3.6$. The results are as in Figure 5 and Figure 6. We may recognize the existing pattern in fractional-order bifurcation diagram where the structures of each diagram resemble the previous stage.

DISCUSSION

The combination between theory of fractional calculus and nonlinear dynamical system provides the novel idea for exploring the unexplored region. Even simple known chaotic systems have broad ranges of irregular behavior that are not yet examined. Fractional calculus helps in exploring the unexplored areas in dynamical system. The RCSJ model is one of the simple known systems that there exhibit chaotic behavior at certain ranges. Theory of fractional differential equations has proved to be a valuable tool for the modeling of many physical phenomena. In this paper, we have applied theory of fractional calculus to examine the fractional-order bifurcation diagram in The Resistively and Capacitively Shunted Junction-model (RCSJ) model. We may see that physical system does not only depend on the instant of time but also on the history of the earlier stage, which can achieved by numerical calculation with fractional calculus. The numerical results show that the patterns of the fractional-order bifurcation diagram do not differ from the integer order that much. We may conclude that integer-order bifurcation diagram explains the behaviors of dynamics subject to change in parameters. The results in fractional order bifurcation diagram are the deviations from the previous stages since the fractional operator has memory effect.

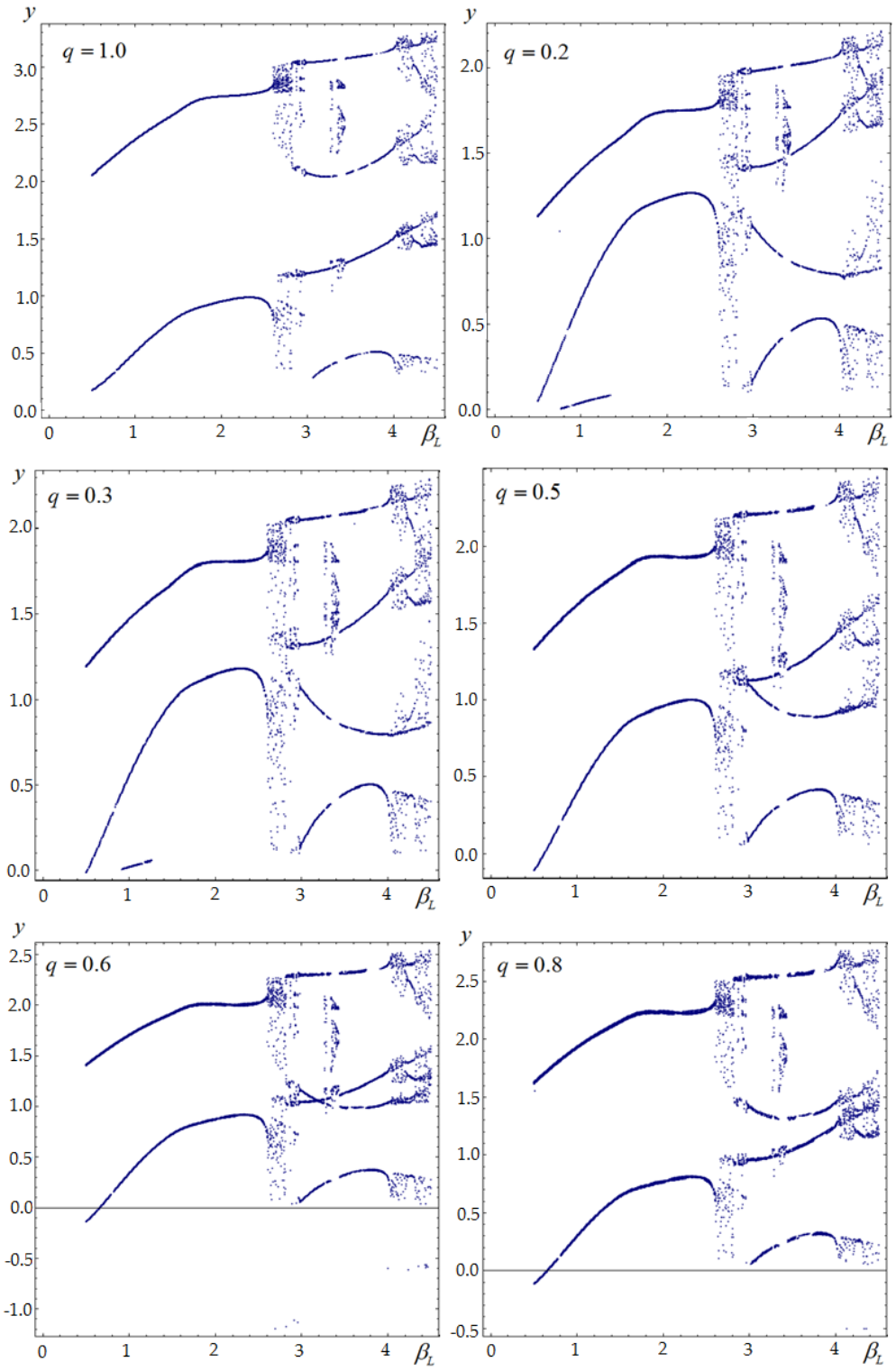

Figure 6. Fractional-order Bifurcation diagram of the following parameter $i = 1.11, \beta_c = 0.707, \beta_L = 2.68, g = 0.0478$.

Conflict of Interests

The author(s) have not declared any conflict of interests.

REFERENCES

Bagley RL, Calico RA (1991).Fractional order state equations for the control of viscoelastically damped structures. J. Guid. Contr. Dynam.

14(2):304-311. http://dx.doi.org/10.2514/3.20641
Bagley RL, Torvik PJ (1983). A theoretical basis for the application of fractional calculus. J. Rheol. 27: 201-210. http://dx.doi.org/10.1122/1.549724
Baleanu D, Diethelm K, ScalasE, Trujillo JJ (2009). Fractional Calculus Models and Numerical Methods. World Scientific Publishing, Singapore.
Cao J, Ma C, Xie H, Jiang Z (2010). .Nonlinear dynamics of doffing system with fractional order damping. J. Comput. Nonlin. Dyn. 5(4):041012-041018. http://dx.doi.org/10.1115/1.4002092
Chen DY, Zhao WL, Ma XY, Zhang RF (2012). Control and Synchronization of Chaos in RCL-Shunted Josephson Junction with Noise Disturbance Using Only One Controller Term. Abstr. Appl. Anal. 2012. http://dx.doi.org/10.1155/2012/378457
Clarke J, Braginski AI (2006). The SQUID Handbook, Vol. II Applications of SQUIDs and SQUID Systems, Wiley-CH.
Dreyer K, Hickey FR (1991). The route to chaos in a dripping water faucet. Am. J. Phys. 59 (7):619. http://dx.doi.org/10.1119/1.16783
Erturk V, Zaman G, Momani S (2012). A numeric analytic method for approximating a giving up smoking model containing fractional derivatives. Comput. Math. Appl. 64(10):3065-3074. http://dx.doi.org/10.1016/j.camwa.2012.02.002
Erturk VS, Momani S, Odibat ZM (2008). Application of generalized differential transform method to multi-order fractional differential equations. Commun. Nonlin. Sci. Numer. Simul. 13(8):1642-1654. http://dx.doi.org/10.1016/j.cnsns.2007.02.006
Feng YL, Shen K (2008). Chaos synchronization in RCL-shunted Josephson junctions via a common chaos driving. Eur. Phys. J. 61:105-110. http://dx.doi.org/10.1140/epjb/e2008-00037-9
Ge ZM, Ou CY (2007).Chaos in a fractional order modified Duffing system. Chaos Solit. Fract. 34:262-291. http://dx.doi.org/10.1016/j.chaos.2005.11.059
Hartley TT, Lorenzo CF, Qammer HK (1995). Chaos on a fractional Chua's system. IEEE Trans Circuits Syst. 42(8):485-490. http://dx.doi.org/10.1109/81.404062
Li C, Chen G (2004).Chaos and hyper chaos in the fractional-order Rossler equations. Physica A. 341:55-61. http://dx.doi.org/10.1016/j.physa.2004.04.113
Li C, Deng W (2007). Remarks on fractional derivatives, Appl. Math. Comput.187(2):777-784. http://dx.doi.org/10.1016/j.amc.2006.08.163
Li CP, Zhang FR (2011). A survey on the stability of fractional differential equations. Eur. Phys. J. Special Topics 193:27-47. http://dx.doi.org/10.1140/epjst/e2011-01379-1
Li TY, Yorke JA (1975). Period Three Implies Chaos. Am. Math. Monthly. 82:985. http://dx.doi.org/10.2307/2318254
Lorenz EN (1963). Deterministic Non-periodic Flow. J. Atmos. Sci. 20:130-141. http://dx.doi.org/10.1175/1520-0469(1963)020<0130:DNF>2.0.CO;2
Lu JG (2005). Chaotic dynamics and synchronization of fractional-order Arneodo's systems. Chaos Solit. Fract. 26(4):1125-1133. http://dx.doi.org/10.1016/j.chaos.2005.02.023
Lu JG, Chen G (2006). A note on the fractional-order Chen system. Chaos Solit. Fract. 27:685-688. http://dx.doi.org/10.1016/j.chaos.2005.04.037
Matignon D (1996).StabilityResults for Fractional Differential Equations with Applications to Control Processing. Comput. Eng. Syst. Appl. pp. 963-968.
May RM (1976).Simplemathematicalmodels with very complicated dynamics.Nature 261:459-67. http://dx.doi.org/10.1038/261459a0
Miller KS, Ross B (1993). An Introduction to the Fractional Calculus and Fractional Differential Equations. John Wiley & Sons. New York NY USA.
Momani S, Odibat ZM (2008). A novel method for nonlinearfractional partial differential equations: Combination of DTM and generalized Taylor's formula.J. Comput. Appl. Math. 220:85-95. http://dx.doi.org/10.1016/j.cam.2007.07.033
Odibat ZM, Bertelle C, Aziz-Alaoui MA, Duchamp GHE (2010). A multi-step differential transform method and application to non-chaotic or chaotic systems. Comput. Math. Appl. 59(4):1462-1472. http://dx.doi.org/10.1016/j.camwa.2009.11.005
Odibat ZM, Momani S (2008a). A generalizeddifferential transform method for linear partial differential equations of fractional order. Appl. Math. Lett. 21(2):194-199. http://dx.doi.org/10.1016/j.aml.2007.02.022
Odibat ZM, Momani S (2008b). An Algorithm for the numerical solution of differential equations of fractional order. J. Appl. Math. Inform. 26:15-27.
Odibat ZM, Momani S, Erturk VS (2008c).Generalized differential transform method: Application to differential equations of fractional order. Appl. Math. Comput. 197(2):467-477. http://dx.doi.org/10.1016/j.amc.2007.07.068
Oldham KB, Spanier J (1974). The FractionalCalculus. Academic Press New York NY USA.
Petras I (2009). Stability of fractional-order systems with rational orders: A survey. Fract. Calc. Appl. Anal. 12(3):269-298.
Petras I (2008). A note on the fractional-order Volta's system. Commun. Nonlin.Sci. Numer. Simul. 15:384-393. http://dx.doi.org/10.1016/j.cnsns.2009.04.009
Petras I (2008). A note on the fractional-order Chua's system. Chaos Solit. Fract. 38:140-147. http://dx.doi.org/10.1016/j.chaos.2006.10.054
Podlubny I (1999). Fractional Differential Equations, Vol. 198. Academic Press, San Diego, Calif, USA.
Radwan AG, Moaddy K, Momani S (2011). Stability and non-standard finite difference method of the generalized Chua's circuit. Comput. Math. Appl. 62(3):961-970. http://dx.doi.org/10.1016/j.camwa.2011.04.047
Sabatier J, Agrawal OP, Machado JAT (2007). Advances in Fractional Calculus: Theoretical Developments and Applications in Physics and Engineering. Springer, Dordrecht, The Netherlands. http://dx.doi.org/10.1007/978-1-4020-6042-7
Sandri M (1996). Numerical Calculation of Lyapunov Exponents. Mathematica J. 6 (3):78-84.
Wang X, Tian L (2006).Bifurcationanalysis and linear control of the Newton–Leipnik system, Chaos Solit. Fract. 27:31-38. http://dx.doi.org/10.1016/j.chaos.2005.04.009
Xiang-Jun W, Zheng-Mao W, Jun-Guo L (2008). Stability Analysis of a Class of Nonlinear Fractional-Order Systems. IEEE Circuits Syst. II 55(11):1178-1182. http://dx.doi.org/10.1109/TCSII.2008.2002571
Yu Y, Li HX, Wanga S, Yu J (2009). Dynamicanalysis of a fractional-order Lorenz chaotic system. Chaos Solit. Fract. 42:1181-1189. http://dx.doi.org/10.1016/j.chaos.2009.03.016
Zaslavsky GM (2002). Chaos, fractional kinetics, and anomalous transport. Phys. Rep. 371(6):461-580. http://dx.doi.org/10.1016/S0370-1573(02)00331-9
Zhang W, Zhou S, Li H, Zhu H (2009). Chaos in a fractional-order Rössler system. Chaos.Solit. Fract. 42:1684-1691. http://dx.doi.org/10.1016/j.chaos.2009.03.069

academicJournals

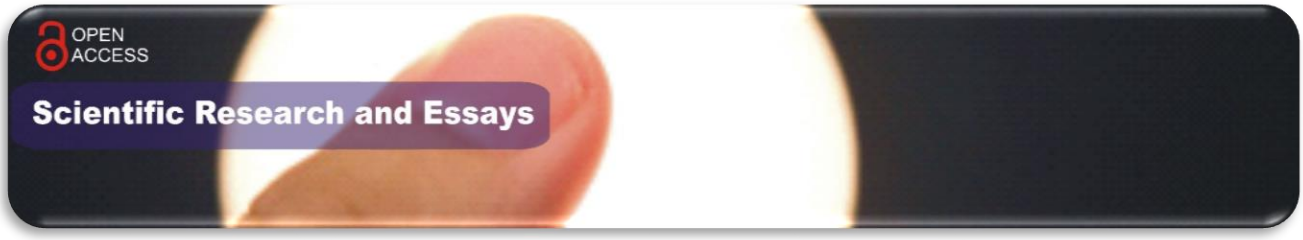

Related Journals Published by Academic Journals

- International NGO Journal
- International Journal of Peace and Development Studies